PERFORMANCE ANALYSIS OF EJECTOR ENHANCED MULTI EVAPORATOR CASCADE REFRIGERATION SYSTEM

A

THESIS

Submitted in partial fulfillment of the requirements for the award of degree of

Master of Engineering (M.E.)

In

Thermal Engineering

Submitted by

FAISAL SHABIR

(ROLL NO. 801283009)

UNDER THE GUIDANCE OF

Dr. M.K.MITTAL

(Assistant Professor)

DEPARTMENT OF MECHANICAL ENGINEERING

THAPAR UNIVERSITY, PATIALA – 147004

JULY 2014

CERTIFICATION

I, Faisal Shabir, hereby declare that this thesis report entitled ***"Performance analysis of ejector enhanced multi evaporator cascade refrigeration system"*** submitted in the partial fulfilment of the requirements for the award of degree of Master of Engineering in Thermal Engineering, in the Mechanical Department, Thapar University, Patiala, is wholly my own work. This matter embodied in this report has not been submitted in part or full to any other university or institute for the award of any degree.

Date: 07-07-2014
Place: Patiala

Faisal Shabir
801283009

This is to certify that above statement made by the student concerned is correct and true to the best of my knowledge & belief.

Supervisor:
7/7/2014
Dr. Madhup Kumar Mittal
Assistant Professor
Mechanical Engineering Department
Thapar University, Patiala

Countersigned by

Dr. Ajay Batish
Professor and Head
Mechanical Engineering Department
Thapar University, Patiala

Dr.S.K.Mohapatra
Dean Academic Affairs
Thapar University, Patiala

ACKNOWLEDGEMENT

With deep sense of gratitude I would like to express deepest appreciation to my advisor, Dr. Madhup Kumar Mittal, who has the attitude and the substance of a genius. Dr. Mittal continually and convincingly conveyed a spirit of adventure in regard to research and an excitement in regard to teaching. Without his guidance and persistent help this dissertation would not have been possible.

The opportunity, support, exposure and atmosphere provided by the Thapar University, Patiala, to carry out my studies is highly appreciated.

A special debt of gratitude is owed to the authors whose works I have consulted and quoted in this work.

Last but not least, I am forever grateful to my parents for their unconditional support and best wishes.

(Faisal Shabir)

ABSTRACT

Refrigeration and air conditioning is one of the leading uses of electric power in the world. Reduction of power input to the compressor by incorporating a low grade heat operated pre compression device is one of the efficient ways to reduce fossil fuel consumption and thereby reduce the environmental hazards. In the present study, an improved cooling cycle for multi evaporator cascade refrigeration system enhanced by incorporation of ejectors for pre compression of refrigerant vapour is analyzed. The ejector enhanced multi evaporator cascade refrigeration system (EEMECRS) consists of two stages; the lower stage has three evaporators to achieve low temperature cooling at different temperatures , the upper stage has two evaporators, one for air conditioning purposes, and other to absorb heat rejected from the lower stage. The two stages are interconnected through an intercooler which acts as a condenser to the lower stage and one of the evaporators for the upper stage.

A mathematical model based on mass and energy conservation in each component is developed to analyze the performance of EEMECRS. For ejector, one dimensional mathematical model previously developed by Kairouani *et al*.(2009) for constant area ejector flow is modified to account for the losses in primary nozzle and so that it could be applied to EEMECRS operating with several working refrigerants. Four refrigerants in each stage of EEMECRS giving a total of sixteen combinations of refrigerants in upper and lower stage of EEMECRS were analyzed to identify the pair of refrigerants which give best performance. R1270 and R142b in lower and upper stage of EEMECRS respectively were found to give best performance. The novel system has been theoretically investigated for various performance characteristics. The comparison between novel and unenhanced multi evaporator cascade refrigeration system (UMECRS) has been made under same operating conditions. EEMECRS is developed keeping in view needs of medical industry where medicines are required to be cooled at different low temperatures and also requires air conditioning for working spaces of employees. The results show that COP is improved by 28% for best refrigerant pair *i.e* R1270 in lower stage and R142b in upper stage of EEMECRS.

TABLE OF CONTENTS

LIST OF FIGURES

LIST OF TABLES

NOMENCLATURE

a	Sound speed[m/sec]
A	Area of cross section [m^2]
COP	Coefficient of performance
C_p	Specific heat capacity at constant pressure [J Kg^{-1} K^{-1}]
C_v	Specific heat capacity at constant volume [J Kg^{-1} K^{-1}]
D	Diameter [m]
F	Friction factor
h	Enthalpy[J Kg^{-1}]
k	Ratio of specific heats(C_p/ C_v)
L	Length of mixing chamber[m]
M	Mach number
m	Mass flow rate [Kg s^{-1}]
P	Pressure [Pa]
Q	Heat load[W]
R	Gas constant
r	Compression ratio (P_4/P′)
s	entropy[J Kg^{-1} K^{-1}]
T	Temperature
U	Entrainment ratio [m″/m′]
V	Velocity [m s^{-1}]
W	Mechanical work[J kg^{-1}]
X	Distance between primary nozzle exit and mixing chamber inlet[m]

η	Efficiency
ξ	Driving pressure ratio(P'/P_4)
Γ	Driving pressure ratio(P''/P')
$\emptyset$	Ejector area ratio
θ	Temperature ratio
Δ	Increment
f	Function
ρ	Density

Subscripts and superscripts

C	Condenser
un	unenhanced
cm1	Compressor 1
cm2	Compressor 2
e1	Motive nozzle outlet
e2	Mixing chamber inlet
e3	Diffuser inlet
e4	Diffuser outlet
ev1	Evaporator1
ev2	Evaporator 2
ev3	Evaporator 3
ev4	Evaporator 4
ej1	Ejector 1

ej2	Ejector 2
ej3	Ejector 3
int	Intercooler
m	mixed
r	Relative to unenhanced system
s	Isentropic
sat	Saturation
sup	Superheat
0	Stagnation
′	Primary
″	Secondary
*	Nozzle throat
1	Lower stage
2	Upper stage
R	Relative
SYS	System

Chapter 1

Introduction

1.1 Historical background

Many industrial and medical applications, conservation of food, and air conditioning of living spaces makes cooling indispensable for human being in modern world. Currently, the mechanical vapour compression systems used for this purpose uses large amounts of electrical power that is produced predominantly by fossil fuel combustion, which is a cause of the global warming. Increasing concerns about environmental issues makes imperative need to develop alternative technologies that will allow carrying out cooling applications reducing the use of electrical energy with negligible environmental impacts.

The mechanical compression refrigeration system consumes a massive amount of high grade energy. This has motivated researchers to focus on utilization of low grade heat operated systems that can use abundantly available low grade energy to carry out cooling applications. The heat operated systems include absorption, adsorption and ejector compression system. Among these low grade heat-operated systems, the absorption refrigeration system requires a relatively high temperature heat source. On the other hand, the ejector refrigeration system is found attractive because it requires a relatively low temperature heat source. Compared to absorption systems, ejector systems have advantages of low heat source requirement, simplicity, reliability, and low installation and operational costs. These systems can be widely used in with low-temperature energy sources such as solar energy, geothermal energy and waste heat *etc*. Use of ejector heat operated system will reduce the fossil fuel consumption and consequently lessen the environmental hazards. The main disadvantages of ejector refrigeration system are:

- Ejectors are designed to operate within a small range of temperatures. Any deviation from this range results in dramatic deterioration of the ejector performance.

- Its poor performance. It has a COP of order of 0.2 on an average when the evaporating temperature is at 10^{o}C.

The use of ejector in vapour compression system for performance improvement was first proposed by Kornhauser, 1990.The ejector enhanced compression cycle reduces the work of compression by raising the suction pressure to a level higher that in the evaporator leading to the improvement of COP. Use of ejector will give two benefits: work recovery (COP improvement) and flash gas bypass (evaporator size reduction).

1.2 Ejector operation

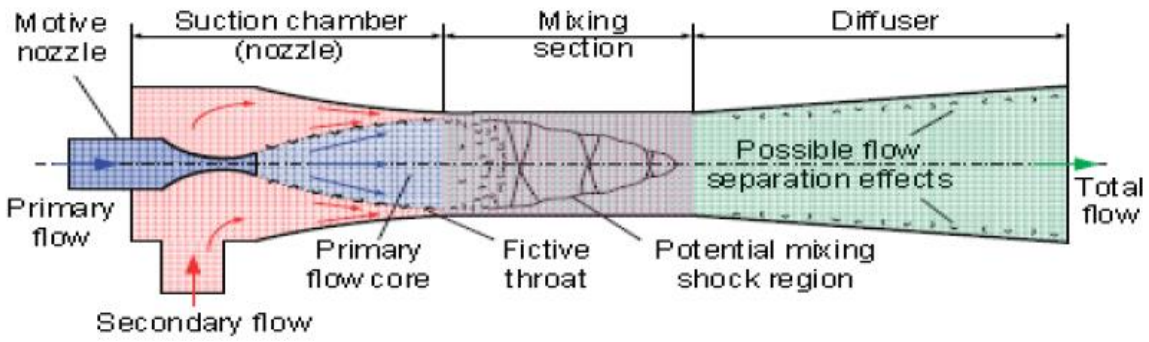

Fig. 1.1: Behaviour of primary and secondary fluid stream inside ejector.

As shown in Fig. 1.1, a typical ejector is composed of a primary nozzle, a mixing chamber and a diffuser. The working principle for the ejector is straight forward. An ejector has two inlets: one to admit the motive fluid stream at high pressure fluid and other to admit the secondary fluid stream at low pressure. The motive fluid enters the converging-diverging nozzle where, the pressure energy of the motive fluid is converted to kinetic energy, as a result, at the exit of the nozzle, the fluid velocity becomes supersonic and a low pressure zone is created .This low pressure created enables the secondary fluid to be entrained or pumped through other inlet.

The entrained vapour flow subsequently mixes with motive fluid flow while they move through the converging section of the ejector, thereby, increasing pressure at expense of kinetic energy. The motive fluid slows down and the entrained stream speeds up and, at some point downstream the mixing chamber, the mixed flow reaches the speed of sound. A stationary shock wave is produced thereby results in a sharp rise in absolute pressure. The shock wave in the diffuser throat shifts the velocity of mixed stream from supersonic to sub-sonic. Then, in the diverging section,

the increasing cross sectional area increases the pressure at the expense of kinetic energy. The net result, being an increase of the absolute pressure of the mixture on discharge to several times the pressure at which secondary fluid entered the ejector inlet.

1.3 Ejector refrigeration system

A simple ejector refrigeration system consists of the following equipment

i) Evaporator ii) Condenser iii) Boiler/Generator iv) Ejector v) Pump vi) Expansion Device

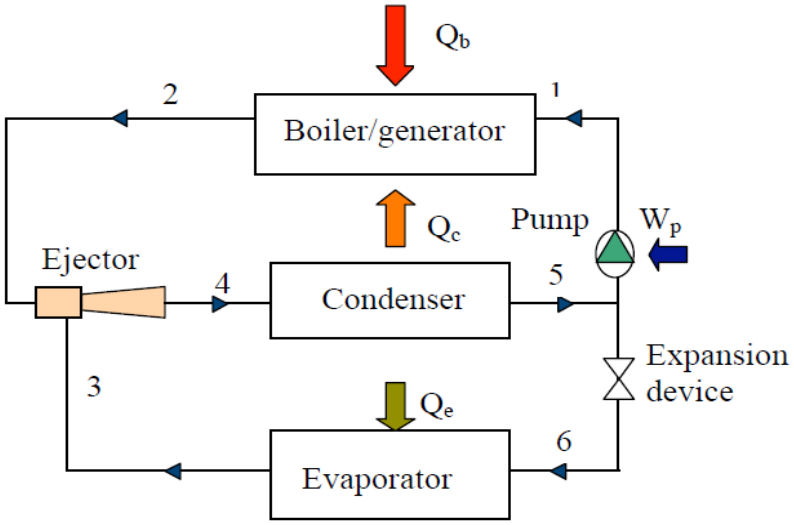

Fig. 1.2: Schematic diagram of ejector refrigeration cycle (source: Grimsby)

Referring to the basic ejector refrigeration cycle in Fig.1.2, the ejector refrigeration system is composed of two sub cycles, the power sub-cycle and the refrigeration sub-cycle. In the power sub-cycle, low-grade heat, Q_b , is supplied to boiler or generator to evaporate high pressure liquid refrigerant (process 1-2). At state point 2, the high pressure vapour generated, known as the motive fluid, enters the ejector and expands through the converging-diverging nozzle creating a low pressure zone. This reduction in pressure entrains vapour from the evaporator, known as the secondary fluid, at point 3. The entrained vapour flow subsequently mixes with motive fluid flow before entering the diffuser, while combined flow moves through the diffuser, the flow decelerates and pressure recovery occurs. The combined fluid then flows to the condenser where it is condensed rejecting heat to the environment, Q_c. At the condenser outlet the fluid stream is divided into two parts at point 5, one portion is

then pumped to the boiler for the completion of the power cycle. The other portion is expanded through an expansion device and enters the evaporator of the refrigeration sub-cycle at point 6. The refrigerant absorbs latent heat of vaporisation producing a refrigeration effect, Q_e, and the resulting vapour is then entrained into the ejector at point 3.

1.4 Hybrid ejector-compression system

Sokolov and Hershgal (1989) were the first to propose a combined cycle between an ejector refrigeration system and a vapour compression system, eliminating the main limitations of each technology. On one side, the ejector refrigeration sub-system opens its application range and increases its efficiency. On the other hand, the mechanical compression refrigeration system reduces its electrical energy consumption.

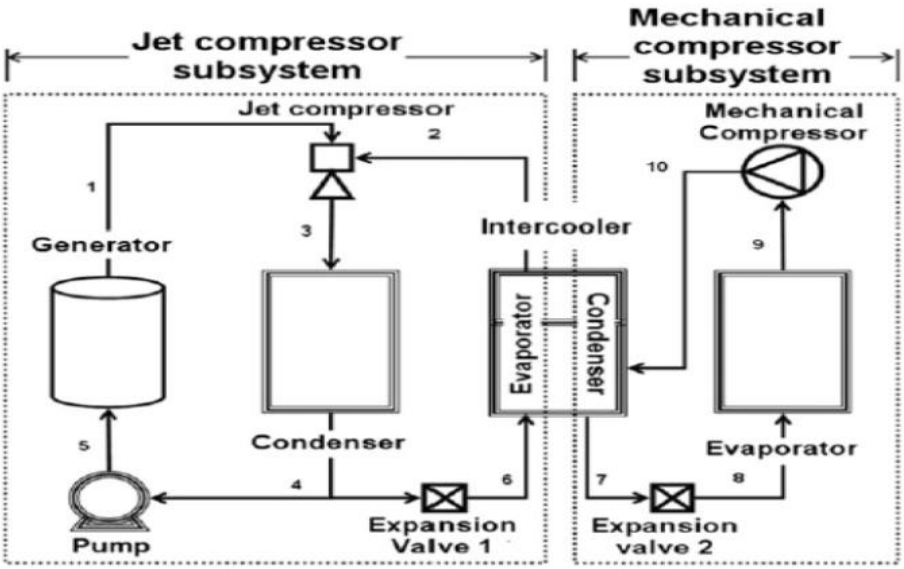

Fig. 1.3: Hybrid ejector-compression refrigeration system (Sokolov and Hershgal ,1989)

The interface between both systems is a heat exchanger called intercooler (Sokolov and Hershgal, 1990). The intercooler can act as heat and sometimes also as a mass exchanger; it can be seen as the evaporator of the ejector system and as the condenser of the mechanical compression refrigeration. The authors obtained significant improvements in the overall performance of the system.

1.5 Motivation for research

During the past twenty years researchers have focussed on investigating the possibility of improving the performance of vapour compression systems through various hybrid configurations. Many theoretical and experimental configurations of integration of ejector into compression system have been proposed. However, very little literature has been cited on use of ejectors in multi evaporator systems. Multi evaporator systems with low temperature cooling are indispensable in various medical and industrial applications. To achieve such low temperature, it becomes necessary to cascade the low temperature multi evaporator system to conventional compression system. The upper stage of cascade does the function of heat rejection. The enhancement of multi evaporator systems by ejectors is of much importance as this configuration reduces the power input to the system.

The present study is carried out to develop and analyze a novel multi evaporator cascade refrigeration configuration with integrated ejectors for use in medical industry where low temperature cooling is required at different temperatures. The proposed system has three low temperature evaporators in the lower stage of the system for cooling of three compartments at different temperatures. This stage is interconnected with upper stage of the system through intercooler which acts as condenser for lower stage. The upper stage has two evaporators; one to absorb the heat of the lower stage and other to provide cooling for air conditioning of working spaces in medical industry. Ejectors have been incorporated into the system for pressure recovery, saving a substantial amount of power input to the system. No literature has been cited on enhancement of multi evaporator cascade refrigeration system by ejectors.

1.6 Objectives of the present work

The present study has been carried out to develop a mathematical model for performance analysis of the ejector enhanced multi evaporator cascade refrigeration system (EEMECRS). The EEMECRS is analysed for following objectives:

1. To determine the entrainment ratio U_{ej} and the back pressure of ejector for different temperatures of motive and secondary stream.
2. To compare the entrainment ratio for various refrigerants.
3. To identify a best pair of refrigerants in upper and lower stage of system among the alternatives considered.

4. To compare the system performance of ejector enhanced multi-evaporator cascade refrigeration system (EEMECRS) with unenhanced conventional refrigeration system.
5. To investigate effect of ejector geometry on EEMECRS performance.
6. To investigate the effect of operating temperatures on EEMECRS performance.

A computer code using MATLAB 7.01 is developed to compute the results of mathematical model in order to achieve above mentioned objectives. Refrigerant properties have been evaluated using REFPROP 7.01 subroutines.

1.7 Organisation of thesis

The present study is mainly divided into five chapters as given below:

Chapter1:

This chapter presents the overview of the historical background of ejector enhanced systems and advantages of incorporation of ejectors into conventional compression system. The basic working of ejector and ejector refrigeration system along with a generalised hybrid configuration have been have been discussed. Motivation for present research along with its main objectives are being listed in the chapter.

Chapter2:

This chapter has been divided into three segments. The first segment discusses the types of ejector modelling regimes and basic governing equations in different regimes cited in literature. The second section provides a comprehensive review of various mathematical and numerical models of an ejector. The third section discusses various ejector enhanced compression system configurations along with their merits and demerits.

Chapter 3:

This chapter discusses the novel system description and development of mathematical model for EEMECRS. The computational methodology of simulation model has also been presented.

Chapter 4:

This chapter deals with the results of simulation. Validation of developed mathematical model with experimental data is presented. Strategy for selection of best pair of refrigerants along with effect fluid nature on system performance is discussed. Effect of operating temperatures and ejector geometry on system performance are presented in graphical and tabular form.

Chapter 5:

The conclusion drawn from the results of simulation are presented in this chapter along with the scope for future work.

Chapter 2

Literature Review

This chapter is divided into three sections; the first section discussed the basic of ejector, parameters influencing the performance and basic governing equations of ejector. Second section provides comprehensive review of various mathematical and numerical models available in literature. The third section discusses various hybrid compression-ejection systems configurations along with their merits and demerits.

2.1 Ejectors

Ejectors are devices used to induce a secondary fluid by momentum and energy transfer from a high velocity primary jet. Depending on the application, ejectors operated with incompressible fluids (liquids) are normally referred to as jet pumps or eductors. On the other hand, the terms ejector and injector are generally employed when ejectors are operated with compressible fluids (gases and vapours). Another difference between the two, besides the working fluid states is that incase of ejector working with compressible fluids, the nozzle is supersonic. The supersonic approach allows the greater conversion of primary flow pressure head to secondary flow pressure head increase. Fig.2.1 and 2.2 show typical cross sectional views of liquid jet pump and steam ejector.

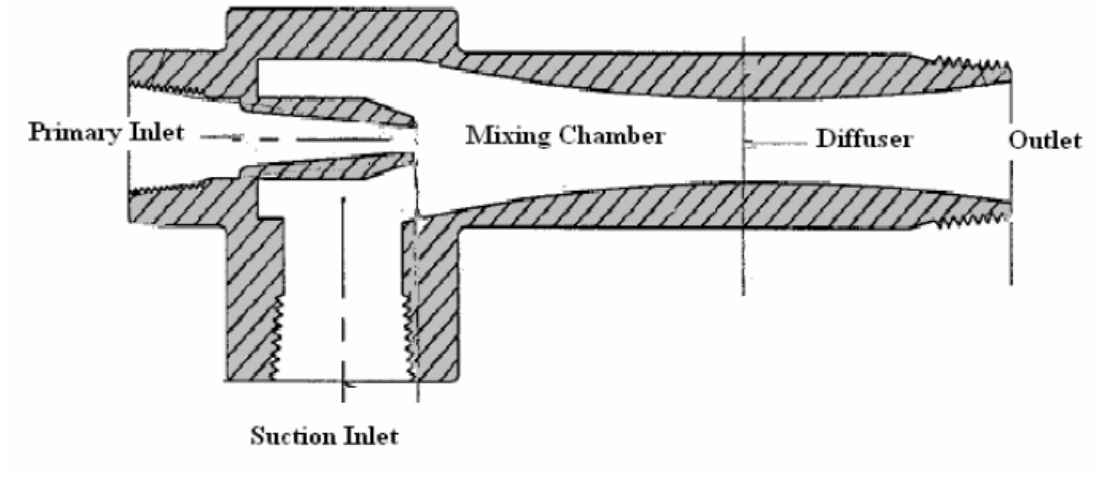

Fig. 2.1: Cross sectional view of a typical liquid jet pump**.**

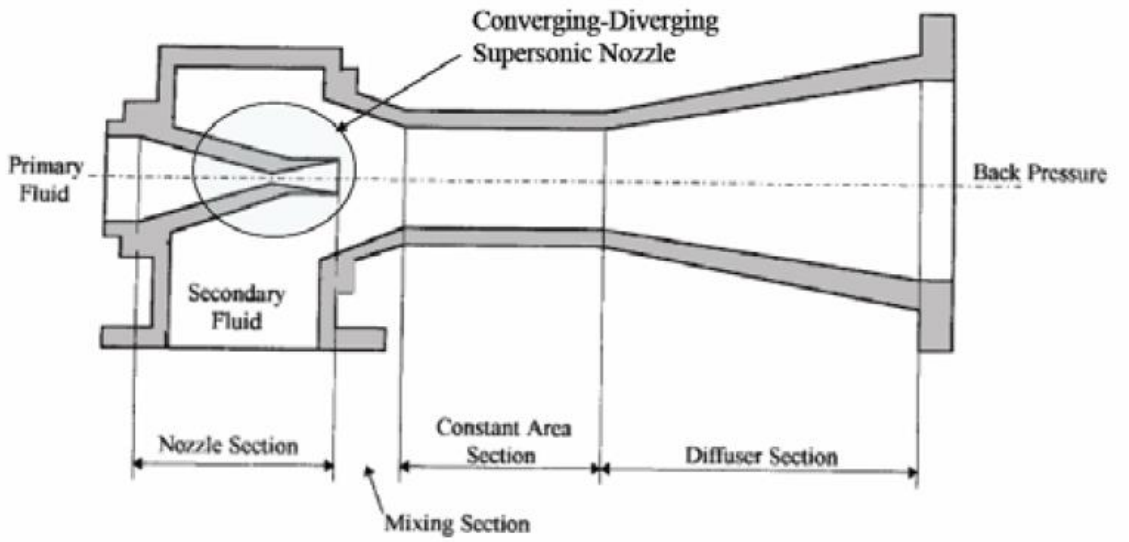

Fig. 2.2: Cross sectional view of a typical gas ejector.

The working principle of liquid jet pumps and gas ejectors is same; a high-pressure fluid known as motive fluid is accelerated to high velocity jet through a converging nozzle for the liquid jet pump or a converging-diverging supersonic nozzle for the gas ejector. The pressure head is partly converted to kinetic energy at the nozzle exit according to the Bernoulli equation. The high velocity, low static pressure motive fluid jet entrains secondary flow from the suction port and accelerates it in the direction of the motive jet. The two streams mix inside the mixing chamber. A diffuser is installed at mixing chamber exit to lift the static pressure of mixed flow at expense of its kinetic energy. Thus, ejector plays two fundamental roles: the entrainment and recompression of mixed fluid stream.

2.1.1 Theoretical background of one dimensional ejector:

Fabri and Paulon (1956) described that in general there are two regimes of ejector operation *i.e* the supersonic regime and the mixed flow regime. The supersonic regime is characterized by certain part flow being supersonic over the whole cross-sectional area in the mixing chamber. In this type of flow regime the exit pressure, P_4, does not influence the performance characteristics (P_o', P_o'' and U). While as, in case of mixed flow regime the exit pressure, P_4, reduces the length of fully supersonic part of the flow field in the mixing chamber until it breaks down. Then, the flow at the exit

of primary nozzle and in center of mixing chamber is still supersonic whereas the flow near the mixing chamber walls is subsonic. For most cases, the supersonic jet attaches to one side of the wall known as Coanda effect. The secondary flow stagnation pressure in this regime is a function of the exit pressure P_4.

Ubelhack (1972) gives detailed analyses of inviscid one dimensional ejector. Experimental investigations on supersonic ejectors have delineated that wide range of ejector operation can be described by fundamental conservation laws. In order to make this chapter self-contained, it is necessary to replicate some part of work done by Ubelhack (1972).

2.1.1.1 Supersonic regime

This regime can be subdivided into:

(i) The supersonic-saturated regime, where M_2'' is sonic,

(ii) The actual supersonic regime, $1 > M_2'' > 0.3$

(iii) The supersonic regime with low secondary flow $0.3 > M_2'' > 0$ (or $U \rightarrow 0$).

Supersonic regime in a supersonic ejector is shown in Fig. 2.3

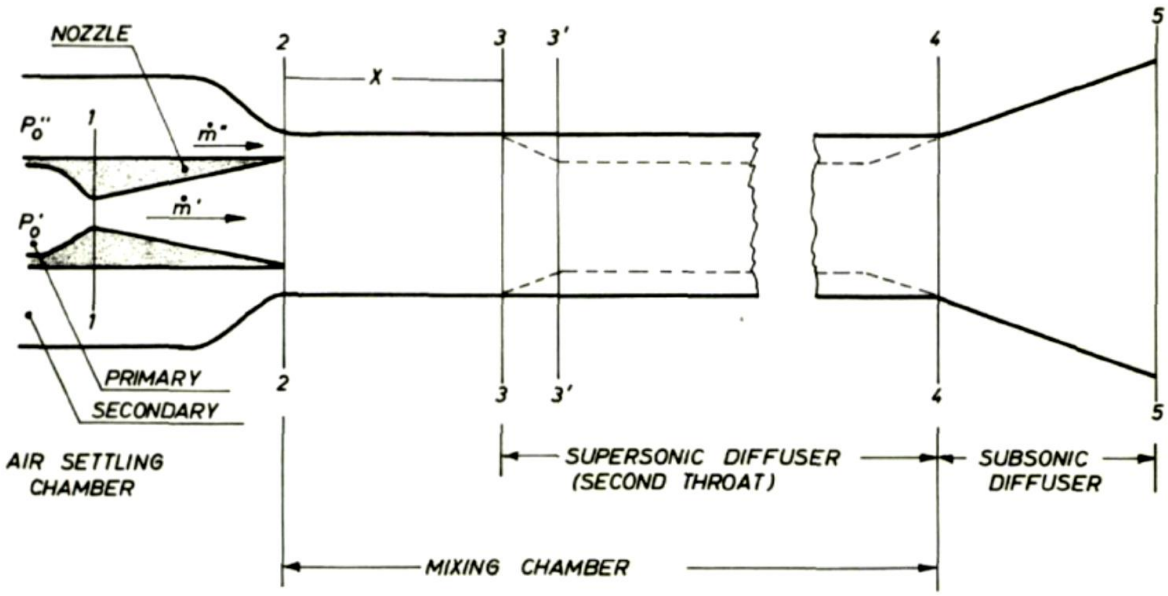

Fig. 2.3: Cross sectional view of supersonic ejector and reference stations.

2.1.1.1.1 Conservation laws

1. Continuity Equation

The mass flow in a duct is given by

$$m = \rho V A = \rho_o a_o A \frac{\rho_{cr}}{\rho_o} \frac{A_{cr}}{A_o} \sqrt{\frac{T_{cr}}{T_o}} \tag{1}$$

$$m = \frac{\rho_o a_o}{R T_o} \frac{\rho_{cr}}{\rho_o} \sqrt{\frac{T_{cr}}{T_o}}\ A\ q(M_{cr}) \tag{2}$$

where,

$$q(M_{cr}) = \frac{A_{cr}}{A} = \left(\frac{\gamma+1}{2}\right)^{1/(\gamma-1)} M_{cr} \left(1 - \frac{\gamma-1}{\gamma+1}\ M_{cr}^2\right)^{1/\gamma-1} \tag{3}$$

is a dimensionless function of the Mach number and the specific heat ratio only. It has been found useful for numerical calculation to introduce dimensionless functions of M_{cr}.

2. Momentum Equation

The momentum equation can be represented by the balance of jet thrusts in different sections of the ejector.

The vacuum thrust is defined by

$$F = PA + PV^2 A = P_o A(1 + \rho M^2) \tag{4}$$

or

$$F = P_o A f(M_{cr}) \tag{5}$$

where

$$f(M_{cr}) = (1 + M_{cr}^2)\left(1 - \frac{\gamma-1}{\gamma+1}\ M_{cr}^2\right)^{1/\gamma-1} \tag{6}$$

The quantity F can also be expressed in terms of the mass flow m, using Equation (2).

$$F = P_o \frac{A_{cr}}{A_o} A_{cr}\ f(M_{cr}) = P_o A_{cr} \frac{f(M_{cr})}{q(M_{cr})} \tag{7}$$

The ratio

$$\frac{f(M_{cr})}{q(M_{cr})} = \left(\frac{2}{\gamma+1}\right)^{1/(\gamma-1)} Z(M_{cr}) \tag{8}$$

where

$$Z(M_{cr}) = M_{cr} + \frac{1}{M_{cr}} \tag{9}$$

and

$\left(\frac{2}{\gamma+1}\right)^{1/(\gamma-1)}$ represents $\frac{P}{P_o}$

Using these relations in above equations yields

$$F = P_o \frac{\rho_{cr}}{\rho_o} A_{cr} Z(M_{cr}) \tag{10}$$

2.1.1.1.2 Supersonic saturated regime

The performance characteristics in this regime can be determined from the condition of sonic velocity at Station 1 for the primary jet and Station 2 for the secondary jet only.

The relation between the entrainment ratio *U* and the stagnation pressure ratio P_o''/P_o' is found from Equation (1).

$$U = \frac{m''}{m'} = \frac{A_2''}{A_1'} \frac{P_o''}{P_o'} \tag{11}$$

2.1.1.1.3 Actual supersonic regime

The calculation of this regime is based on the following assumptions:

(i) The primary and the secondary jets are isentropically accelerated between stations 2 and e shown in Fig. 2.4. The mixing of the two jets is neglected.
(ii) The secondary jet reaches sonic speed at station e.

The performance characteristics of the supersonic regime can thus be determined by applying the conservation laws between Stations 2 and e as shown in Fig. 2.4.

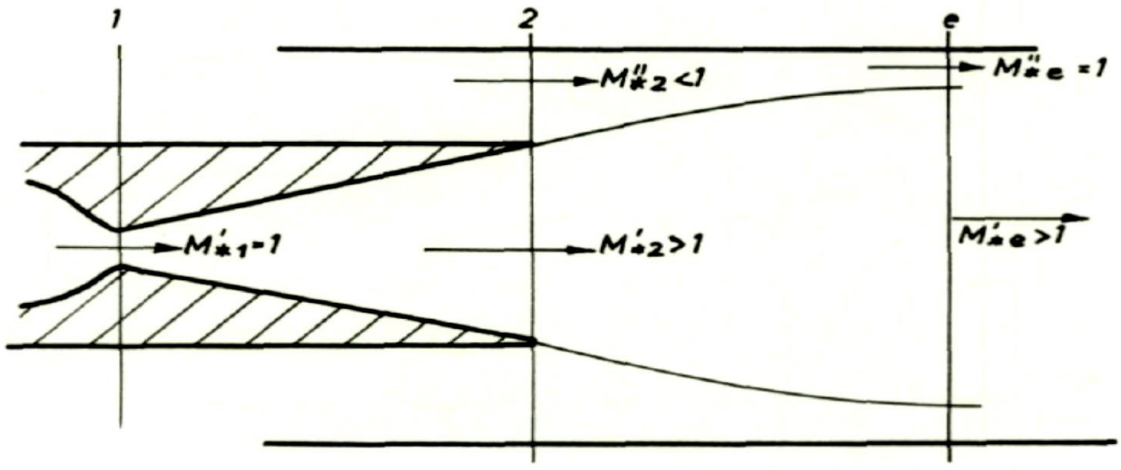

Fig. 2.4: Actual supersonic regime

For the particular case of equal stagnation temperature

$T_o' = T_o''$ and therefore $a_{cr}' = a_{cr}''$ (12)

The momentum equation yields

$$m'z_2' + m''z_2'' = m'z_e' + m''z_e'' \quad (13)$$

Introducing the entrainment ratio $U = m''/m'$ and the condition $M_{cre}'' = 1$, $Z_{cre}'' = 2$, equation (13) takes the form,

$$U = \frac{z_e' - z_2'}{z_e'' - 2} \quad (14)$$

The entrainment ratio can also be represented equation (1),

$$U = \frac{m''}{m'} = \frac{P_o''}{P_o'} \frac{A_2''}{A_1'} \frac{q(M_2'')}{q(M_{1cr}')} \quad (15)$$

Solving for $\frac{P_o''}{P_o'}$ and noting that $q(M_{1cr}') = 1$ yeilds

$$\frac{P_o'}{P_o''} = \frac{1}{U} \frac{A_2''}{A_1'} q(M_{cr2}'') \quad (16)$$

Equations (13) and (15) represent the solution for supersonic regime.

2.1.1.2 Mixed flow regime

Referring to Fig. 2.3, in the mixed flow regimes there exists a subsonic region of the flow pattern between the secondary flow settling chamber and the exit of the mixing

chamber *i.e* station 4. The exit pressure P_4 thus influences the pressure P_o'' in the secondary settling chamber. The value of P_o'' increases when P_4 is increased and vice versa (for *U* = constant). Above a certain value of the P_2'' flow in the primary nozzle will separate and thus cause the thrust of the nozzle to decrease and influence the whole characteristic performance.

The characteristics of this mixed flow regime can be determined by the continuity and momentum equations applied between stations 2 and 4.

2.1.1.2.1 Conservation laws

1. Continuity Equation

$$m'' + m' = m_4 \tag{16}$$

or

$$P_o' A_1' \, q(M_{cr1}') + (1 + U) = P_{o4} A_4 \, q(M_{cr4}) \tag{17}$$

2. Momentum equation

$$P_o^{'} A_2^{'} \, f\left(M_{cr2}^{'}\right) + P_o^{''} A_2^{''} \, f\left(M_{cr2}^{''}\right) = P_{o4} A_4 \, f(M_{cr4}) \tag{18}$$

Together with the definition of U,

$$U = \frac{m''}{m'} = \frac{P_o''}{P_o'} \frac{A_2''}{A_1'} \, q(M_{cr2}'') \tag{19}$$

The Equations (17) and (18) display the relation between $\frac{P_o'}{P_4}$ and $\frac{P_o''}{P_4}$ for a certain entrainment ratio. Here also M_{cr2}'' is the parameter relating $\frac{P_o''}{P_o'}$ and *U*.

To solve the above equations an arbitrary value for P_o', is assumed, P_o'' then is found from Equation (19). Equation (17) can be solved for $P_{o4} A_4 \, q(M_{cr4})$ (introducing the same value of M_{cr2}''). In the same manner $P_{o4} A_4 \, f(M_{cr4})$ is found from Equation (18). The exit Mach number M_{cr4}'' is then determined by,

$$\frac{P_{o4} A_4 \, f(M_{cr4})}{P_{o4} A_4 \, q(M_{cr4})} = \left(\frac{2}{\gamma + 1}\right)^{1/(\gamma - 1)} Z(M_{cr4}) \tag{20}$$

The function $Z(M_{cr4})$ is double valued. The subsonic solution has to be chosen in this case. The resulting procedure to determine P'_{04} , $\frac{P''_o}{P_4}$ and $\frac{P'_o}{P_4}$ is straightforward.

2.1.1.3 Effect of friction

In the supersonic regimes, friction does not greatly influence the ejector performance since the distance over which the secondary flow is accelerated to supersonic speed is rather short (of the order of two diameters). In the mixed flow regime, however, friction at the mixing chamber walls influences the characteristic line of this regime. If friction is considered in the theoretical calculation equation (18) should read as:

$$F'_2 + F''_2 - F_F = F_4 \qquad (21)$$

In other words, the pressure losses due to friction reduce P_4 and therefore increase both pressure ratios $\frac{P''_o}{P_4}$ and $\frac{P'_o}{P_4}$.

2.1.1.4 Diffuser

In the preceding calculations the effect of the subsonic diffuser was not taken into account. The best possible influence of a subsonic diffuser following Station 4 has already been given in the calculations in Section 2.1.1.2, where P_4 and P_{04} were determined through M_{cr4}. In the ideal case, P_5 would equal P_{04} (100% diffuser efficiency). In most practical applications M_{cr4} varies in the narrow range between 0.45 and 0.65 only. Assuming a mean exit velocity of M_{cr4} = 0.55 and a diffuser efficiency of 75%, we would get an improvement in pressure ratios of 15%. This value was found as a mean value in many experiments.

2.1.1.5 Mixing chamber length

The effect of the mixing chamber length on the ejector characteristics is shown in the experimental curve in Fig. 2.5. It can be observed that at transition from the supersonic to the mixed flow regime a minimum length of the mixing chamber is required in order to get approximately a uniform flow and the exit pressure P_4. Fig. 2.5 shows the typical pressure distribution in the mixed flow regime, very close to transition to the supersonic regime. From Fig. 2.5, it can be concluded that for this

particular ejector configuration and entrainment ratio the optimum mixing chamber length is $(L/D)_{opt}$ = 12 . For larger values of *L/D*, the exit pressure decreases due to friction. At lower L/*D* than $(L/D)_{opt}$ it is not possible to reach $(P_4)_{opt}$. The supersonic regime breaks down sooner. It is therefore advisable to choose a L/*D* > $(L/D)_{opt}$.

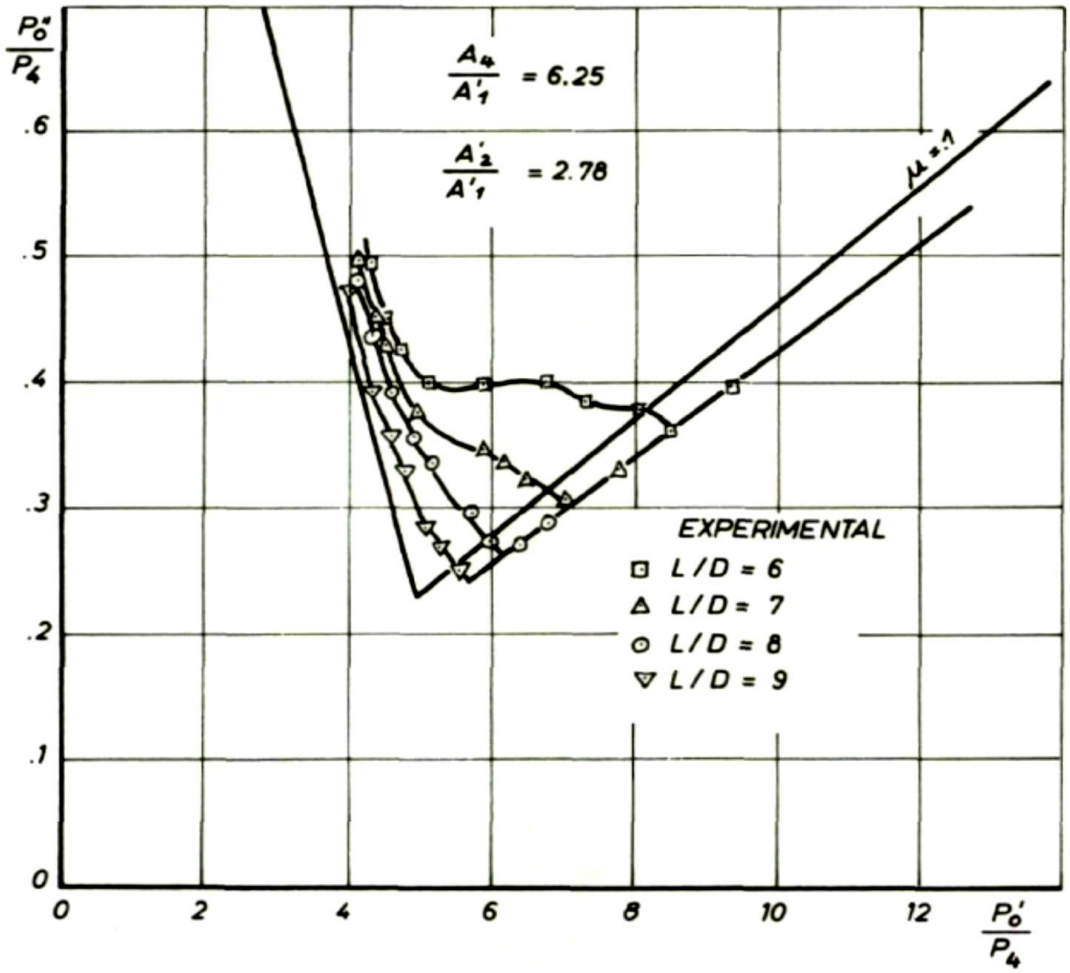

Fig. 2.5: Influence of diffuser length on performance of ejector (Ubelhack ,1972)

The main parameters which determine the optimum length of an ejector are:

(i) the area ratio A_3/ A_1, which determines the initial Mach number. At higher Mach numbers the shock waves angles are smaller and the whole supersonic flow pattern (*i.e.*, at transition to the mixed flow regime) is stretched out. A larger L/D is required.

(ii) the entrainment ratio U , Larger entrainment ratios smooth the above-mentioned effect. This is, however, an upper limit of U for the addition of a second throat.

(iii) the nozzle outlet angle. Larger nozzle outlet angles provoke a stronger interaction of the primary jet with the secondary jet and the wall. The resulting shock waves are stronger and steeper. A lower $(L/D)_{opt}$ is therefore to be expected.

2.1.1.6 Effect of temperature

The ejector performance characteristics were derived in Section 2.1.1.1 for equal stagnation enthalpies of both jets. In the case of different stagnation enthalpies the energy equation has to be used in order to determine T_{04} at the exit. In the calculation for the mixed flow regime a complete mixture of the two jets must be assumed. In calculating the characteristics of the supersonic regime the additional assumption of no heat exchange between Stations 2 and e is necessary. The simplest way to show the temperature influence is to look at the supersonic-saturated regime.

From Equation (1) it follows that,

$$m = \frac{P_o A}{\sqrt{T_o}} \times const. \tag{22}$$

Thus, for different T_0 equation (11) yields

$$U\sqrt{\frac{T_0''}{T_o'}} = \frac{P_o''}{P_o'}\,\frac{A_2''}{A_1'} \tag{23}$$

The characteristics derived for equal stagnation temperatures $T_o' = T_0''$, can be used when the parameter U is replaced by $U\sqrt{\frac{T_0''}{T_o'}}$.

2.2 Review of ejector models

A typical ejector is composed of two major components, a primary nozzle and a mixing chamber. The mathematical models of ejectors can be classified into two theories based on the shapes of the mixing chamber, *"constant-pressure mixing ejector"* and *"constant-area mixing ejector"*.

2.2.1 Constant area ejector model

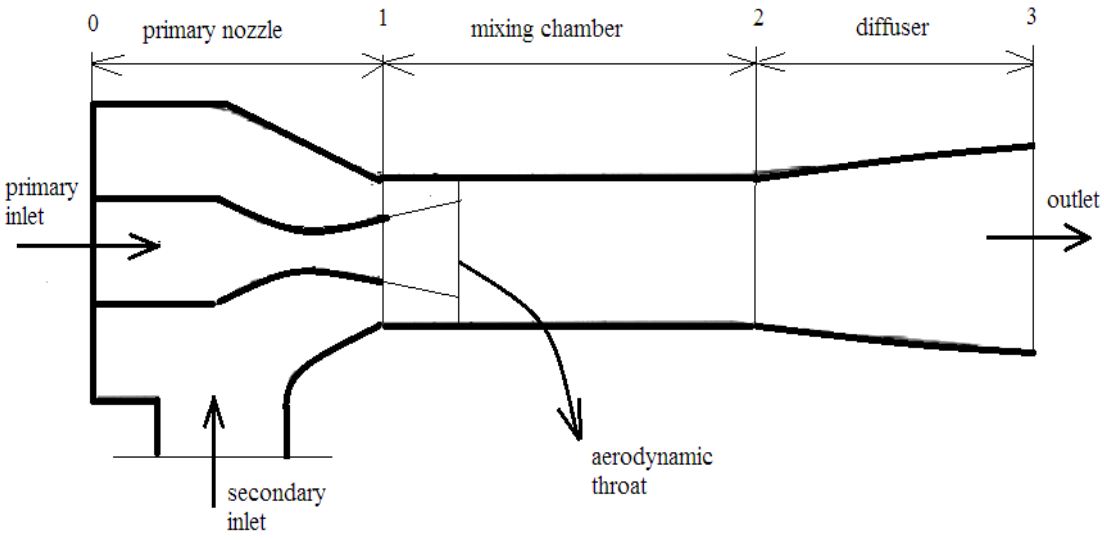

Fig. 2.6: Constant-area mixing model of ejector.

Fig.2.6 shows a schematic diagram of constant-area ejector model. For this mixing model, the primary nozzle exit is placed within the constant-area section of the mixing chamber. The mixing process takes place within the constant-area section of ejector. The primary stream expands against the secondary stream and an aerodynamic throat is formed somewhere downstream the mixing chamber (Fabri and Siestrunck,1958). Thus, primary stream behaves as an aerodynamic nozzle for the secondary stream and secondary stream could be chocked at aerodynamic throat if the downstream pressure is low enough.

2.2.1.1 Assumptions of constant area mixing model

The constant-area ejector mixing model is based on following assumptions:

1. Both streams are in steady state.

2. Both streams at section 1 are uniform and are completely mixed at section 3.

3. Both streams are considered as perfect gases.

4. The inner wall between section 1 and 3 is considered adiabatic.

5. The secondary steam is chocked at section 2.

2.2.2 Constant pressure ejector model

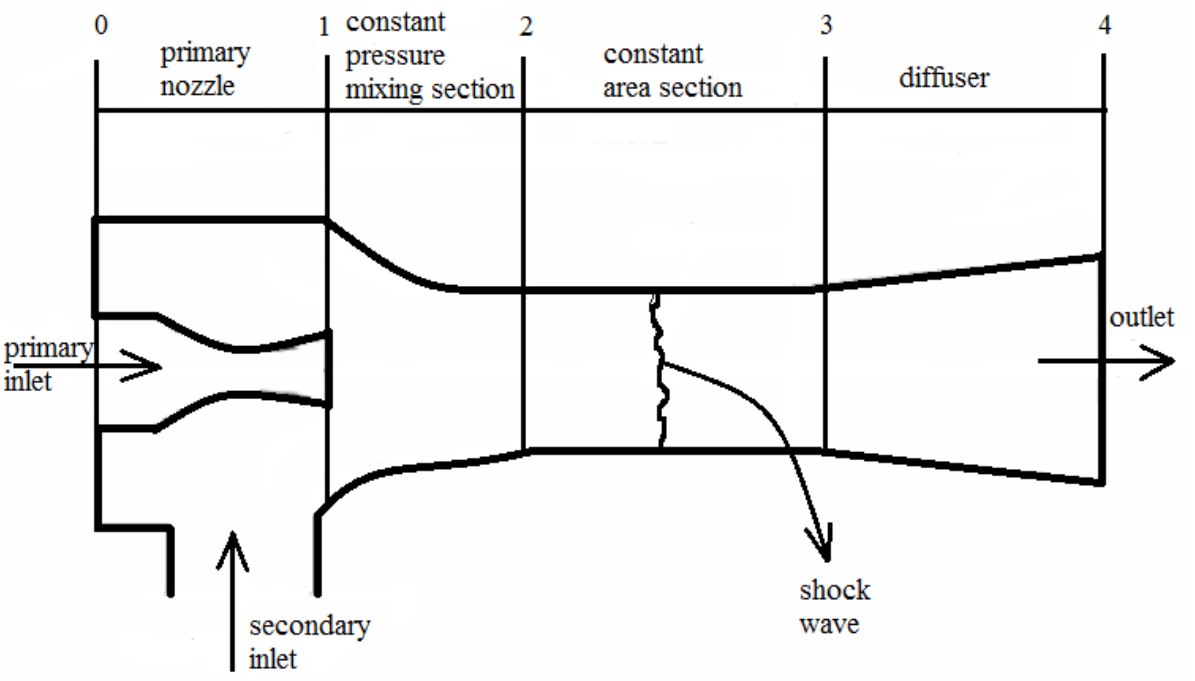

Fig. 2.7: Constant-pressure mixing model of ejector.

Fig. 2.7 shows the schematic diagram of constant-pressure mixing model. Constant-pressure mixing ejector has its nozzle exit position placed in a convergent chamber upstream of the constant-area section, the static pressure through the mixing process is assumed to be constant.

2.2.2.1 Assumptions of constant-pressure mixing model.

The constant-pressure ejector mixing model is based on following assumptions:

1. Both streams are at inlet and mixed flow at outlet of ejector, are considered to be at stagnation conditions.

2. Velocities are uniform at all sections.

3. The two streams are mixed at constant pressure between sections 1 and 2.

4. The mixed flow is supersonic at section 2.

5. A shock wave occurs between sections 2 and 3 and the flow is subsonic at 3.

2.2.3 Mathematical models

Keenan *et al.* (1950) presented a 1- dimensional model of ejectors. They developed two models each for mixing of primary and secondary flow at constant pressure and constant area. They used a set of five basic equations to model both ejectors *i.e.* momentum equation, continuity equation, energy equation and perfect gas relations. Keenan was able to reasonably predict the ejector performance characteristics firstly for constant area mixing ejectors then also for constant pressure mixing ejectors. Furthermore they concluded that constant pressure ejector model shows better performance. This later became a classical theory.

Munday and Bagster (1977) indicated that the primary flow fans out without mixing with the second flow after discharging from the nozzle exit, and a steam ejector model was developed by defining a fictive throat effective area. They modified the Keenan theory to account for loss coefficients at the primary nozzle, the mixing chamber and the diffuser. They also performed experimentation on a steam jet refrigeration system.

Aphornratana and Eames (1994) performed experiments on a small scale steam ejector refrigerator using ejector with adjustable primary nozzle and showed that a single optimum primary nozzle position cannot be defined to meet all operating conditions.

Huang *et al*. (1999) developed a 1-dimentional mixing model of ejector performance at critical-mode operation. Constant-pressure mixing was assumed to occur inside the constant-area section of the ejector and the entrained flow at choking condition was analysed. They also carried out an experiment using 11 ejectors and R141b as the working fluid to verify the analytical results. To account for non-ideal process, the effects of frictional and mixing losses were taken into account by using some coefficients introduced in the isentropic relations. This allowed authors to design an ejector, including the effect of supersonic shock such that model and experimental data generally agreed within about 10% and showed that the model can accurately predict the performance of the ejectors.

El-Dessouky *et al*. (2002) developed semi-empirical models for design and rating of steam jet ejectors. The model gives the entrainment ratio as a function of the expansion ratio and the pressures of the entrained vapour, motive steam and compressed vapour. Correlations were developed for the motive stream pressure at the nozzle exit as a function of the evaporator and condenser pressures and the area ratios as a function of the entrainment ratio and the stream pressures. This model included correlations for the choked flow with compression ratios above 1.8. In addition, a correlation was provided for the non-choked flow with compression ratios below 1.8.

The idea of designing an ejector with minimum losses from normal shock was proposed and named 'the Constant Rate of Momentum Change method, (CRMC) by Eames (2001). CRMC provided a way to gradually increase the static pressure of the mixed flows entry to exit while passing through the ejector. The CMRC method produced a diffuser geometry that removes the thermodynamic shock. Without the shock, therefore, there is no stagnation pressure loss. Author claimed that the pressure lift ratio of the CRMC ejector was increased while the entrainment ratio remained unchanged. However, it was found that the ejector lost it function if the throat diameter was too small.

Ouzzane and Aidoun (2003) developed one dimensional mathematical model and computer programs for ejector studies in refrigeration cycles. The model analysed compressible refrigerant flow, based on a forward marching technique of solution for the conservation equations. The entrainment ratio, the compression ratio and geometric parameters such as diameters and axial dimensions were used to assess performance. Authors concluded that local distributions of pressure, temperature and mach number can be obtained for typical conditions and the mixing chamber greatly influenced the operation and performance, by controlling the shock wave occurrence and intensity. Model predictions for ejector sizing and operation were compared with available experimental data and a fairly good agreement was obtained.

Chunnanond and Aphornratana (2004) provided a literature review on ejectors and their applications in refrigeration. A number of studies were grouped and discussed under several topics, *i.e.* background and theory of ejector and jet refrigeration cycle, performance characteristics, working fluid and improvement of jet refrigerator. They also discussed selection of appropriate working fluid. Moreover, other applications of

an ejector in other types of refrigeration system were also described. They concluded that new assumptions on mixing and flowing characteristic were always established and applied on the mathematical model and computer simulation analysis.

Riffat *et al.* (2005) presented a review of studies carried out on ejectors and their applications during the period of 1995 to 2005. The performance of ejectors had been carefully considered theoretically and by experiment. The use of water, halocarbon compounds and working pairs such as LiBr-H_2O were reviewed. The use of different heat sources *e.g.,* solar energy, and low-grade energy were discussed. This included the use of combined systems *i.e* solar-powered ejector refrigeration systems, absorption ejector hybrid refrigeration systems, adsorption-ejector systems, and ejector-mechanical compressor systems.

Liu and Groll (2008) presented an analysis of a two phase flow controllable ejector for the transcritical CO_2 cycle to determine the efficiencies of the motive nozzle, suction nozzle, and mixing section using measured data. Authors pointed out that motive nozzle efficiency decreases as ejector throat area decreases and that the suction nozzle efficiency is affected by the outdoor temperature and ejector throat area. Moreover, the distance between the motive nozzle exit and the mixing section constant area entry not only affects the suction nozzle efficiency, but also affects the mixing section efficiency.

Elbel and Hrnjak (2008) provided an overview of historical and recent developments regarding air-conditioning and refrigeration systems that use ejectors. They studied more than 150 papers in the open literature and important findings and trends were summarized. The authors discussed early invention, use of ejectors in various systems and utilization of low grade heat to operate ejectors. Another major field, expansion work recovery by two-phase ejector, was described. Moreover, authors described various ejector flow theories to point out the importance of flow choking and shock wave phenomena. However, they pointed out significantly less literature is available on the topic of two-phase ejectors which can be used to recover expansion work. While many of the flow theories and design guidelines developed for single-phase ejectors should be transferable to two-phase ejectors, a number of significant differences exist.

Bruce (2009) proposed a developed a one-dimensional ejector model draft of ejector modelling in HYSYS. However his ejector was only applicable in the design case. It did not include sizing data which was necessary for rating calculations. This ejector simulation had four parameters that need to be specified in addition to the inlet stream conditions

Boumaraf and Lallemand (2009) developed a simulation program includes a correlation of the ejector entrainment ratio established in different operating conditions at critical point from the conservation equations of the 1-D constant-area mixing model available in the previous literature. All the components of the system were dimensioned for a refrigerating power of 10 kW. Authors investigated system performance dimensioning conditions and in off-dimensioning conditions for refrigerants R142b and R600a.The results showed that the system COP decreases when the hot source temperature is higher than that of its dimensioning. Also, it was noted that R142b leads to better performance of the system in all cases.

Zhu and Li (2009) made modifications to the first is the Shock circle model (Zhu, 2007), to better account for the boundary layer secondary flow in the mixing chamber prior to mixing. The novel ejector model was proposed for the performance evaluation on ejectors with both dry and wet vapour working fluids at critical operating mode. A simple linear function was defined in order to approach the real velocity distribution inside the ejector. Experimental data from different ejector geometries and various operation conditions reported earlier were used to verify the effectiveness of the new model. Results show that the model had a good performance in predicting the mass flow rates and the entrainment ratio for both dry and wet vapour ejectors. It contained only one energy conservation equation and was independent of the mixing chamber and the diffuser.

Ma *et al.* (2010) experimentally investigated the use of variable geometry ejectors in novel steam jet refrigerator suitable for solar energy applications. The primary flow of the ejector was controlled using a spindle in order to provide fine tuning and for ejector operation as well as optimum coefficient of performance. The nominal 5 kW steam ejector with a generator temperature of 90^{o}C was designed. The influence of the spindle position, and the boiler temperature, as well as that of evaporating temperature

on the performance of the ejector was assessed. They concluded that there exists an optimum entrainment ratio and COP related to optimum ejector area ratio.

Valle *et al.* (2012) proposed a new one-dimensional model approach for the evaluation of the entrainment ratio of double choked ejectors. The model was based on a perturbation procedure of linearized and axisymmetric supersonic flow. This model was evaluated against experimental results and average deviation of model entrainment ratio with respect to experimental data was of the order of 7%.

Antonio *et al.* (2012) developed a thermodynamic model of one-dimensional flow inside ejector to study the dimensioning of the cylindrical mixing chamber of ejector used in particular in sugar refineries for degraded vapour re-compression, during the evaporation phase. Characteristic curves and envelope curves plotted are an interesting tool from which the characteristic dimensions of the ejector can be rapidly obtained for preliminary dimensioning. These ejectors were specifically designed for the process rather than selected from a catalogue of standard devices. They obtained a fair agreement for more than three hundred steam ejectors with a discrepancy between calculation and measurements of less than 5% and suggested that this method could be exploited for the dimensioning of compressible fluid ejectors with a conical mixing chamber.

Zhu *et al.* (2014) proposed a new type of dual-nozzle ejector enhanced vapour-compression cycle (DEVC) for solar assisted air source heat pump systems. They tested the model for refrigerant R410A for the range of given operating conditions, and indicated that the COP and volumetric heating capacity of the novel cycle using were theoretically improved by 4.60-34.03% and 7.81-51.95% over conventional ejector enhanced vapour-compression cycle (CEVC), respectively. These results implied that the solar-air source heat pump systems could take advantage of the best features of the DEVC.

2.2.4 Numerical Models (CFD)

With advances in hardware computational capability, computational Fluid Dynamics (CFD) has matured over the last decade allowing researchers to examine the ejector processes in far greater detail for effects of supersonic shock, real gas behaviour, metastable refrigerant states, boundary layer flow and flow separation *etc*.

Perhaps the most important factor in CFD analysis of ejectors is the selection of a turbulence model. It has been found that the standard k-e turbulence model is inadequate for describing expanding supersonic jets. Researchers have indicated that the hybrid k-e-sst model offers good results.

The results of CFD studies are fairly in agreement with experimental data for entrainment ratios but limited to double chocking condition only. Despite this CFD models are not able to predict the performance of ejectors for off design conditions. Insights into real ejector flows are provided by advanced visualisation techniques and will become important as a means to verify CFD predictions.

Sriveerakul *et al.* (2007, Part1) investigated performance of a steam ejector used in refrigeration applications by the use of CFD. The effects of operating conditions and geometries on its performance were investigated. Average errors of the predicted entrainment ratio and the critical back pressure were both found to be less than −7%.

Sriveerakul *et al.* (2007, Part2) presented a study after validation in Sriveerakul et *al.*(2007, Part1) to analyse the flow phenomena inside the steam ejector when its operating conditions and geometries were varied. The flow structure of the modeled ejectors was created graphically, and the phenomena inside the flow passage were explored. Their results show that the effective area as proposed by Huang (1999) does exist. Two series of oblique shocks were found in the simulation. The first series was found immediately after the primary fluid stream leaves the primary nozzle and begins to mix with the secondary fluid stream. The second series of oblique shock was found at the beginning of the diffuser section as a result of a non-uniform mixed stream.

Vargaa *et al.* (2009) used an axis-symmetric CFD model to determine ejector efficiencies for the primary nozzle, suction, mixing and diffuser. The authors considered water as working fluid and the operating conditions were selected in a range that would be suitable for an air-conditioner powered by solar thermal energy. Influence of ejector area ratio was studied which indicated there exists an optimal ratio, depending on operating conditions. Ejector efficiencies were calculated for different operating conditions. It was found that while nozzle efficiency can be considered as constant, the efficiencies related to the suction, mixing and diffuser sections of the ejector depend on operating conditions.

2.3 Review of ejector enhanced vapour compression systems

In 1989 Sokolov and Hershgal (1989) proposed a combined cycle between a ejector refrigeration system and a conventional mechanical compression system, as shown in Fig.1.3, ameliorating the main limitations of each technology. On one side, the ejector system opens its application range and increases its efficiency. On the other hand, the vapour compression refrigeration system reduces its electrical energy requirements.

This attracted many researchers and many works have been carried out in order to further investigate the possibility of improving the system

Few years later, Sun (1997) theoretically investigated hybrid ejector-compression refrigeration system, which used different refrigerant for each subsystem; water and R134a were used as working fluids for the ejector refrigeration system and the vapour compression refrigeration system respectively. The system used low grade energy sources with 80 ºC generator temperatures and was designed for air conditioning applications. Very high COP values between 4 and 6.8 were obtained as author did not consider cost of solar energy and only considered the electrical energy utilized. This resulted in reduction of electrical energy consumption by 50%.

Sun (1998) performed a comparative study of the effect of using different working pairs in a HJCRS system (Sun, 1998a, b). Refrigerant R718, the CFC's R11, R12, R113, the HCFC's R21, R123, R142b, the HFC's R134a, R152a, the organic compound RC318 and the azeotrope R500 were evaluated for both upper and lower stage. A refrigerant pair selection strategy was developed. R718 (water) for ejector

system and R21 for compression gave the best results, reaching an overall COP of over 0.7.

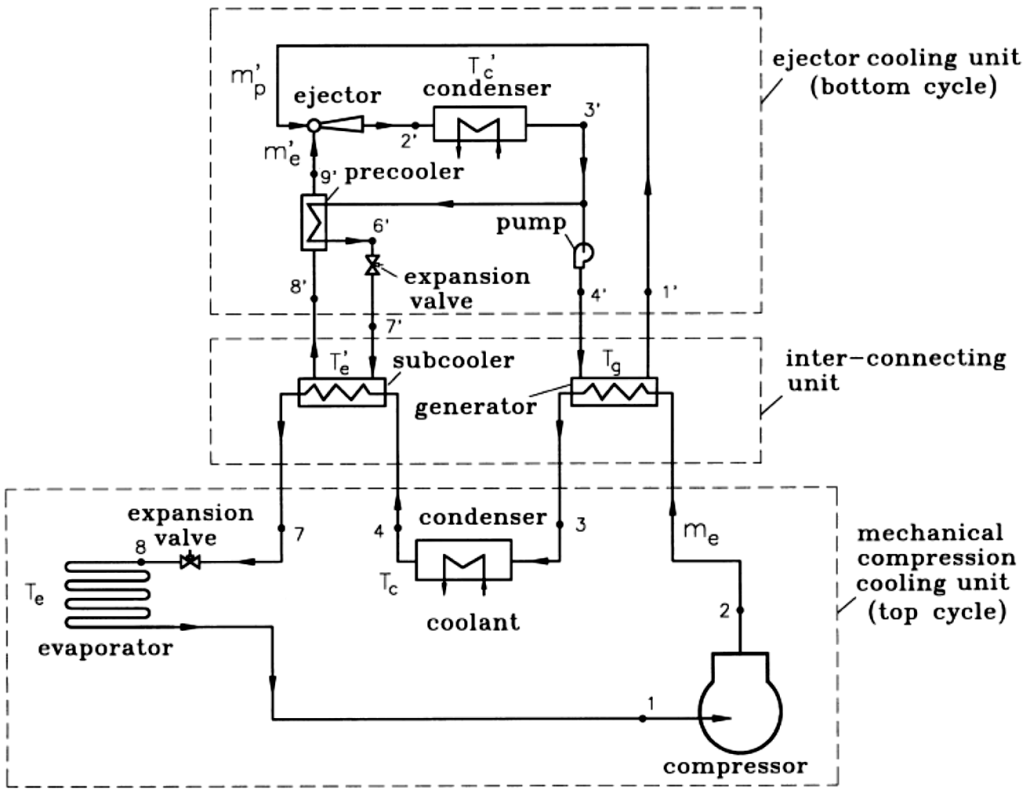

Fig. 2.8: Hybrid system with ejector cooling system as bottoming cycle. (Huang *et al.*,2000)

An interesting configuration was developed by Huang et *al.* (2000) as shown in Fig. 2.8 that utilized waste heat from the vapour compression cycle to drive ejector compression system and acts as a bottom cycle of the hybrid system. Refrigerant R141b was used in both subsystems and was designed for air conditioning applications. For the simulation and design, they used their own ejector model previously developed. The study concluded that COP improvement over conventional compression system was 18.4% for the evaporating temperature T_e= -5^{o}C and for T_e =5^{o}C COP was be improved by 24%. Authors stressed that using ejector cycle as bottom cycle in hybrid system is more viable.

Arbel and Sokolov (2004) presented a theoretical study of a solar driven hybrid compression-ejection refrigeration system using R142b as working fluid. The authors compared the performance of the system with previous studies developed by Sokolov,

where R114 was used. The new system not only accounted for technical improvements but also ecological improvements. The optimization process, in which the best operating conditions for a given system are achieved, were discussed. Authors only varied generator temperature, for optimization and indicated that system will have maximum efficiency at the optimized Tg. The overall COP obtained was 5.

Herna´ndez *et al*. (2004) presented a theoretical comparative study comparing of R134a and R142b in a hybrid compression-ejection system. The system was designed for ice production applications. The effect of generator, condenser and intercooler pressure on system performance was evaluated. For unitary cooling capacity of 1 kW with evaporator temperature of 10^{O}C and moderate condenser and generator temperatures of 30 and 85^{O}C, respectively were taken. With theses working temperatures R134a had the best operation with a highest coefficient of performance of 0.48 and an exergy efficiency of 0.25 was achieved. On the other hand, for higher condenser temperatures R142b showed better performance. Authors pointed out, working fluid in the ejector subsystem is determinant of system performance. Nevertheless, it is important to point out that this refrigerant was employed for the very high condenser temperatures managed in air cooled systems or heat pumps.

Elakdhar *et al.*(2007) made a theoretical study of hybrid compression-ejection system for domestic refrigeration. The behaviour of the system with different working fluids (R123, R124, R141b, R290, R152a, R717, R600a and R134a) was studied. This system configuration did not have an intercooler; the exit of the ejector was connected to the entrance of the compressor, as shown in Fig. 2.9. The results of study indicated that there exists an inversely proportional relation between the COP and the decrement of the secondary evaporator temperature. They obtained the best results for R141b with COP improvement of 32% over conventional cycle.

Vidal and Colle (2010) carried out the simulation and thermo-economic optimization of a hybrid compression ejection system. R134a and R141b were used for compression and ejection system respectively. Solar energy was used as the driving source for ejector system for a 10.5 kW cooling capacity system .The results showed solar fraction of 82% with 105 m^2 of flat plate collector and overall COP of 0.89 was reached. The authors discussed the importance of the proper selection of system components to obtain adequate payback periods.

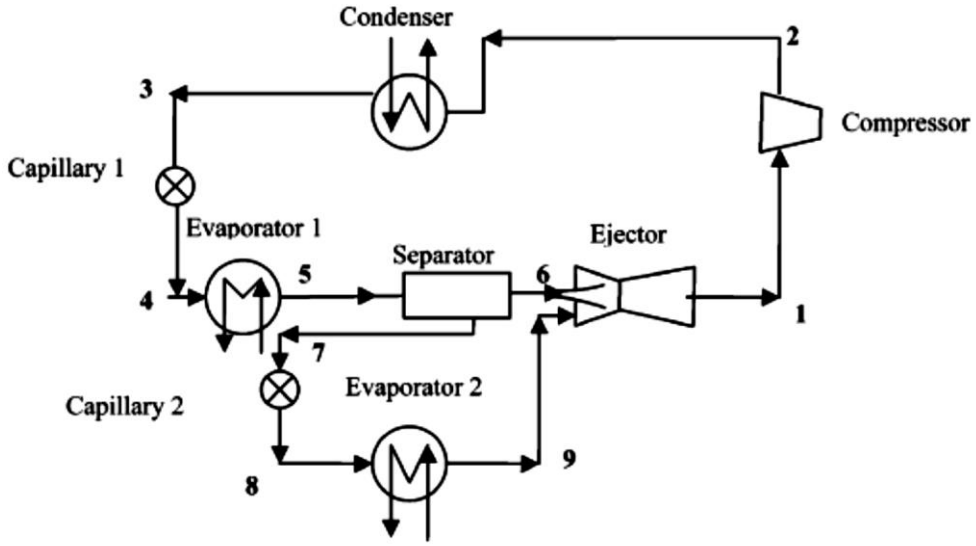

Fig. 2.9: Hybrid compression ejection system with two evaporators. (Elakdhar *et al.*, 2007)

Petrenko *et al*. (2011) investigated the performance of a trigeneration system that consisted of a cogeneration subsystem and a hybrid cooling subsystem using R744 (CO_2) and R600 (butane) as working fluids, respectively. The system was developed for a capacity of 10 kW performance was analysed over wide ranges of critical condensing temperatures Tc= 28-40^oC, and generating temperatures Tg of 80, 100, 120,140^oC at the fixed evaporating temperature of 14^oC.They reached a COP of 1.4 under design conditions.

Zhu and Jiang (2012) proposed a new configuration that utilized the waste heat of basic compression system to drive the ejector as shown in Fig.2.10. Results indicated that the COP shows significant improvement at compressor discharge temperature larger than 100 ºC. With R152a COP was increased by 5.5% over the basic system and by 8.6% with R22. The average COP increase with R134a was about 0.7% due to low compressor discharge temperature 70-90 ºC.

Suhas and Deshmukh (2013) investigated the hybrid configuration developed by Zhu and Jiang (2012) for R600a. Results indicated an increase in COP by 3.086% over conventional system. They also pointed out that the ejector is the key component of the hybrid refrigeration system. The ejector geometries and operating conditions greatly influence the ejector performance and refrigeration system as a whole, and

therefore ejector area ratio need to be carefully designed to optimize the hybrid refrigeration system for the best performance.

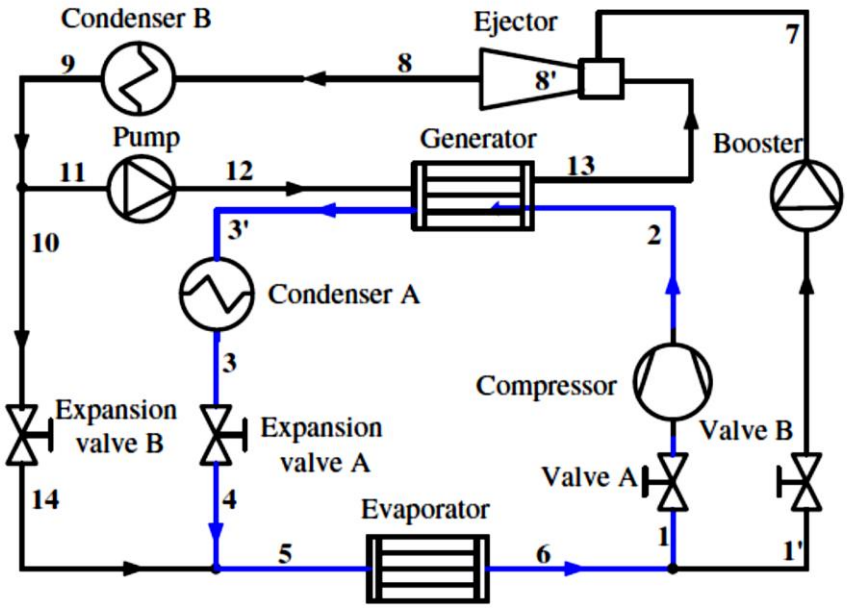

Fig. 2.10: Hybrid system driven by waste heat at compressor outlet.
(Zhu and Jiang ,2012; Suhas and Deshmukh ,2013)

The operating and performance parameters of combined ejector- compression cycles studied by various researchers in past are summarised in table 2.1

Table 2.1: Operating and performance parameters of combined ejection compression cycles from 1989 to 2013

Author(year)	**Refrigerant**	**Temperature(°C)**	**Cooling capacity(kW)**	**Total COP**	**Nature of study**
Sokolov and Hershgal (1989)	R114	Tevap = -8 Tint= NA Tcond= 30 Tgen = 86	2.9	0.4	Experimental
Da-Wen Sun *et al.* (1996)	LiBr-R717	Tevap = 10 Tint =NA Tcond = 22 Tgen = 210	NA	1.8	Theoretical
Da-Wen Sun (1997)	R718 and R134a	Tevap =5 Tint = 25 Tcond = 35 Tgen = 80	5	5	Theoretical
Da-Wen Sun (1998 a,b)	R21 and R718	Tevap = 5 Tint = 30 Tcond = 40 Tgen = 70	NA	0.65	Theoretical
Huang *et al.* (2001)	R141b and R22	Tevap = 5 Tint = 25 Tcond = 40 Tgen = 70	5.2	2.5	Experimental
Arbel and Sokolov (2004)	R142b	Tevap = 4 Tint = 38 Tcond = 50 Tgen = 100	3.5	5	Theoretical
Herna´ndez *et al.* (2004)	R134a and R1142b	Tevap=-10 Tint= NA Tcond= 30 Tgen = 85	1	0.48	Theoretical

Elakdhar *et al.* (2007)	R123, R124, R141b, R290, R152a, R717, R600a and R134a	Tevap1= 5 Tevap2 = -30 Tcond = 42 Tgen = NA	NA	1.38	Theoretical
Petrenko *et al.* (2011)	R744, R600	Tevap = -20 Tint = 20 Tcond = 36 Tgen = 120	10	1.4	Theoretical
Vidal and Colle (2010)	R134a, R141b	Tevap = 8 Tint = 19 Tcond= 34 Tgen = 80	10.5	0.89	Theoretical
Yinhai Zhu, Peixue Jiang (2012)	R134a, R152a, R22	Tevap = -5 Tint =NA Tcond=50 Tgen = 82.55	5.99	2.40	Theoretical
Kshirsagar,D.S., Deshmukh,M.,M. (2013)	R600a	Tevap = -5 Tint =NA Tcond=50 Tgen = NA	NA	0.397	Theoretical

Chapter 3

Mathematical modelling and Simulation

3.1 Cascade refrigeration systems

Low temperature cooling has become indispensible for various medical, chemical and industrial applications. To achieve such low temperature and maintain the pressure of the system within reasonable limits, two refrigeration cycles that use two different refrigerants are linked through a heat exchanger. The lower cycle is used to achieve cooling at low temperature by absorbing heat from the refrigerated space. Lower cycle rejects heat to the upper stage through a heat exchanger, while the upper cycle is hot and can reject heat to a very hot reservoir. This configuration has an advantage of using two different refrigerants over multi pressure systems.

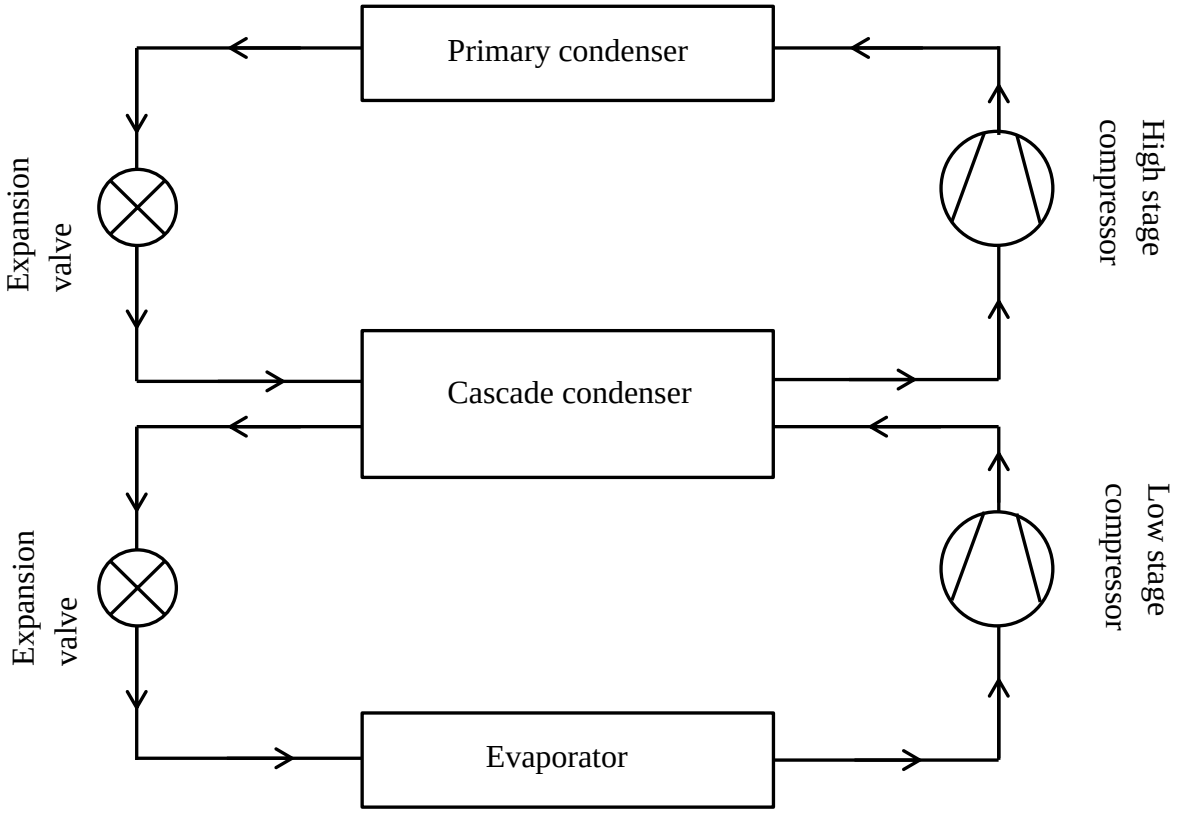

Fig. 3.1: Schematic diagram of cascade refrigeration system

Fig.3.1 shows the schematic of a simple cascade system the refrigerant in lower stage absorbs heat in the evaporator and is compressed to cascade condenser pressure. In cascade condenser the lower stage rejects heat which is absorbed by refrigerant in upper stage. The liquid refrigerant is expanded in expansion valve to evaporator pressure and lower cycle is complete, whereas refrigerant from the cascade condenser rejects heat to environment after being compressed in high stage compressor.

Cascade systems have many important applications like liquefaction of petroleum vapours and industrial gases, manufacturing of dry ice, deep freezing etc.

3.2 Ejector enhanced multi evaporator cascade refrigeration system (EEMECRS)

In conventional cascade refrigeration system, entire cooling load is carried by a single evaporator, but in many refrigeration application such as medical industry different temperature are required to be maintained for different applications. In, such cases each location needs to be cooled by its own evaporator in order to obtain a more satisfactory control of condition. In present study a configuration is developed to obtain low temperature cooling at three different levels by cascading lower multi evaporator stage to a higher temperature upper stage through an inter cooler. The upper stage is a two evaporator system, one evaporator acts as intercooler and absorbs heat from the lower stage, and the other evaporator kept at a relatively higher temperature and is designed for air conditioning of living spaces. The system is specifically designed to meet the needs of medical industries that require low temperature cooling at different level and also require air conditioning for working spaces. An improvement to this configuration is proposed by incorporation of ejectors into the latter system. The incorporation of ejectors in the system allows for recovery of pressure ratio reducing the compression work of compressor and thereby increasing the COP of system (EEMECRS) over unenhanced multi evaporator cascade refrigeration system (UMECRS).

Fig. 3.2 and Fig. 3.3 presents schematic diagram of unenhanced multi evaporator cascade refrigeration system (UMECRS) along with the P-h diagram respectively. In the proposed EEMECRS, the back pressure valves in the upper and lower stage of UMECRS are replaced by three ejector devices. This configuration increases the suction pressure reducing specific compressor work.

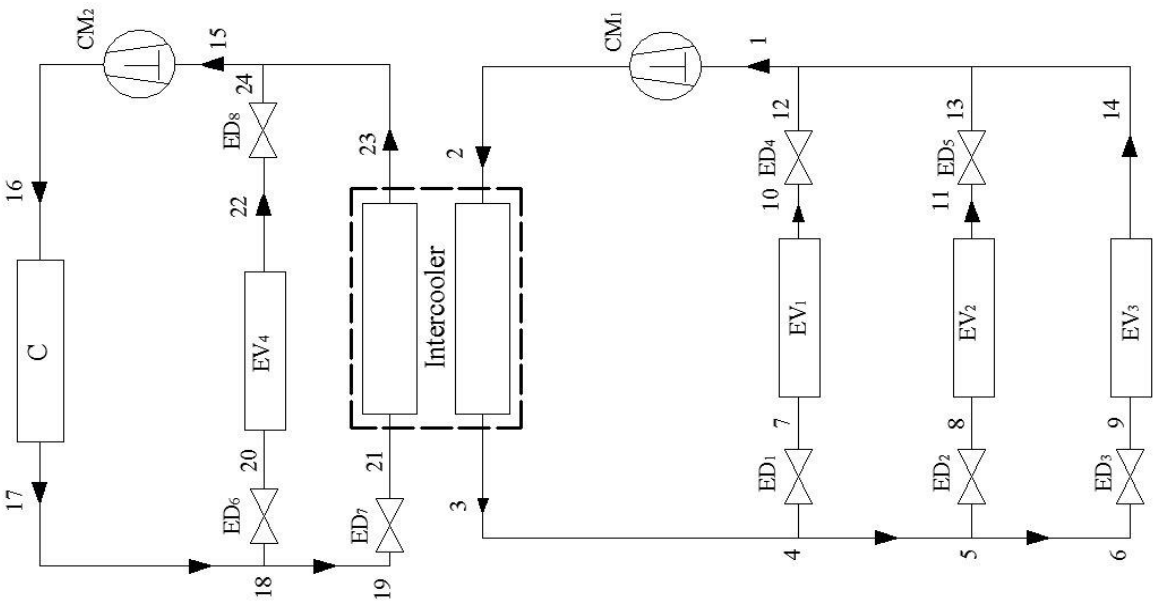

Fig. 3.2: Schematic diagram of unenhanced multi evaporator cascade refrigeration system (UMECRS)

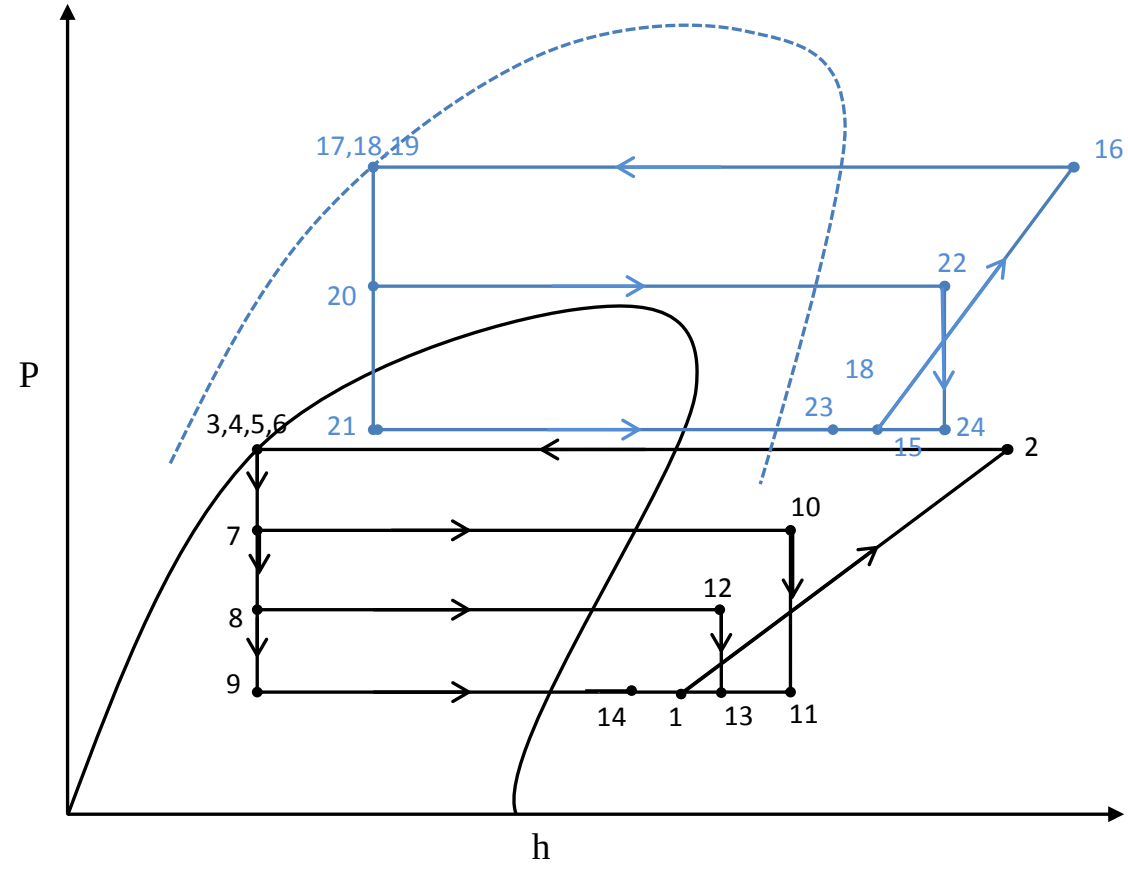

Fig. 3.3: P-h plot of unenhanced multi evaporator cascade refrigeration system

3.3 System description

Fig. 3.4 and Fig. 3.5 presents schematic diagram and P-h chart respectively for ejector enhanced multi-evaporator cascade refrigeration system (EEMECRS).

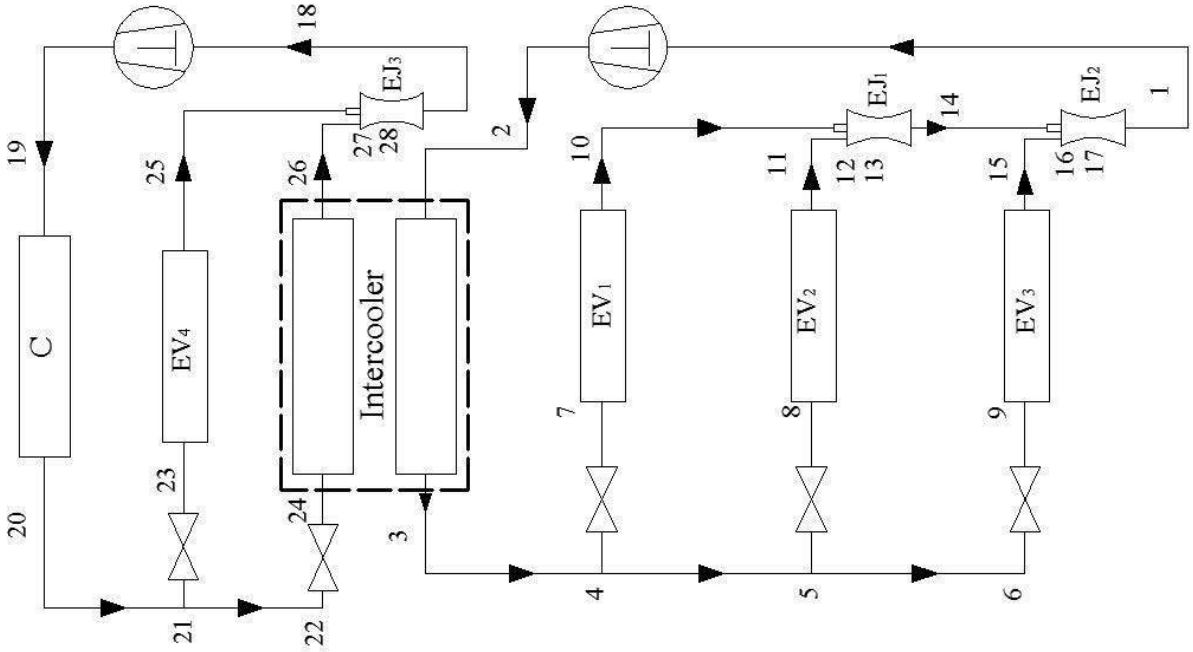

Fig. 3.4: Schematic diagram of ejector enhanced multi evaporator cascade refrigeration system (EEMECRS)

The arrangement consists of two stages interconnected through a heat exchanger called intercooler. The lower stage used to achieve cooling at low temperatures has three evaporators EV_1, EV_2 and EV_3 operating at different temperatures with individual expansion valves and a single compressor. The upper stage is a two evaporator system with individual expansion valves and a single compressor. The evaporator at lower pressure is designed to absorb heat from the lower stage while the other evaporator at relatively higher temperature is designed for catering the needs of air conditioning applications. In the lower stage, the two back pressure valves as shown in Fig. 3.2 are replaced by two ejectors EJ_1 and EJ_2 and for the upper stage backpressure valve is replaced by a single ejector EJ_3 (Fig. 3.4).

Referring to Fig. 3.4, low pressure (P_L) refrigerant at state point (1) enters the compressor 1 and is compressed to high side pressure (P_H) at state point (2).The fluid enters the intercooler which acts as condenser for lower stage and one of the evaporators for upper stage. Heat rejected by the lower stage is absorbed by upper

stage at intermediate temperature and refrigerant in lower stage condenses to state point (3).

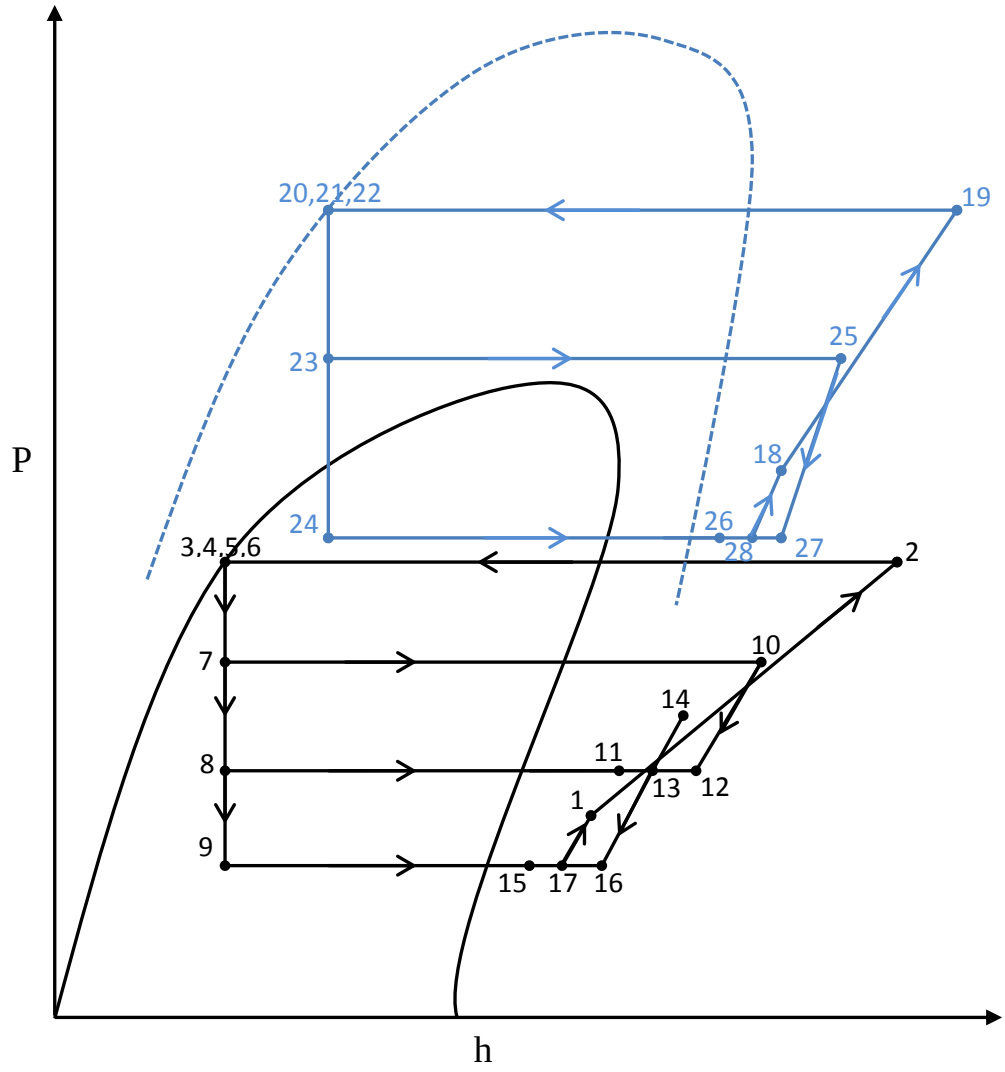

Fig. 3.5: P-h plot for ejector enhanced multi evaporator cascade refrigeration system (EEMECRS)

The condensate is divided into three parts, state points (4), (5) and (6) and is passed to corresponding evaporators through individual expansion valves. One enters the evaporator 1 after a pressure reduction in the individual expansion valve 1, state point (7), the other enters the evaporator 2 after a pressure reduction in the individual expansion valve 2, state point (8) and the last enters the evaporator 3 after a pressure reduction in the individual expansion valve 3, state point (9). The refrigerant coming from individual expansion valve 1 enters the evaporator 1 and draws heat from the refrigerated space coming out at superheated state (10). The refrigerant coming from individual expansion valve 2 enters the evaporator 2 and draws heat from the

refrigerated space coming out at superheated state (11). The fluid entering the evaporator 3 is vaporised from state (9) to superheated state (15). The flow at state (10) enters ejector 1 (EJ_1) primary nozzle and expands to a mixture at state (12). The superheated secondary vapour enters the ejector (EJ_1) at pressure P_{ev2} corresponding to state (11). The two vapours mix in the ejector corresponding to state (13). The mixture then flows through diffuser of (EJ_1) where it recovers to pressure Pej_1 at state 14. The mixture vapour leaving the ejector 1 at state (14) enters the primary nozzle of the ejector 2 (EJ_2) entraining vapour into the ejector 2 from evaporator 3 and expands to state (16). The two vapours mix to state (17) and leave the ejector 2 after a recovery of pressure Pej_2 in the diffuser part at state (1) and thereby completing the cycle for lower stage.

For the upper stage, refrigerant vapour enters the compressor 2 at state point (18) and is compressed to the condenser pressure at state point (19). The superheated refrigerant enters the condenser rejecting heat to the surrounding and the liquid condensate at state point (20) is divided into two parts. One part after expansion through individual expansion valve enters the evaporator 4 drawing heat from the refrigerated space and comes out at superheated state (25), while the other part of fluid after expansion through individual expansion valve is passes through the intercooler absorbing the heat rejected by lower stage and coming out at superheated state (15). The fluid at state point (25) enters the ejector 3(EJ_2) primary nozzle and expands to a mixture state (27), the superheated secondary fluid from the intercooler (26) enters the ejector through secondary inlet. The two streams mix in the ejector corresponding to state point (28) and after passing through diffuser of (EJ_3) , the mixture comes out (18) after recovery of pressure Pej_3.

3.4 Mathematical modelling

3.4.1 Ejector

Fig. 3.6 represents the schematic of constant area ejector .The refrigerant vapour at high pressure enters the ejector primary convergent-divergent nozzle causing it to expand and thereby creating a pressure depression for entraining low pressure refrigerant vapour at secondary inlet. The two streams come in contact in the mixing chamber before passing through the diffuser where the pressure recovery takes place.

The dimensions of various parts forming the nozzle, the suction chamber, mixing chamber and diffuser, together with fluid flow rate and properties define ejector capacity and performance. Some basic definitions related to ejector performance are described below:

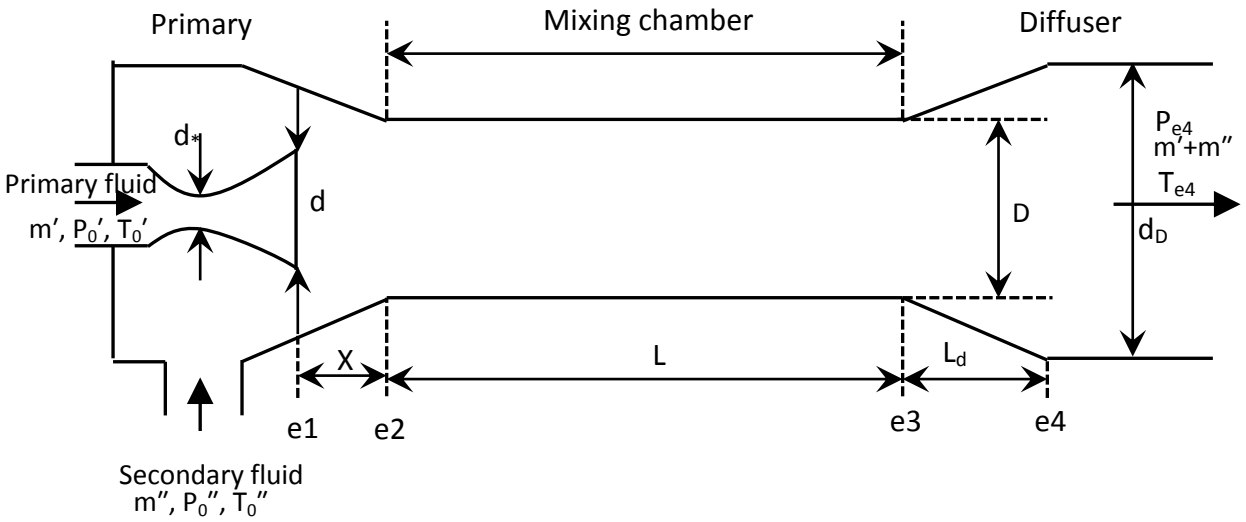

Fig. 3.6: Schematic of constant area ejector with reference stations.

1. Entrainment ratio, U: It is the ratio of flow rate of entrained vapour to the flow rate of motive vapour.

2. Expansion ratio, Γ: It is defined as the ratio of the motive fluid vapour pressure to the entrained fluid vapour pressure.

3. Compression ratio, r: It is the pressure ratio of compressed mixed flow to the entrained flow.

4. Driving pressure ratio, ξ: It is defined as the ratio of motive vapour pressure to back pressure.

5. Ejector area ratio, Ø: It is defined as the ratio of area of mixing chamber to the throat area of primary nozzle.

6. Diffuser area ratio, Ω: It is defined as the ratio of area of diffuser outlet to diffuser inlet.

7. Temperature ratio, θ: Ratio of secondary fluid stream temperature to primary stream.

There are three different operating regimes of a constant area ejector (Le Grives and Fabri, 1969; Ubelhack, 1972) classified on the basis of dependence of ejector entrainment ratio on the back pressure or driving pressure ratio (ζ). These regimes are the supersonic regime (SR), the transition regime (TR) and the mixed regime (MR). In supersonic regime the primary fluid pressure at section e1 as shown in Fig. 3.6, is higher than that of secondary fluid. The primary expands against the secondary fluid and somewhere down the mixing chamber an aerodynamic throat is formed which causes the velocity of secondary stream to reach supersonic speed. As a result of secondary stream chocking, the secondary mass flow rate becomes independent of the back pressure. The mixed regime (MR) accounts for all cases for which secondary fluid is not be chocked. In such case the secondary stream cannot reach the sonic speed within the mixing chamber and therefore secondary mass flow rate is dependent on back pressure. In transition regime (TR) the secondary fluid reaches the supersonic speed at the point of conjunction of two streams and this gives the optimum performance of ejector (Nahdi *et al.*, 1993). For this reason, the present study will analyse the ejector in TR. The mathematical model for constant area ejector in TR developed by Kairouni *et al.*(2009) is modified to account for losses in nozzle and such that it could be applied to EEMECRS operating with several refrigerants.

The following assumptions are made for the analysis:

1. The flow inside the ejector is steady and one-dimensional.

2. The working fluid is an ideal gas with constant properties Cp and k.

3. For simplicity in deriving the 1-D model, the isentropic relations are used before mixing.

4. The two fluids are completely mixed at the exit of the mixing chamber.

5. $X \neq 0$.

With $X \neq 0$ the flow in convergent part is sonic which implies that the aerodynamic throat is situated at the entry of the mixing chamber. So, we deduce that, for TR with a distance $X \neq 0$

$$M''_{e2} = 1 \tag{24}$$

To form the sonic throat of the secondary fluid at the section e2, the motive fluid must expand against secondary flow, which imposes $P'_{e2} > P''_{e2}$. After the section e2, we can only have $P'_{e2} > P''_{e2}$, since the case $P'_{e2} < P''_{e2}$is physically impossible. For the condition $P'_{e2} > P''_{e2}$, the primary fluid is going to continue to expand, the sonic throat is situated then downstream the section e3 and the regime becomes supersonic. Therefore, the TR is characterized by

$$P'_{e2} = P''_{e2} \tag{25}$$

By applying the mass, momentum and energy balances to the control volume defined between section e2 and section e3 (Fig. 3.6), we can write the following equations.

1. Continuity equation:

$$m'' + m' = m_{e3} \tag{26}$$

With $U = m''/m'$, the equation (26) can be expressed as:

$$\frac{m_{e3}}{m'} = 1 + U \tag{27}$$

2. Energy equation:

$$m' C_p T'_0 + m'' C_p T''_0 = m_{e3} C_p T_{0e3} \tag{28}$$

Here, T_{0e3} is the stagnation temperature at the section e3. Dividing the equation by $m' C_p T'$, the energy equation can be expressed as follows:

$$(1 + U\theta) = (1 + U)\left(\frac{T_{0e3}}{T'}\right) \tag{29}$$

Where θ is defined as

$$\theta = \frac{T''}{T'} \tag{30}$$

3. Momentum equation:

$$m_{e3} V_{e3} + P_{e3} A_{e3} + \Delta P A_{e3} = m' V'_{e2} + P'_{e2} A'_{e2} + m'' V''_{e2} + P''_{e2} A''_{e2} \tag{31}$$

$$\Delta P A_{e3} = F\left(\frac{\rho V_m^2}{2}\right)\left(\frac{L}{D}\right) A_{e3} \tag{32}$$

Where F is the friction factor.

With the assumption $\rho V_m^2 = \rho_{e3} V_{e3}^2$, equation (32) can be expressed as

$$\Delta P A_{e3} = F\left(\frac{V_{e3}}{2}\right)\left(\frac{L}{D}\right) m_{e3} \tag{33}$$

In order to simplify the equations resolution, the dimensionless velocity $M(M = V/a)$ and the function are $f1(M)$ introduced (Abramovich, 1970; Lu, 1986)

$$f1(M) = M + \frac{1}{M} \tag{34}$$

Where a_*, is the sound speed at nozzle throat and is given by:

$$a_* = \sqrt{kRT} \tag{35}$$

And after a series of transformation of the expression $mV + PA$ we obtain,

$$mV + PA = \left(\frac{(k+1)}{2k}\right) m a_* f1(M) \tag{36}$$

By using equation (33) and (36) and dividing the momentum equation by $\left(\frac{(k+1)}{2k}\right)\left(\frac{(k+1)}{2k}\right) m' a'_*$, equation (33) can be expressed as

$$\left(\frac{a_{*e3}}{a'_*}\right)\left(\frac{m_{e3}}{m'}\right)(f_1(M_{e3}) + xM_{e3}) = f_1(M'_{e2}) + \frac{a''_*}{a'_*}\frac{m''}{m'} f_1(M''_{e2}) \tag{37}$$

Where, $x = (k/k+1)(L/D)F$

The distance L (Fig. 3.6) in the TR is assumed to be 10 D (Paliwoda, 1968). By using the isentropic relations, the momentum equation becomes:

$$1 + U\theta^{1/2}(f_1(M_{e3}) + xM_{e3}) = f_1(M'_{e2}) + U\theta^{1/2} f_1(M''_{e2}) \tag{38}$$

4. Calculation of the stagnation pressure P_{0e3} in the section e_3:

The primary mass flow rate can be expressed as:

$$m' = P'_0 \frac{1}{\sqrt{T'_0}}(A'_*)\left(\frac{k}{R}\right)^{1/2}\left(\frac{2}{k+1}\right)^{(k/k-1)}\left(\frac{k+1}{2}\right)^{1/2} \tag{39}$$

The mass flow rate in the section e3:

$$m_{e3} = P_{0e3} \frac{1}{\sqrt{T_{0e3}}}(A_{*e3})\left(\frac{k}{R}\right)^{1/2}\left(\frac{2}{k+1}\right)^{(k/k-1)}\left(\frac{k+1}{2}\right)^{1/2} \tag{40}$$

Where,A_{*e3} is the fictitious throat in the mixing chamber and can be expressed as follows by using isentropic relations:

$$A_{*e3} = A_{e3} f_2\,(k, M_{e3}\,, \eta_n) \tag{41}$$

Where,

$$f_2\,(k, M_{e3}\,, \eta_n) = \frac{A_*}{A} = \left(\frac{k+1}{2}\right)^{1/k-1} M \left(1 - \frac{k-1}{k+1}\frac{M^2}{\eta_n}\right)^{1/k-1} \tag{42}$$

By using equation (39) attributed to section e2 and equation (40), we obtain:

$$\frac{P_{0e3}}{P_0'} = \frac{m_{e3}}{m_{e2}'}\sqrt{\frac{T_{0e3}}{T_0'}}\,\frac{A_*'}{A_{e3}'}\left(\frac{1}{f_2\,(k, M_{e3}\,, \eta_n)}\right) \tag{43}$$

where,

$$\frac{T_{0e3}}{T_0'} = \frac{1 + U\theta^{1/2}}{1+U}$$

and

$$\frac{m_{e3}}{m_{e2}'} = 1 + U$$

therefore:

$$\frac{P_{0e3}}{P_0'} = \frac{1 + U\theta^{1/2}}{Ø f_2\,(k, M_{e3}\,, \eta_n)} \tag{44}$$

where,

$$Ø = \frac{A_{e3}}{A_*'}$$

5. Calculation of static pressure Pe4 in the section e4:

By using isentropic relations we can write:

$$P_{e4} = P_{0e4} f_3\left(k, M_{e4}\ , \eta_n\right) \tag{45}$$

where,

$$f_3\,(k, M_{e4}\,, \eta_n) = \left(1 - \frac{k-1}{k+1}\frac{M^2}{\eta_n}\right)^{k/k-1} \tag{46}$$

We can also write,

$$P_{e4} = P_{0e3}\eta_D\, f_3\,(k, M\,, \eta_n) \tag{47}$$

Where, η_D, is the pressure coefficient in the diffuser and is expressed as:

$$\eta_D = \frac{P_{04}}{P_{03}} \tag{48}$$

By using relation similar to equation (39), the mass flow rate at the exit of diffuser can be expressed as:

$$m_{e4} = P_{0e4}\frac{1}{\sqrt{T_{0e4}}}(A_{e4})\left(\frac{k}{R}\right)^{1/2}\left(\frac{2}{k+1}\right)^{(k/k-1)}\left(\frac{k+1}{2}\right)^{1/2} \tag{49}$$

By combining equations (40),(41) and (49) we obtain:

$$\frac{m_{e4}}{m_{e3}} = \frac{P_{0e4}}{P_{0e3}} \times \left(\frac{T_{0e4}}{T_{0e3}}\right)^{1/2} \frac{A_{e4}}{A_{e3}} \times \frac{f_2\,(k, M_{e4}\,, \eta_n)}{f_2\,(k, M_{e3}\,, \eta_n)} \tag{50}$$

The heat loss in the diffuser is neglected and the energy conservation in the diffuser imposes:

$$m_3 C_p T_{03} = m_4 C_p T_{04} \tag{51}$$

By using equations (49),(52) in equation (50) we obtain:

$$f_2\,(k, M_{e4}\,, \eta_n) = \frac{f_2\,(k, M_{e3}\,, \eta_n)}{\Omega\,\eta_D} \tag{52}$$

where, $\Omega = A_{e4}/A_{e3}$

Substituting equations (45) and (52) in equation (47), we can find a relation between the exit parameters P_{e4}, M_{e4} and the inlet parameters P_0', θ:

$$f_2\,(k, M_{e4}\,, \eta_n) = f_3\,(k, M_{e4}\,, \eta_n)\,\xi\,\frac{1 + U\theta^{1/2}}{\Omega\,\emptyset} \tag{53}$$

6. Entrainment ratio,U:

Similar to equation (44), entrainment ratio can be written as

$$U = \frac{m''}{m'} = \frac{P_0''}{P_0'}\sqrt{\frac{T_0'}{T_0''}}\,\frac{A_{e2}''}{A_*'}\,f_2\left(k, M_{e2}'', \eta_n\ \right) \tag{54}$$

Finally, by using Ø we obtain:

$$U\theta^{1/2} = \frac{1}{\Gamma}\left(\emptyset - \frac{1}{f_2\left(k, M'_{e2}, \eta_n\right)}\right) f_2\left(k, M''_{e2}, \eta_n\right) \tag{55}$$

On the other hand, by using the hypothesis expressed by $P'_{e2} = P''_{e2}$ and similarly to equation (47), we have:

$$P'_{e2} = P'_0 f_3\left(k, M'_{e2}, \eta_n\right) \tag{56}$$

and

$$P''_{e2} = P''_0 f_3\left(k, M''_{e2}, \eta_n\right) \tag{57}$$

so,

$$\frac{P''_0}{P'_0} = \frac{f_3\left(k, M''_{e2}, \eta_n\right)}{f_3\left(k, M'_{e2}, \eta_n\right)} \tag{58}$$

By combining equations (55) and (58),

$$\frac{f_2\left(k, M''_{e2}, \eta_n\right)}{f_3\left(k, M'_{e2}, \eta_n\right)} = \frac{U\theta^{1/2}}{\left(\emptyset - \frac{1}{f_2\left(k, M'_{e2}, \eta_n\right)}\right) f_3\left(k, M'_{e2}, \eta_n\right)} \tag{59}$$

7. System of equations:

The final system of equations used for transition regime is given by:

$$\left(1 + U\theta^{1/2}\right)\left(f_1\left(M'_{e3}\right) + xM'_{e3}\right) = f_1\left(M'_{e2}\right) + U\theta^{1/2} f_1\left(M''_{e2}\right) \tag{60}$$

$$f_2\left(k, M_{e4}, \eta_n\right) = \frac{f_2\left(k, M_{e3}, \eta_n\right)}{\Omega\, \eta_D} \tag{61}$$

$$f_2\left(k, M_{e4}, \eta_n\right) = f_3\left(k, M_{e4}, \eta_n\right) \xi\, \frac{1 + U\theta^{1/2}}{\Omega\, \emptyset} \tag{62}$$

$$U\theta^{1/2} = \frac{1}{\Gamma}\left(\emptyset - \frac{1}{f_2\left(k, M'_{e2}, \eta_n\right)}\right) f_2\left(k, M''_{e2}, \eta_n\right) \tag{63}$$

$$\Gamma = \left(\frac{2}{k+1}\right)^{(k/k-1)} \frac{1}{f_3\left(k, M'_{e2}, \eta_n\right)} \tag{64}$$

In which,

$$\Gamma = \frac{P_0'}{P_0''} \tag{65}$$

$$\xi = \frac{P_0'}{P_{e4}} \tag{66}$$

$$r = \frac{P_{e4}}{P_0''} \; or \; r = \frac{\Gamma}{\xi} \tag{67}$$

The system of equations has nine parameters: $U\theta^{1/2}$, Γ, ξ, Ω, Ø, M'_{e2}, M''_{e2}, M_{e3}, M_{e4} considering diffuser efficiency η_D and the friction factor F are fixed. Thermodynamic parameters $U\theta^{1/2}$, Γ, ξ and geometric parameters: Ω, Ø are the most important. To have a solution of the system, it is necessary to fix four initial parameters. Thus, the system of equations (60)–(64) translates the relation between five variables among the set of nine parameters in which four are fixed. In our case, the four fixed variables are M''_{e2}, Γ, Ø, Ω and the five unknown parameters are: $U\theta^{1/2}$, ξ, M'_{e2}, M_{e3}, M_{e4}. The aim of the ejector modeling is to find the back pressures of the three ejectors and their corresponding entrainment ratios.

LOWER STAGE

3.4.2 Evaporator 1 (EV_1):

The refrigerating effect caused by evaporator 1 (EV_1) can be expressed as:

$$Q_{EV1} = m_1 (h_{10} - h_7) \tag{68}$$

where,

$$h_7 = h_3 = f_{sat} (P_2) \tag{69}$$

$$h_{10} = f (P_{10}, T_{10}) \tag{70}$$

$$T_{10} = T_{10sat} + \Delta T_{sup} \tag{71}$$

3.4.3 Evaporator 2 (EV_2):

The refrigerating effect caused by evaporator 2 (EV_2) can be expressed as:

$$Q_{EV2} = m_2 (h_{11} - h_8) \quad (72)$$

where,

$$h_8 = h_3 = f_{sat} (P_2) \quad (73)$$

$$h_{11} = f (P_{11}, T_{11}) \quad (74)$$

$$T_{11} = T_{11sat} + \Delta T_{sup} \quad (75)$$

3.4.4 Evaporator 3 (EV_3):

The refrigerating effect caused by evaporator 3 (EV_3) can be expressed as:

$$Q_{EV3} = m_3 (h_{15} - h_9) \quad (76)$$

where,

$$h_9 = h_3 = f_{sat} (P_2) \quad (77)$$

$$h_{15} = f (P_{15}, T_{15}) \quad (78)$$

$$T_{15} = T_{15sat} + \Delta T_{sup} \quad (79)$$

3.4.5 Compressor 1:

The compression is assumed to be non-isentropic process. Process 1-2s is an isentropic compression process, while process 1-2 is the actual compression process. The actual enthalpy of state 2 is expressed as:

$$h_2 = h_1 + (h_{2s} - h_1) / \eta_{cm1} \quad (80)$$

Where, η_{cm1} is the isentropic efficiency of the compression process 1-2 and is given by Brunin *et al*. (1997) as:

$$\eta_{cm1} = 0.847 - 0.0135 \frac{P_2}{P_1} \quad (81)$$

The enthalpy and entropy of the refrigerant at state 1 are determined by the temperature and pressure at ejector 2 EJ_2 outlet:

$$h_1, s_1 = f(T_1, P_1) \quad (82)$$

The refrigerant enthalpy at state 2s for isentropic process is:

$$h_{2s} = f(s_1, P_2) \quad (83)$$

The power input to compressor 1 can be evaluated as:

$$W_{cm1} = (m_1 + m_2 + m_3)(h_2 - h_1) \quad (84)$$

3.4.6. Intercooler:

The intercooler acts as condenser for the lower stage and evaporator for the upper stage. The heat exchange process in the intercooler is considered to be perfect, *i.e*, the heat rejected by refrigerant of lower stage is completely absorbed by low pressure evaporator of the upper stage and is expressed as:

$$Q_{int} = (m_1 + m_2 + m_3)(h_2 - h_3) = m_4 (h_{26} - h_{28}) \quad (85)$$

Where m_1, m_2 and m_3 are the flow rate of refrigerant in evaporator 1,2 and 3 respectively.

$$h_3 = f_{sat}(P_2) \quad (86)$$

$$h_{26} = f(P_{26}, T_{26}) \quad (87)$$

where,

$$T_{26} = T_{26sat} + \Delta T_{sup} \quad (88)$$

$$h_{24} = f_{sat}(P_c) \quad (89)$$

The enthalpy state points (18) and (1) can be evaluated from generalised mathematical model of ejector in transition regime which gives pressure and temperature at the outlet of ejector.

UPPER STAGE

3.4.7 Evaporator 4 (EV_4):

The refrigerating effect caused by evaporator 4 (EV_4) can be expressed as:

$$Q_{EV4} = m_5 (h_{25} - h_{23}) \quad (90)$$

where,

$$h_{23} = h_{20} = f_{sat} (P_C) \quad (91)$$

$$h_{25} = f (P_{25}, T_{25}) \quad (92)$$

$$T_{25} = T_{25sat} + \Delta T_{sup} \quad (93)$$

3.4.8 Compressor 2:

The compression is assumed to be non-isentropic process. Process 18-19s is an isentropic compression process, while process 18-19 is the actual compression process. The actual enthalpy of state 2 is expressed as:

$$h_{19} = h_{18} + (h_{19s} - h_{18})/\eta_{cm2} \quad (94)$$

Where, η_{cm1} is the isentropic efficiency of the compression process 1-2 and is given by Brunin *et al.* (1997) as:

$$\eta_{cm2} = 0.847 - 0.0135 \frac{P_C}{P_{18}} \quad (95)$$

The enthalpy and entropy of the refrigerant at state 18 are determined by the temperature and pressure at ejector 3 EJ_3 outlet:

$$h_{18}, s_{18} = f(T_{18}, P_{18}) \quad (96)$$

The refrigerant enthalpy at state 19s for isentropic process is:

$$h_{19s} = f(s_{18}, P_{19}) \quad (97)$$

The power input to compressor 2 can be evaluated as:

$$W_{cm2} = (m_4 + m_5)(h_{19} - h_{18}) \quad (98)$$

3.4.9 Condenser:

The condenser of the system is assumed to be air cooled and the refrigerant discharges heat to the environment. Assuming that the refrigerant at the exit of condenser (state 20) is saturated liquid, the governing equations for the condenser are:

$$h_{20}, s_{20}, P_{20} = f_{sat}(T_{20}) \tag{99}$$

The heat load on the condenser is given by:

$$Q_c = (m_4 + m_5)(h_{19} - h_{20}) \tag{100}$$

3.4.10 System Performance evaluation:

The governing equations for each component in the upper and lower stage of the system were solved to evaluate the performance of EEMECRS. The working state of ejectors affects the performance of system as a whole. The system has been evaluated for three different coefficients of performances (COP's) as described below:

The performance of lower stage of EEMECRS is evaluated by COP_1, which represents the ratio refrigerating effect caused by the three evaporators in lower stage EV_1, EV_2 and EV_3 to the power input to compressor 1.

$$COP_1 = \frac{Q_{ev1} + Q_{ev2} + Q_{ev3}}{W_{cm1}} \tag{101}$$

The entrainment ratios, U_{ej1} and U_{ej2} are defined as the ratio of mass flow rate of secondary flow to the mass flow rate of the motive stream. Therefore, they can be obtained as follows:

$$U_{ej1} = \frac{m_2}{m_1} \tag{102}$$

$$U_{ej2} = \frac{m_3}{m_1 + m_2} \tag{103}$$

For the upper stage the performance is evaluated by COP_2, which is defined as the ratio heat absorbed in intercooler and evaporator 4 (EV_4) to the power input to compressor 2:

$$COP_2 = \frac{Q_{int} + Q_{ev4}}{W_{cm2}} \quad (104)$$

The entrainment ratio U_{ej3} is obtained as:

$$U_{ej3} = \frac{m_4}{m_5} \quad (105)$$

The performance of system as a whole is evaluated by COP_{sys}, which is expressed as a ratio of total refrigerating effect caused by the system to the power supplied to the system:

$$COP_{sys} = \frac{Q_{ev1} + Q_{ev2} + Q_{ev3} + Q_{ev4}}{W_{cm1} + W_{cm2}} \quad (106)$$

3.5 Computation methodology

A mathematical model is developed for the performance analysis of EEMECRS. The mathematical model is coded in MATLAB 7.01 to compute the results. The computational procedure is carried out in two steps as given below:

Step 1: The ejector performance is computed on the basis of one dimensional constant area ejector. This model includes operating parameters T_0', T_0'', M_{e2}'' and geometric parameters Ω, Ø. The coefficients *F*, η_D , Ω ,L/D are assumed to be: F= 0.06, η_D = 0.96, Ω = 3 (Lu,1986), L/D = 10 (Paliwoda,1968) and η_n =0.90 (Aly *et al.*,1999). This computational procedure yields the output of entrainment ratio, U, the back pressure and back pressure and temperature P_{e4}, T_{e4}. The refrigerant properties are being evaluated using REFPROP 7 subroutines. The flowchart for the computational procedure is shown in Fig 3.7.

Step 2: The output of ejector model obtained from step 1 is then employed to another computer program to evaluate the performance of EEMECRS. The flow chart for performance analysis of EEMECRS is shown in Fig. 3.8.

Two more programs were developed to compare the performance of ejector enhanced multi evaporator refrigeration system (EEMECRS) to the unenhanced system as described in the beginning of chapter. All programs are written in MATLAB 7.01and are appended in appendix.

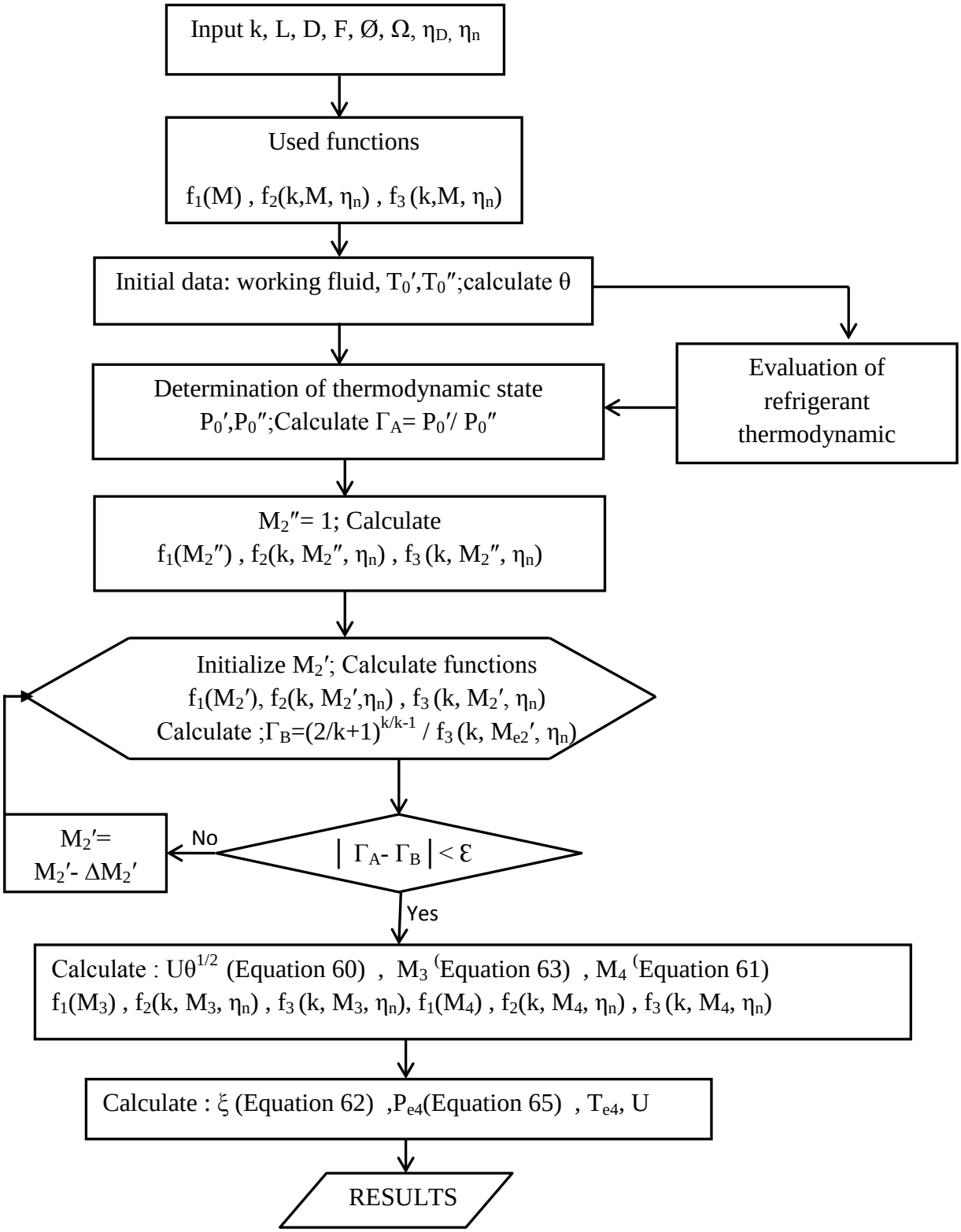

Fig. 3.7: Flowchart for ejector performance analysis

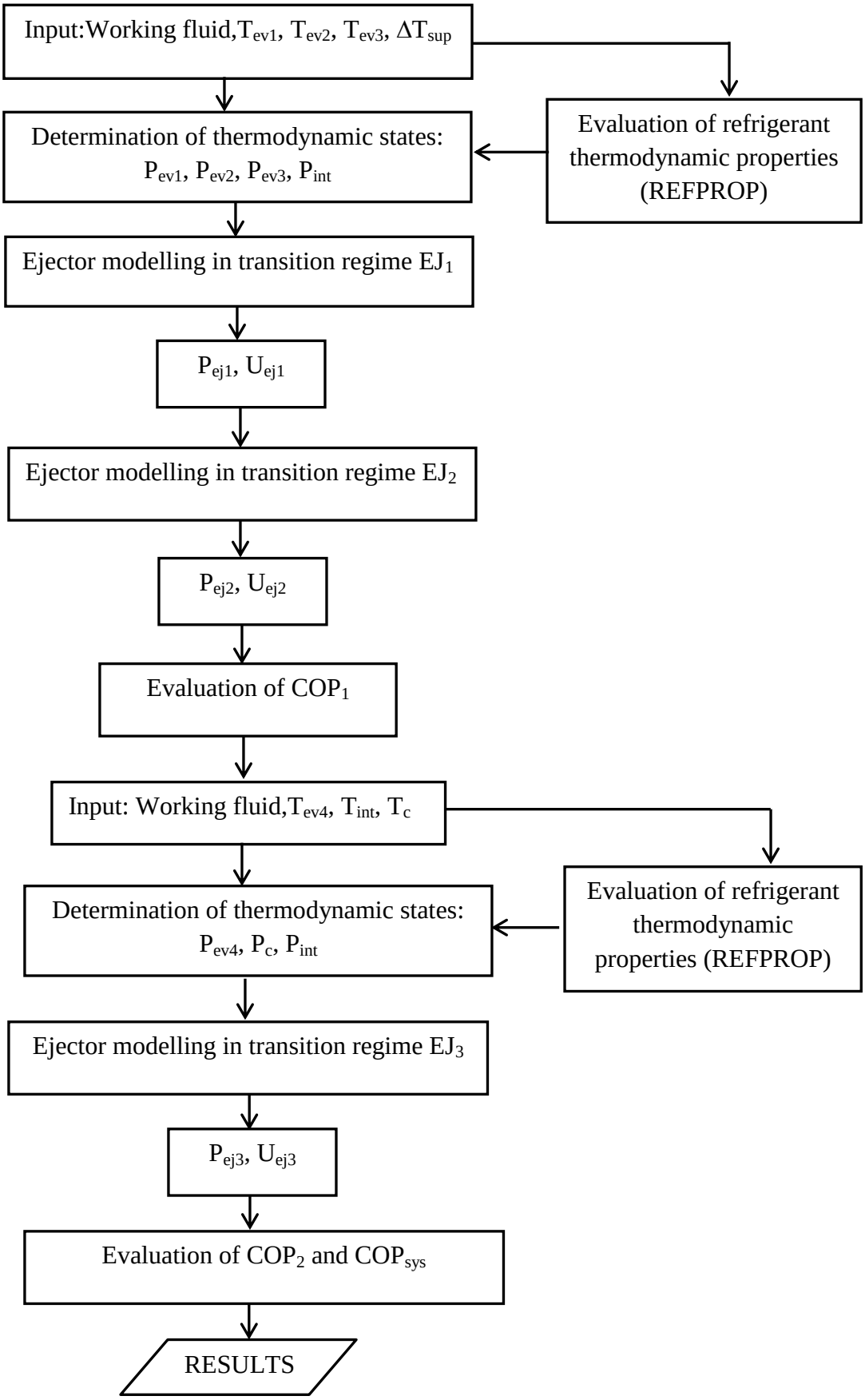

Fig. 3.8: Flowchart for performance evaluation of EEMECRS

Chapter 4

Results and Discussion

Four refrigerants, *i.e.*, R116, R125, R1270 and R23 in lower stage and four refrigerants, *i.e.*, R134a, R141b, R152a and R600a in upper stage of EEMECRS are used as working fluids in the present study. A total of sixteen combinations of refrigerants were simulated in order to identify the best pair of refrigerants. A computer simulation program is developed in MATLAB 7.01, to compute the performance results of EEMECRS. REFPROP 7 subroutines have been used to evaluate refrigerant thermodynamic properties.

The independent design variables considered for the performance analysis of EEMECRS are:

the evaporator 1 temperature ,T_{EV1}, the evaporator 2 temperature, T_{EV2}, the evaporator 3 temperature, T_{EV3}, evaporator 4 temperature ,$T_{EV4,}$ the intercooler temperature ,$T_{INT,}$ the condenser temperature ,T_C , and the ejector area ratio, Ø. The range of these variables used in the study is: $-28 \leq T_{EV1} \leq -20^oC$, $-45 \leq T_{EV2} \leq -35^oC$, $-55 \leq T_{EV3} \leq -48^oC$, $8 \leq T_{EV4} \leq 15^oC$, $-12 \leq T_{INT} \leq -8^oC$, $35 \leq T_C \leq 50^oC$ and the superheating $\Delta T_{SUP} = 5^oC$. Superheating allows ejector to work with dry expansion in the primary and secondary nozzle.

4.1 Model validation

Experimental data for constant area ejector model using R11 reported by Nahdi *et al.*, 1993 were reproduced and selected to validate the current ejector model. The entrainment ratio U is a function of the operating conditions and geometry of ejector defined mainly by ejector area ratio, Ø (Nahdi et al., 1993; Lu, 1986; Paliwoda, 1968). Fig. 4.1 shows the variation of the entrainment ratio U with the compression ratio at different ejector area. It can be seen that entrainment ratio values are very high at low compression ratios and go on decreasing as pressure ratio increases. With increase in area ratio, Ø, entrainment ratio increases at constant pressure ratio, r. The optimum driving pressure ratio, ξ_{opt}, for different values of ejector area ratio, Ø, is also indicated. The results obtained from mathematical model fairly agree with the experimental data within 10% average deviation.

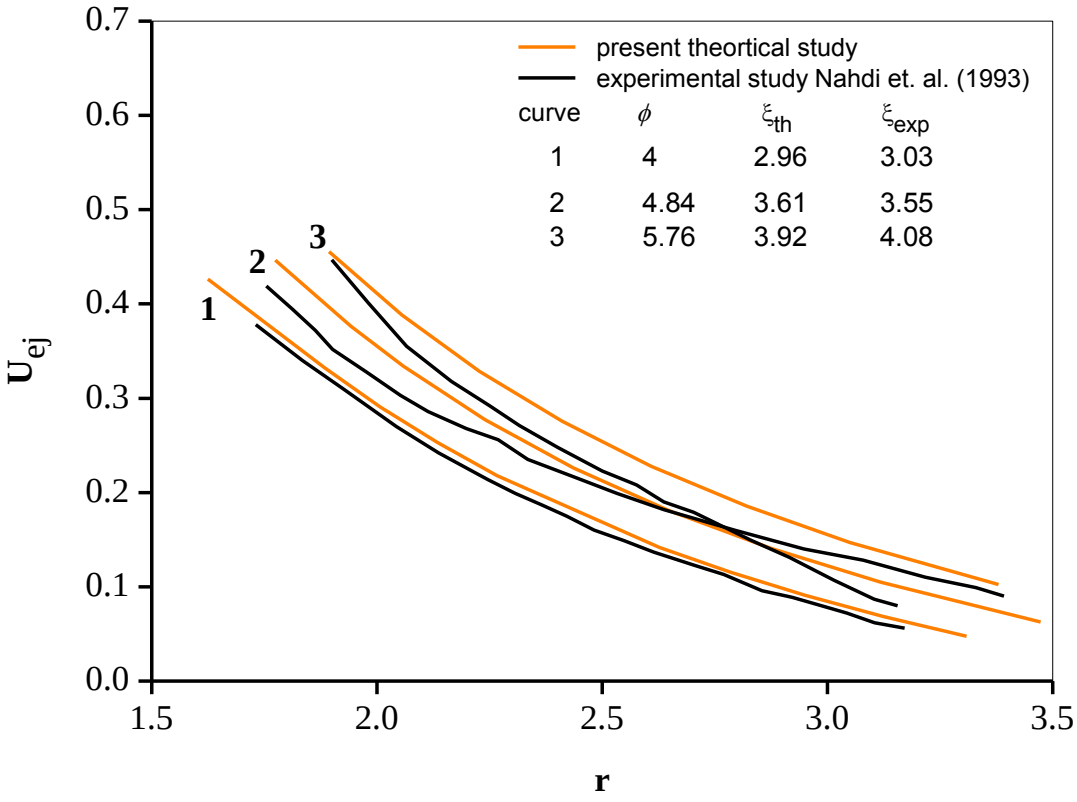

Fig. 4.1: Comparison of simulated results with experimental data of Nahdi et *al.*, 1993

4.2 Effect of Fluid Nature on EEMECRS performance.

The combined cycle can work with a single refrigerant or dual refrigerants. It has been shown that use of dual refrigerants can improve system performance (Sun D.W., 1998). Inorder to identify a suitable refrigerant pair, four refrigerants (R116, R125, R1270 and R23) in lower stage and four refrigerants (R134a, R141b, R152a and R600a) in upper stage of EEMECRS were selected identify the best combination. The refrigerants selected for lower stage have a low normal boiling point (NBP) and the refrigerants in upper stage have a moderate NBP, so that the pressure of the system is maintained close to atmospheric pressure. A total of sixteen combinations were simulated to identify the effect of fluid nature on the various performance characteristics of EEMECRS.

Fig.4.2 shows the values of total refrigerating effect produced and amount of power requested by the EEMECRS at given evaporating and condensing temperatures for various refrigerant combinations. It can be seen that a combination of R1270 (lower

stage) and R142b (upper stage) give the maximum possible refrigerating effect for unit mass flow of refrigerant in lower stage. The power requested by the pair is also comparatively low.

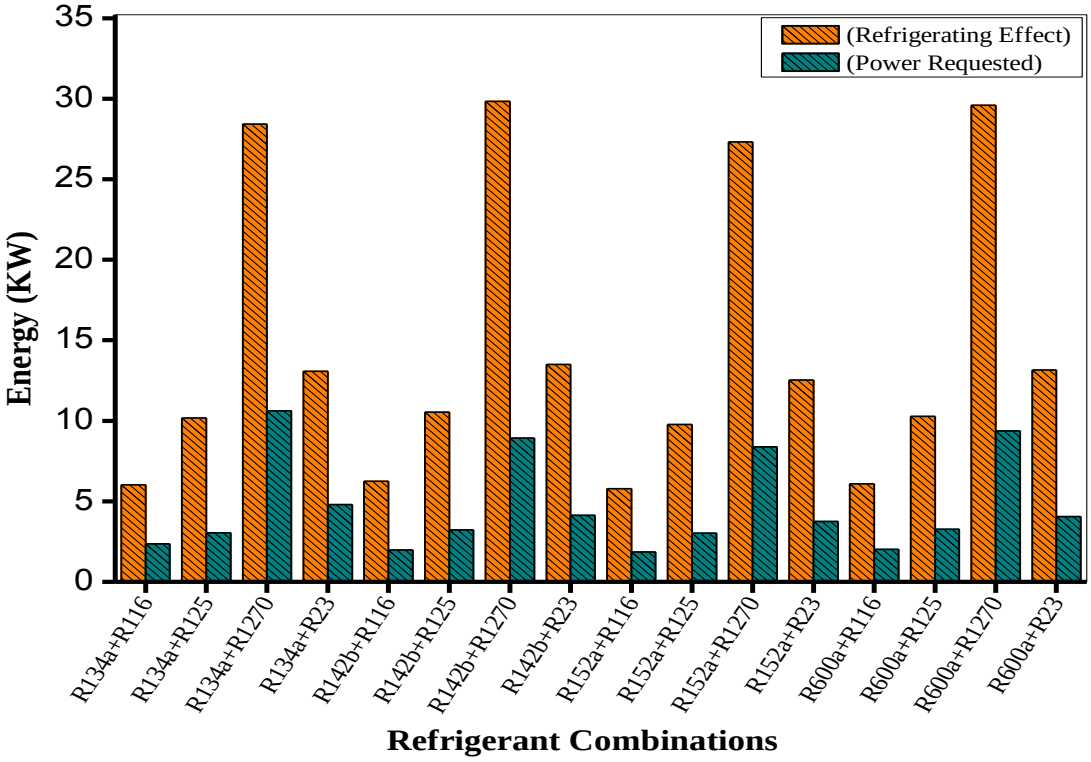

Fig. 4.2: Refrigerating effect and power requested by various refrigerant combinations.

The improvement due to increase of inlet pressure at the compressor aspiration is shown in Fig.4.3. It represents the ratio of pressure at compressor inlet for ejector enhanced system to the pressure at compressor inlet for unenhanced system for various working fluids combinations in upper and lower stage of EEMECRS. The introduction of ejectors into the system increases the pressure at compressor aspiration, which leads to decrease of pressure ratio of compressor and thus COP increases.

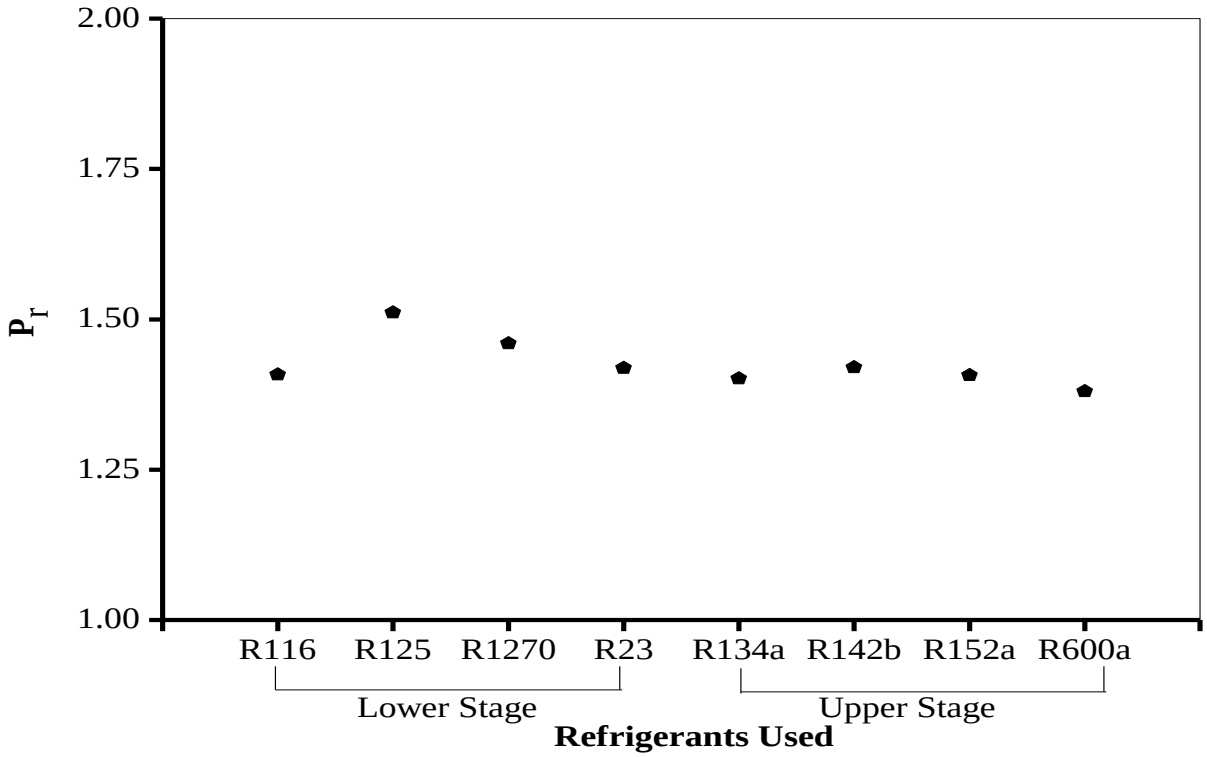

Fig. 4.3: Comparison of pressure ratio at compressor aspiration for various working fluids in EEMECRS

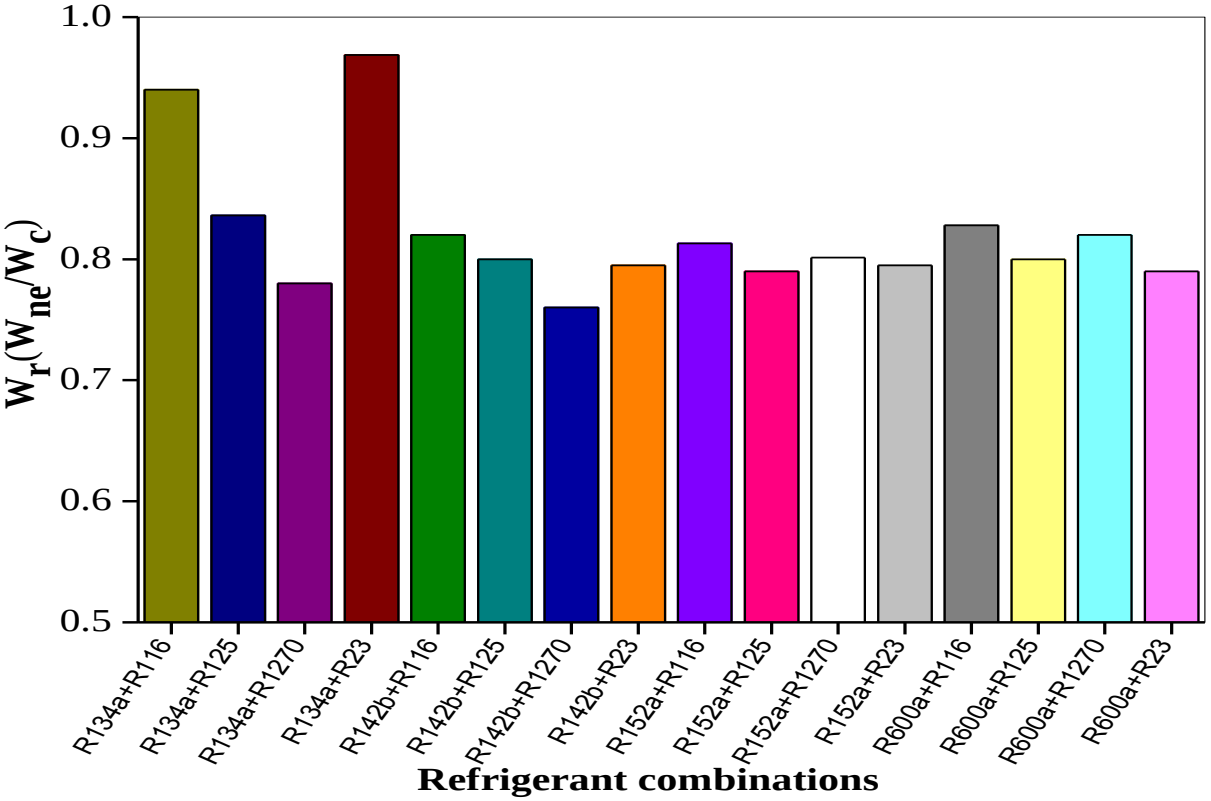

Fig. 4.4: Comparison of work ratio (W_{ne}/W_c) for various refrigerant combinations in EEMECRS.

The work required by the EEMECRS relative to the work required by the unenhanced (UMECRS) system is shown in Fig. 4.4.A combination of R1270 in lower stage with R142b in upper stage saves the most work for the system relative to unenhanced one which corresponds to higher relative COP.

Fig. 4.5 is generated to indicate the variation of entrainment ratios U_{ej1} and U_{ej2} with the corresponding compression ratios r_{ej1} and r_{ej2} for various refrigerants in lower stage of the system. The entrainment ratios U_{ej1} and U_{ej2} are not the only parameters to be considered, one has to find an optimum combination of higher entrainment ratios and pressure ratios. At given evaporating temperatures R1270 is the best suitable option.

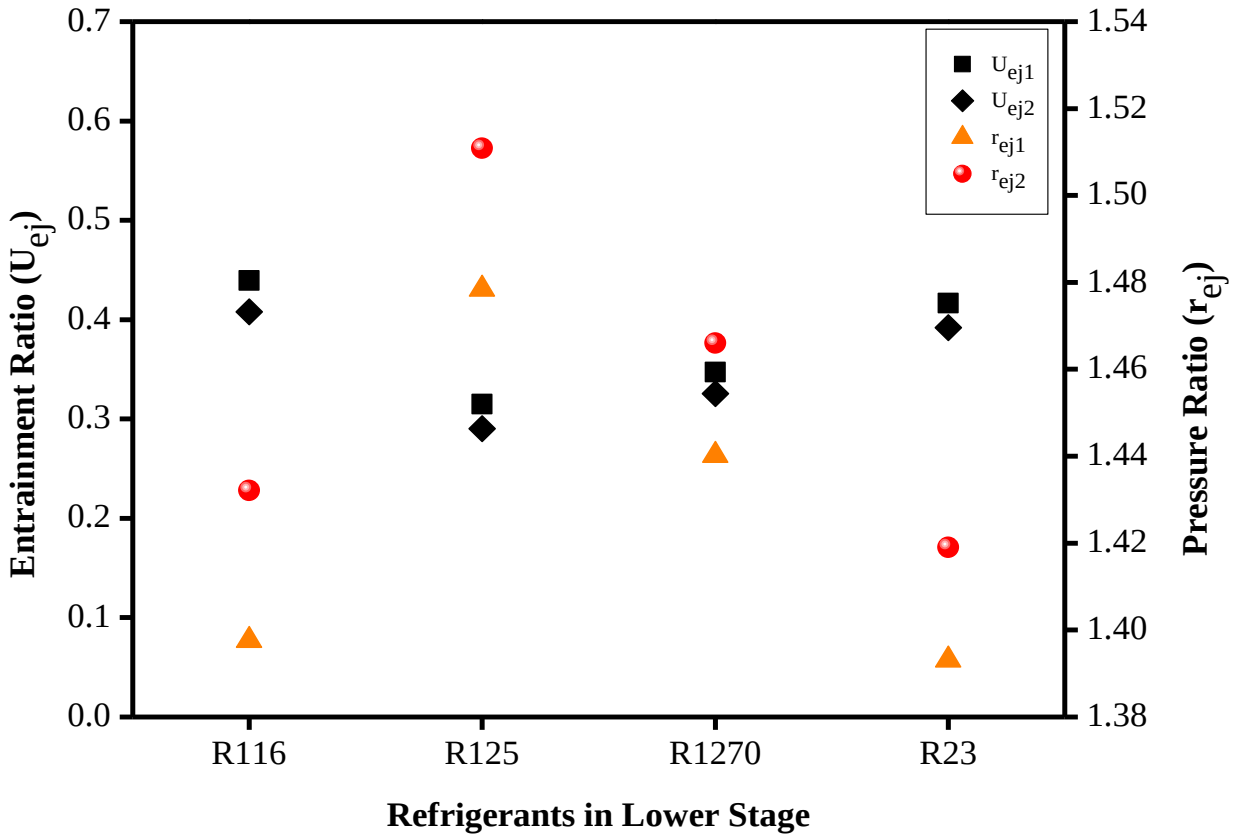

Fig. 4.5: Entrainment ratios U_{ej1} and U_{ej2} with the corresponding pressure ratios r_{ej1} and r_{ej2} for various refrigerants in lower stage of the system

The variation of entrainment ratio U_{ej3} with the corresponding pressure ratios r_{ej3} for various refrigerants selected in higher stage is shown in Fig. 4.6. For the upper stage R142b gives the best optimum values.

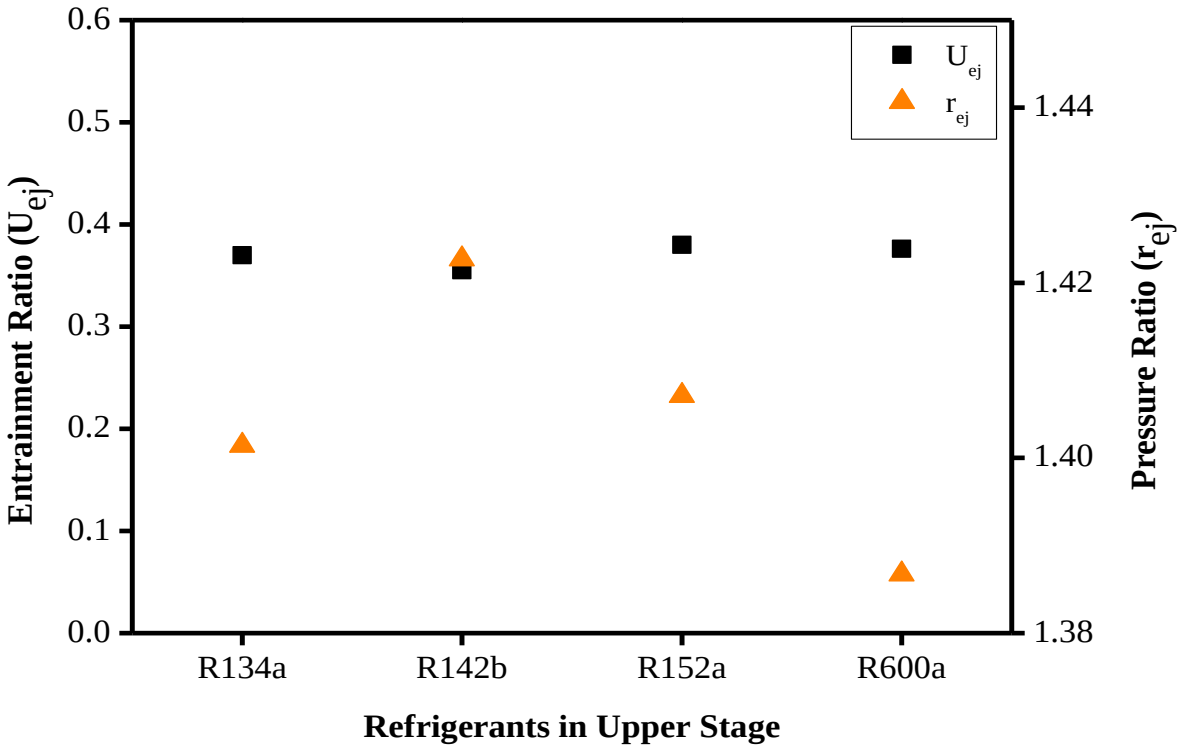

Fig. 4.6: Entrainment ratio U_{ej3} with the corresponding pressure ratio r_{ej3} for various refrigerants in upper stage of the system.

Table 4.1 shows values of COP for various refrigerants simulated for the lower stage of EEMECRS. The increase in COP by introduction of ejectors into conventional system is also indicated.

Table 4.1: Values of COP and relative COP_R for various refrigerants in lower stage

REFRIGERANTS IN LOWER STAGE				
	R116	**R125**	**R1270**	**R23**
COP_1	4.07	4.88	5.14	6.81
COP_{1R}	1.35	1.39	1.38	1.49

Table 4.2: COP_R for various refrigerants in upper stage of EEMECRS

REFRIGERANTS IN UPPER STAGE					
REFRIGERANTS IN LOWER STAGE		R134a	R142b	R152a	R600a
	R23	1.006	1.23	1.23	1.22
	R1270	1.25	1.27	1.22	1.23
	R125	1.16	1.22	1.23	1.21
	R116	1.01	1.18	1.20	1.1

The increase in COP for various refrigerants in upper stage of EEMECRS by introduction of ejector in upper stage of system over the conventional system is listed in table 4.2. It must be noted that COP for each refrigerant in upper stage varies with refrigerants in lower stage.

Table 4.3: Compressor efficiencies for new and conventional system in upper stage

REFRIGERANTS IN UPPER STAGE				
	R134a	**R142b**	**R152a**	**R600a**
η_{cc}	.8362	.8349	.8365	.8370
η_{cne}	.8183	.8158	.8192	.8196

The value of compressor efficiencies (η_c) using various refrigerants for upper and lower stage of EEMECRS and conventional system are listed in Table 4.3 and 4.4.

Table 4.4: Compressor efficiencies for new and conventional system in lower stage

REFRIGERANTS IN LOWER STAGE				
	R116	**R125**	**R1270**	**R23**
η_{cc}	.8227	.8033	.8104	.8204
η_{cne}	.8377	.8272	.8306	.8365

Table 4.5 gives the values of degree of superheat at condenser of EEMECRS for various refrigerants. These values correspond to the extra load on the condenser.

Table 4.5: Degree of superheat at condenser for various refrigerants

REFRIGERANTS USED				
	R134a	**R142b**	**R152a**	**R600a**
DEGREE OF SUPERHEAT	19.99^o	16.08^o	26.53^o	8.06^o

4.3 Selection of Refrigerant pair

In order to identify the best working pair, various performance parameters for all sixteen combinations were studied. A selection strategy has been developed based on coefficient of performance of EEMECRS, COP_{SYS}, and relative coefficient of performance of EEMECRS, COP_{SYSR} as shown in Table 4.6, Fig. 4.7 and 4.8.

Table 4.6: COP Matrix for various refrigerant combinations in EEMECRS

REFRIGERANTS IN UPPER STAGE					
REFRIGERANTS IN LOWER STAGE		**R134a**	**R142b**	**R152a**	**R600a**
	R23	2.71	3.26	3.34	3.24
	R1270	2.67	3.28	3.25	3.16
	R125	2.65	3.25	3.22	3.27
	R116	2.52	3.14	3.10	3.03

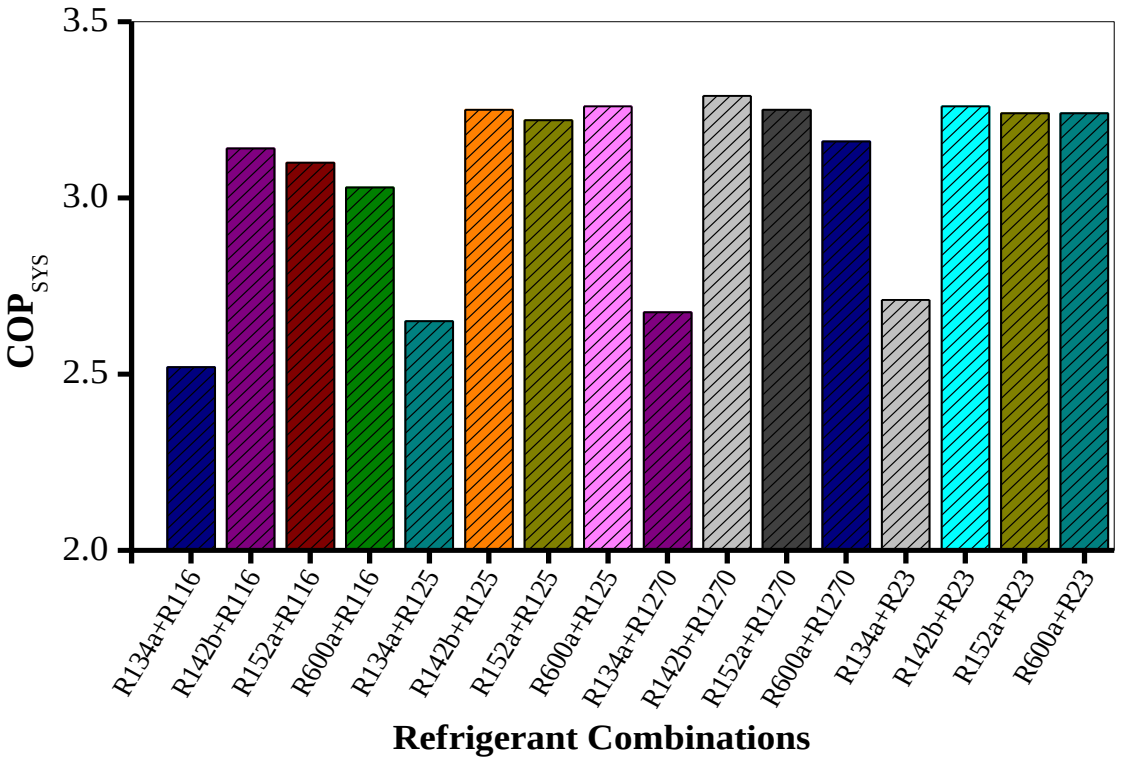

Fig. 4.7: COP of EEMECRS for various refrigerant combinations.

Table 4.6 and Fig. 4.7 indicate that the COP of EEMECRS is highest with refrigerant combination R1270 in lower stage of system and R142b in upper stage.

Variation of COP of EEMECRS to the COP of unenhanced system (UMECRS) for various refrigerant combinations is shown in Fig. 4.8. Refrigerant R1270 in lower stage of system with R142b in upper stage give the best results.

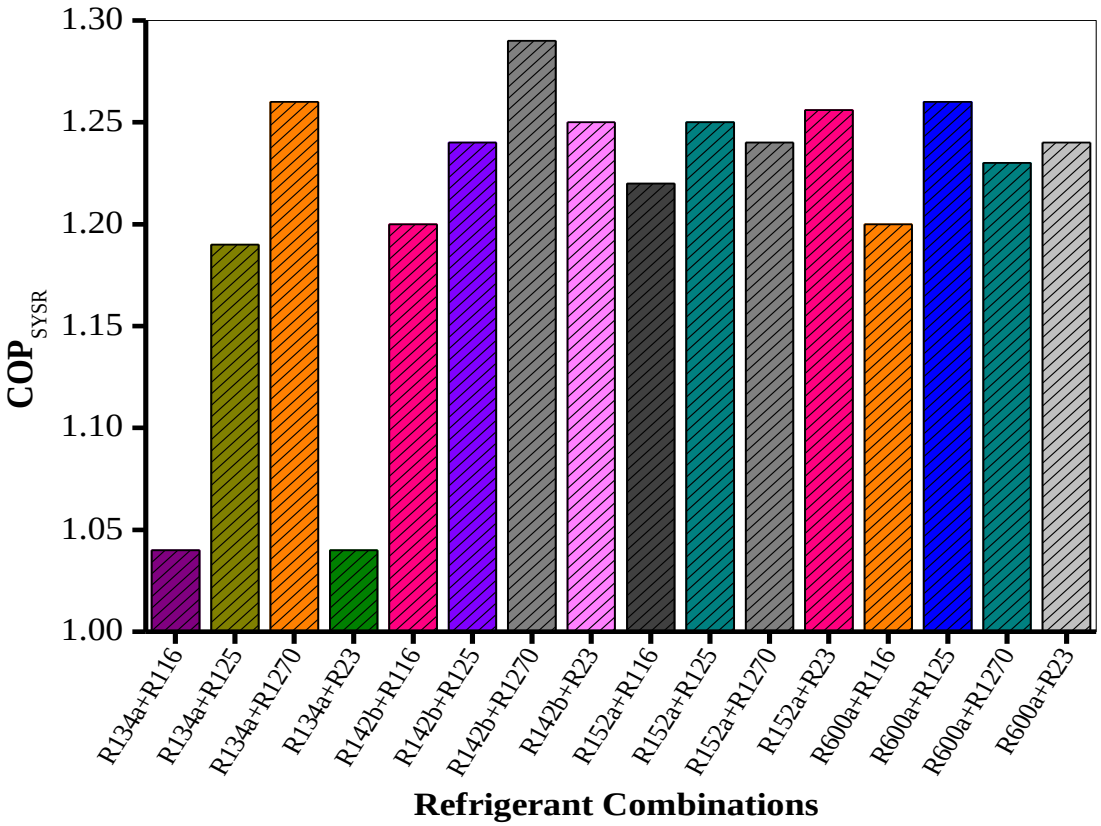

Fig. 4.8: Relative COP of EEMECRS for various refrigerant combinations

From the Fig. 4.7 and 4.8, it is concluded that a combination of R1270 (lower stage) and R142b (upper stage) will give better performance for this combined cycle. The combination also provides advantage of higher refrigerating effect for unit mass of refrigerant in lower system.

4.4 Effect of area ratio on EEMECRS performance

The effect of area ratio, Ø, on the characteristic U(r) using R134a is examined and represented in Fig.4.9. In transition regime model an increase in area ratio, Ø, the characteristic curves U(r) move towards the increasing entrainment ratio and increasing driving pressure ratios, which leads to an increase of ejector performance. A high value of Ø means that the mixing chamber section is relatively greater and primary flow must expand to form the aerodynamic throat, what corresponds to a low value of back pressure. Similar results have been reported by Paliwoda (1968) for

R11.Higher values of Ø give an increased entrainment ratio with a low value of back pressure and correspondingly low pressure ratio. While as, on the other hand low value of Ø increases the compression ratio and back pressure.one has to find an optimum value of Ø which gives an acceptable value of U with a fairly good back pressure. However, the EEMECRS uses ejectors to increase the aspiration pressure at the compressor inlet. For EEMECRS It is therefore suitable to use ejectors with low values of Ø what corresponds to low values of ξ.

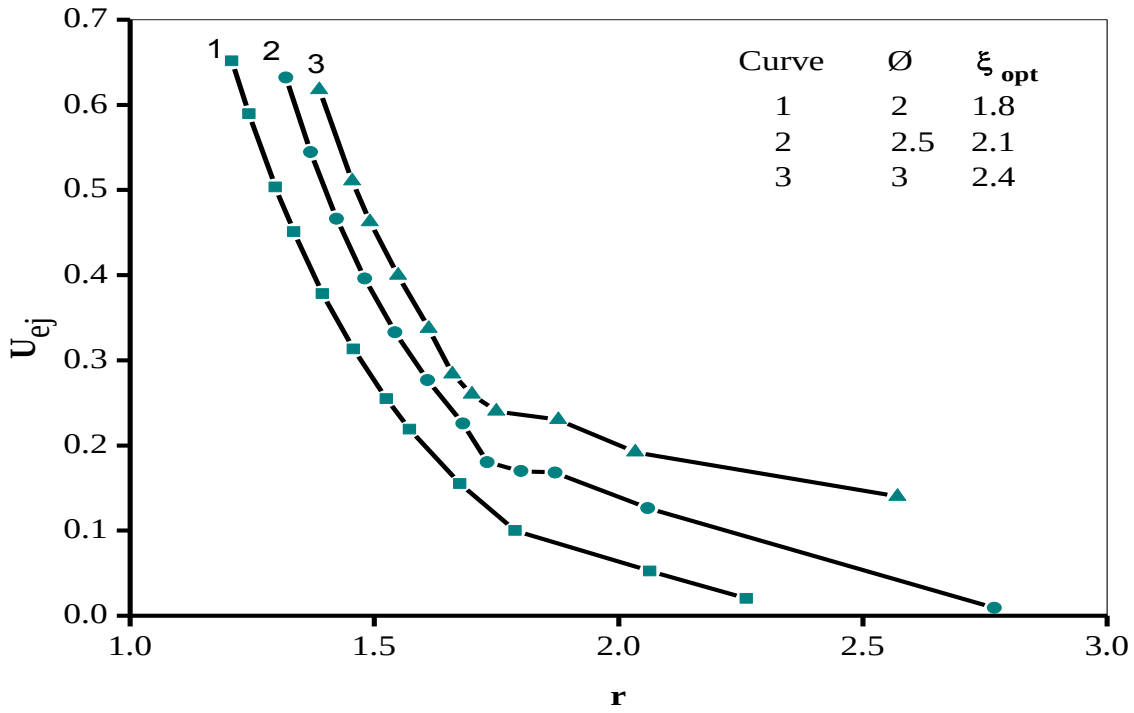

Fig. 4.9: Influence of area ratio Ø on the characteristic U(r) for R134a

THE effect of area ratio of selected refrigerant pair R1270 (lower stage) and R142b (upper stage) on various performance factors of EEMECRS is represented in Fig. 4.10. There is a decrease COP of lower stage (COP_1) with increase in ejector area ratio (Ø).Similar variation is shown by COP of upper stage (COP_2) and COP of EEMECRS (COP_{SYS}).The corresponding relative COP's also show a decrease with increasing in ejector area ratio (Ø).We can see that the COP in EEMECRS is increased by 30% for Ø=1.8 and by 20% for Ø=2.2. It can be concluded that a suitable lower value of Ø which gives justified entrainment ratio can be determinant factor for system optimization.

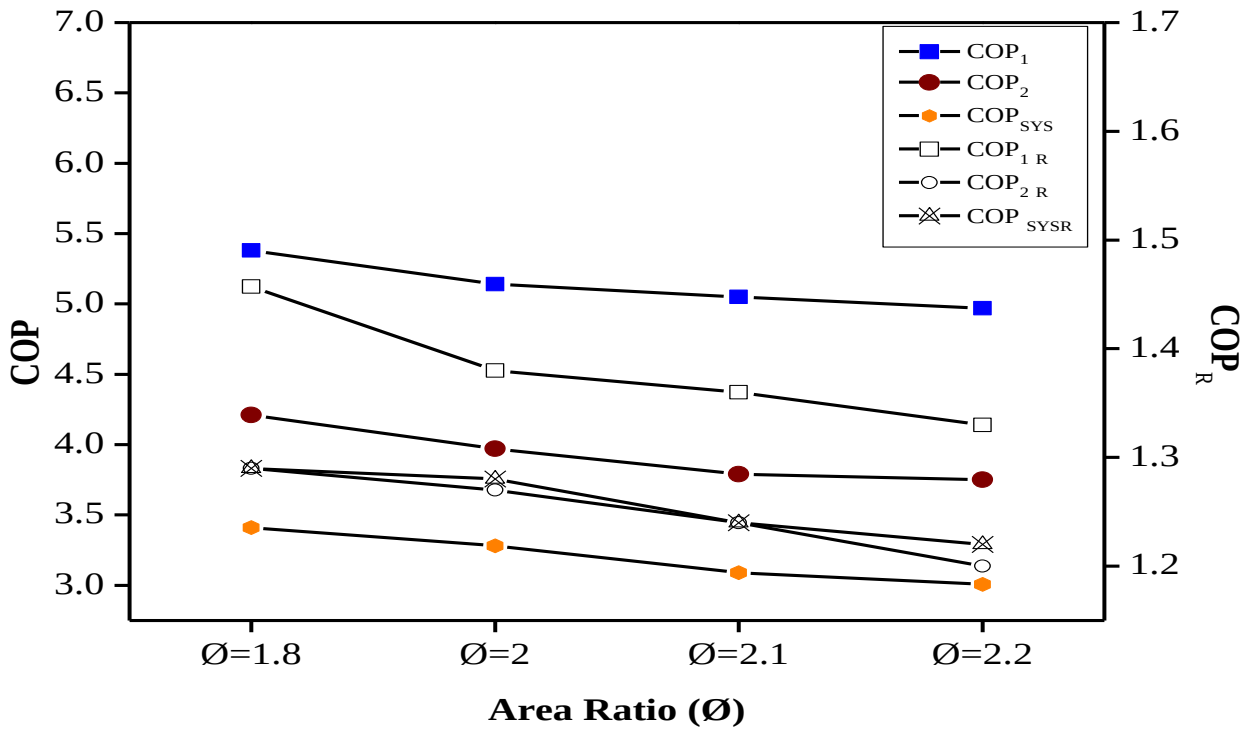

Fig. 4.10: Influence of area ratio on performance of EEMECRS

4.5 Effect of operating temperatures on the EEMECRS performance

The effect of operating temperatures on the performance of EEMECRS is studied for selected refrigerant pair, R1270 (lower stage) and R142b (upper stage). There are six operating parameters which can be varied to evaluate the performance of EEMECRS. This study was conducted for the following range of variables: $-28 \leq T_{ev1} \leq -20^{o}C$, $-45 \leq T_{ev2} \leq -35^{o}C$, $-55 \leq T_{ev3} \leq -48^{o}C$, $8 \leq T_{ev4} \leq 15^{o}C$, $-12 \leq T_{int} \leq -8^{o}C$, $35 \leq T_{C} \leq 50^{o}C$ and the superheating $\Delta T_{sup} = 5^{o}C$. Superheating allows ejector to work with dry expansion in the primary and secondary nozzle.

Fig. 4.11 depicts the influence of the evaporator temperature T_{EV1} on the entrainment ratios U_{ej1} and U_{ej2}, the compression ratios r_{ej1} and r_{ej2} and the coefficient of performances COP_1 and COP_{SYS}. It can be conclude from the figure, that for fixed intercooler and condensing temperature, the compression ratios and COP's show an increase with increasing T_{ev1}, while as the entrainment ratios U_{ej1} and U_{ej2} decrease sharply with increase in evaporating temperature T_{ev1}. When the compression ratios increase, the back pressures at ejector exit increase. Any increase in the back pressure increases COP_1 and COP_{SYS} reducing the driving pressure ratio and subsequently

entrainment ratio. Therefore, critical entrainment ratio decreases when compression ratio increases.

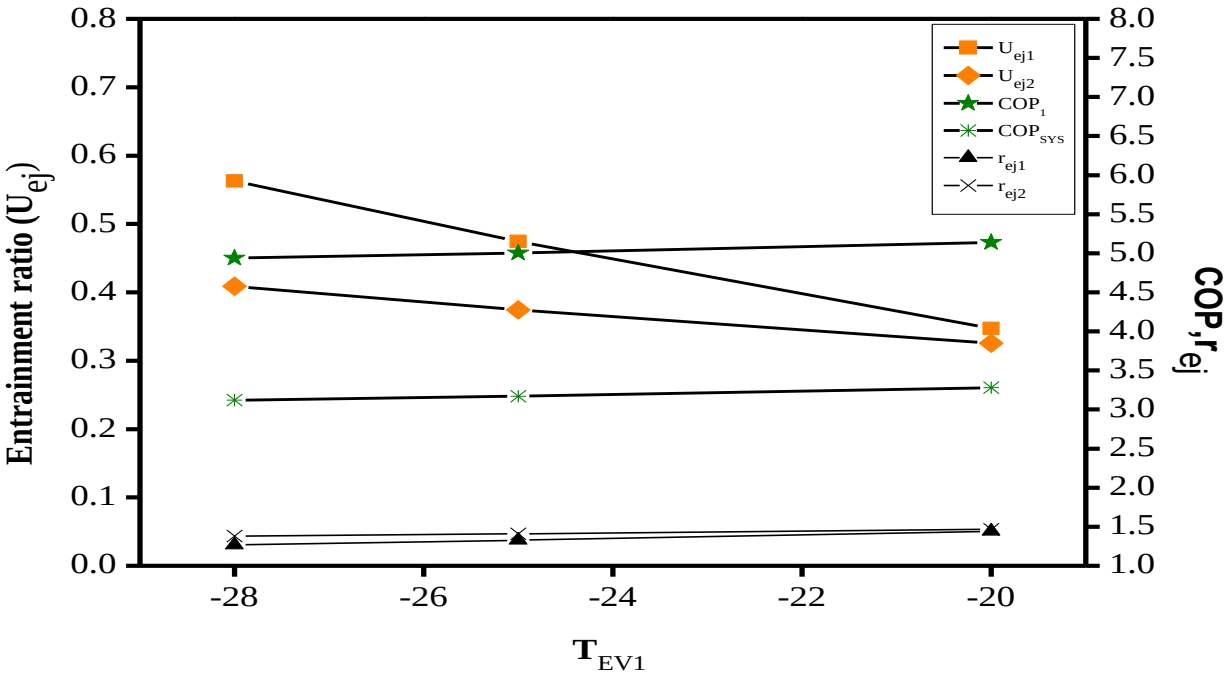

Fig. 4.11: The effect of evaporating temperature T_{ev1} on the entrainment ratios U_{ej1} and U_{ej2}, the compression ratios r_{ej1} and r_{ej2} and the coefficient of performances COP_1 and COP_{SYS}

The effect of evaporating temperature T_{ev2} on the entrainment ratios U_{ej1} and U_{ej2}, the compression ratios r_{ej1} and r_{ej2} and the coefficient of performances COP_1 and COP_{SYS} is depicted in Fig. 4.12.The pressure ratio r_{ej1} is found to decrease with increasing evaporator temperature T_{ev2} , what corresponds to an increasing entrainment ratio U_{ej1}.This increase in U_{ej1} shows that secondary mass flow rate in the ejector 1 increases with T_{ev2}. The entrainment ratio U_{ej2} shows an decrease with increasing evaporating temperature T_{ev2} , since any increase in evaporating temperature T_{ev2} decreases the compression ratio r_{ej2}. COP_1 and COP_{SYS} show a slight increase with T_{ev2}.

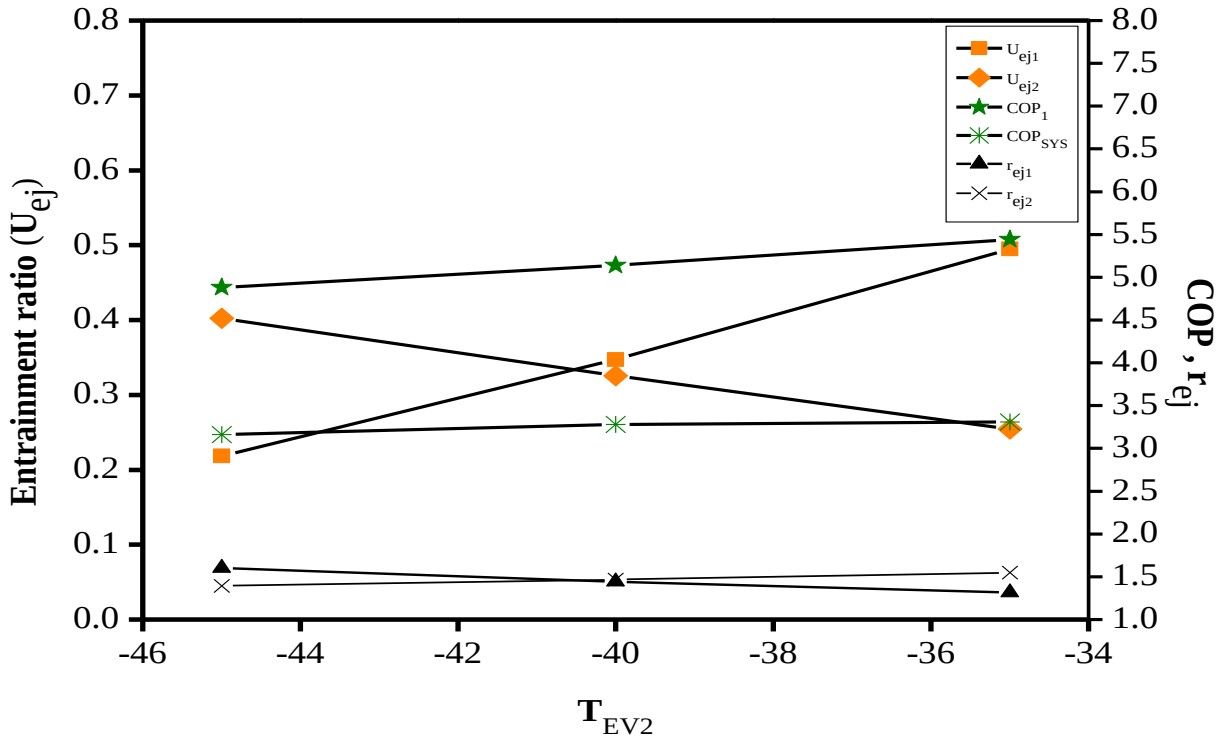

Fig. 4.12: The effect of evaporating temperature T_{ev2} on the entrainment ratios U_{ej1} and U_{ej2}, the compression ratios r_{ej1} and r_{ej2} and the coefficient of performances COP_1 and COP_{SYS}

Fig. 4.13 shows the variation of the entrainment ratios U_{ej1} and U_{ej2}, the compression ratios r_{ej1} and r_{ej2} and the coefficient of performances COP_1 and COP_{SYS} with T_{EV3}. U_{ej1} and r_{ej1} are not affected by varying the evaporator temperature T_{EV3}. U_{ej2} is found to be increasing, since r_{ej2} is decreasing with increasing evaporator temperature T_{EV3}.COP_1 is found to be increasing, while as COP_{SYS} shows a slight increase.

Fig. 4.14 depicts the variation of entrainment ratio U_{ej3}, the compression ratios r_{ej1} and the coefficient of performances COP_2 and COP_{SYS} with evaporating temperature T_{EV4}. The entrainment ratio U_{ej3} shows a decrease with increasing $T_{EV4,}$ since the corresponding pressure ratio r_{ej3} is increasing with increase in T_{EV4}. COP_2 and COP_{SYS} increase slightly with increasing $T_{EV4.}$

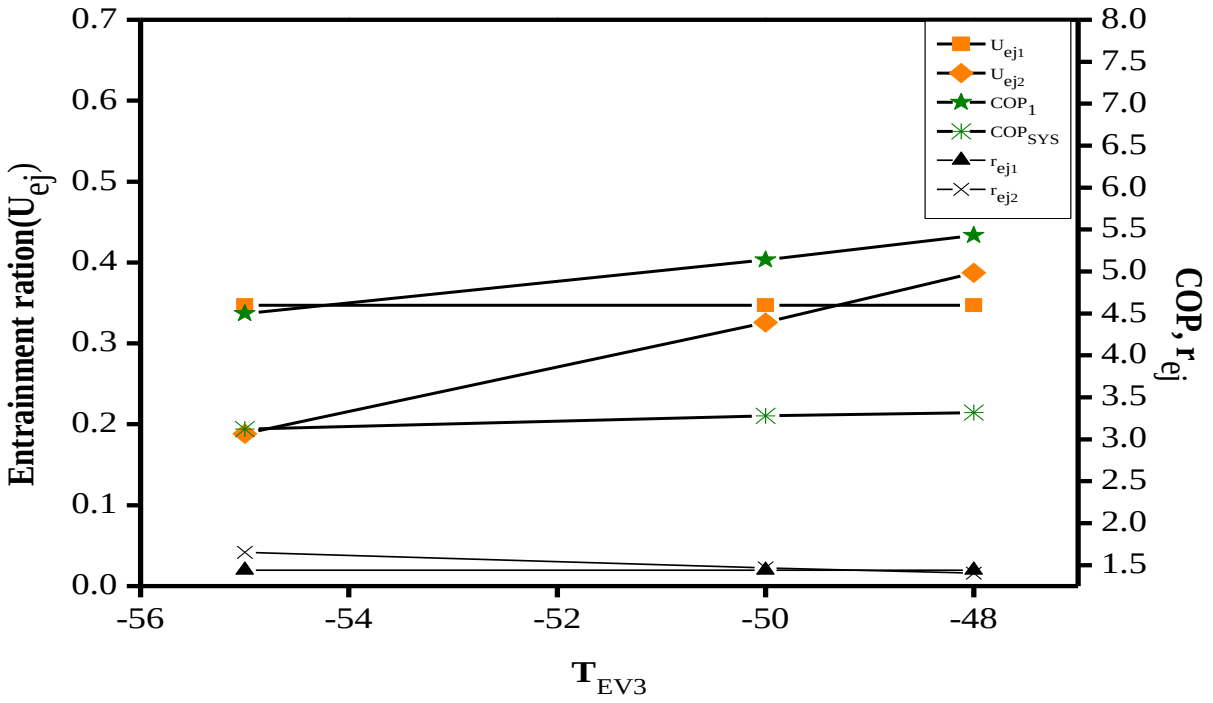

Fig. 4.13: The effect of evaporating temperature T_{ev3} on the entrainment ratios U_{ej1} and U_{ej2}, the compression ratios r_{ej1} and r_{ej2} and COP_1 and COP_{SYS}

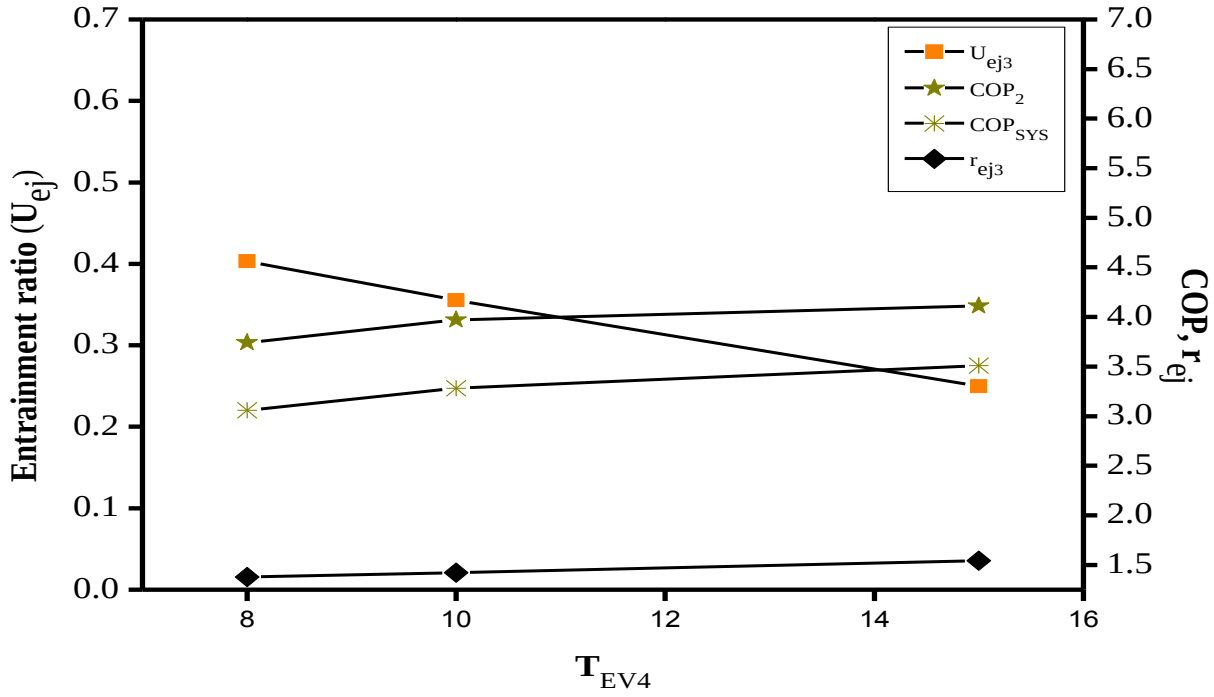

Fig. 4.14: The effect of evaporating temperature T_{ev4} on the entrainment ratio U_{ej3}, the compression ratios r_{ej3} and the coefficient of performances COP_2 and COP_{SYS}

The influence of intercooler temperature T_{INT} on the coefficient of performance COP_1, COP_2 and COP_{SYS} and their relative counterparts COP_{1R}, COP_{2R} and COP_{SYSR} is depicted in Fig. 4.15.The intercooler acts as condenser for the lower stage and evaporator for the second stage. With increasing intercooler temperature T_{INT} ,the COP's of lower stage (COP_1 and COP_{1R}) shows a decrease, the reason being increase in work of compression to a higher intercooler(condenser for lower stage) temperature. The COP's of upper stage (COP_2 and COP_{2R}) shows an increase with increasing intercooler temperature T_{INT}, since the evaporator temperature of upper stage (T_{int}) is increased. The system performance of EEMECRS is measured by COP_{SYS} and COP_{SYSR}, which show a slight increase with increasing intercooler temperature T_{int} , meaning that upper stage of the system has predominant effect on performance of EEMECRS.

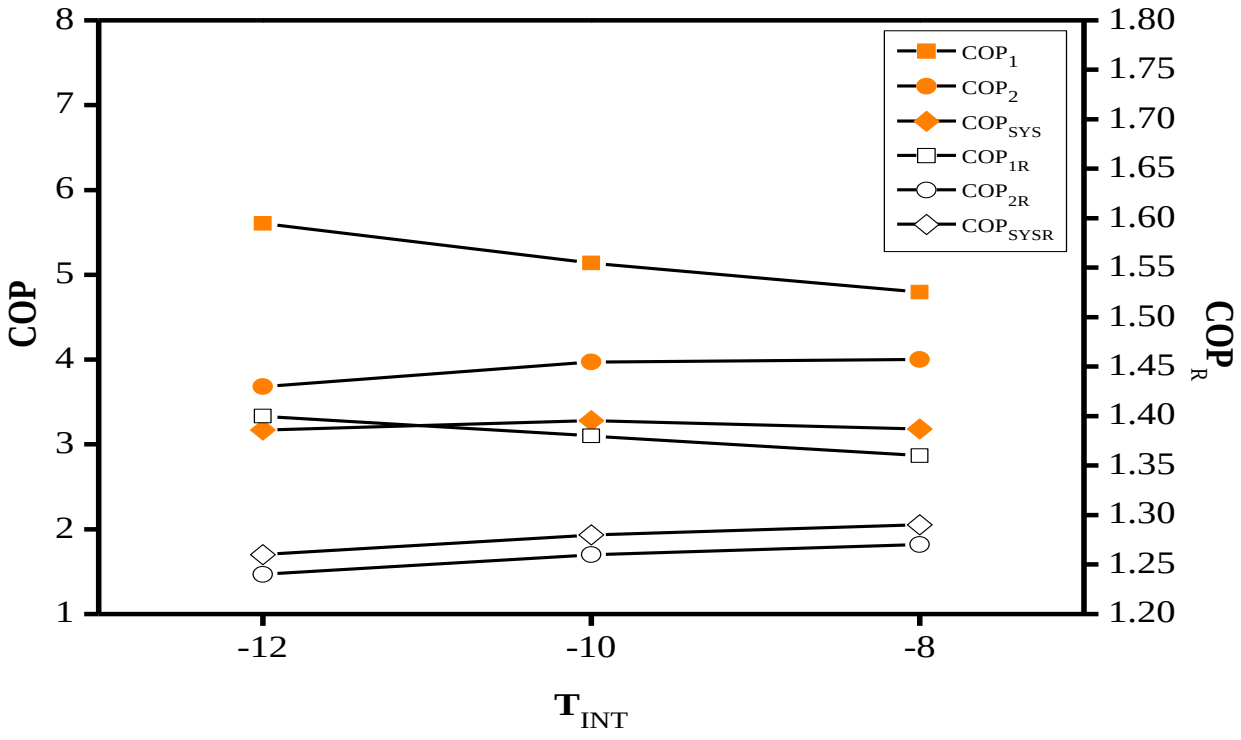

Fig.4.15: The effect of intercooler temperature T_{INT} on the coefficient of performance COP_1, COP_2 and COP_{SYS} and their relative counterparts COP_{1R}, COP_{2R} and COP_{SYSR}.

Fig 4.16 shows variation of entrainment ratio U_{ej3} and pressure ratio r_{ej3} with intercooler temperature. Any increase intercooler temperature T_{INT}, decreases the pressure ratio r_{ej3} which corresponds to an increase in entrainment ratio U_{ej3}

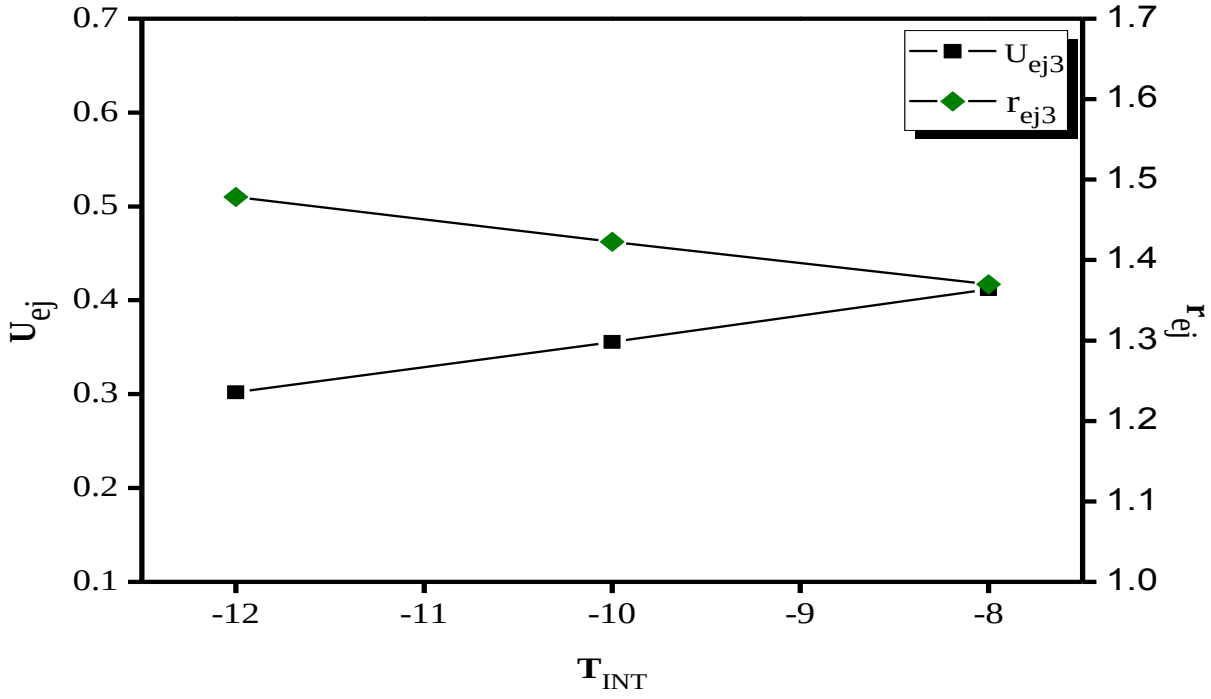

Fig.4.16: The effect of intercooler temperature T_{int} on U_{ej3} and r_{ej3}.

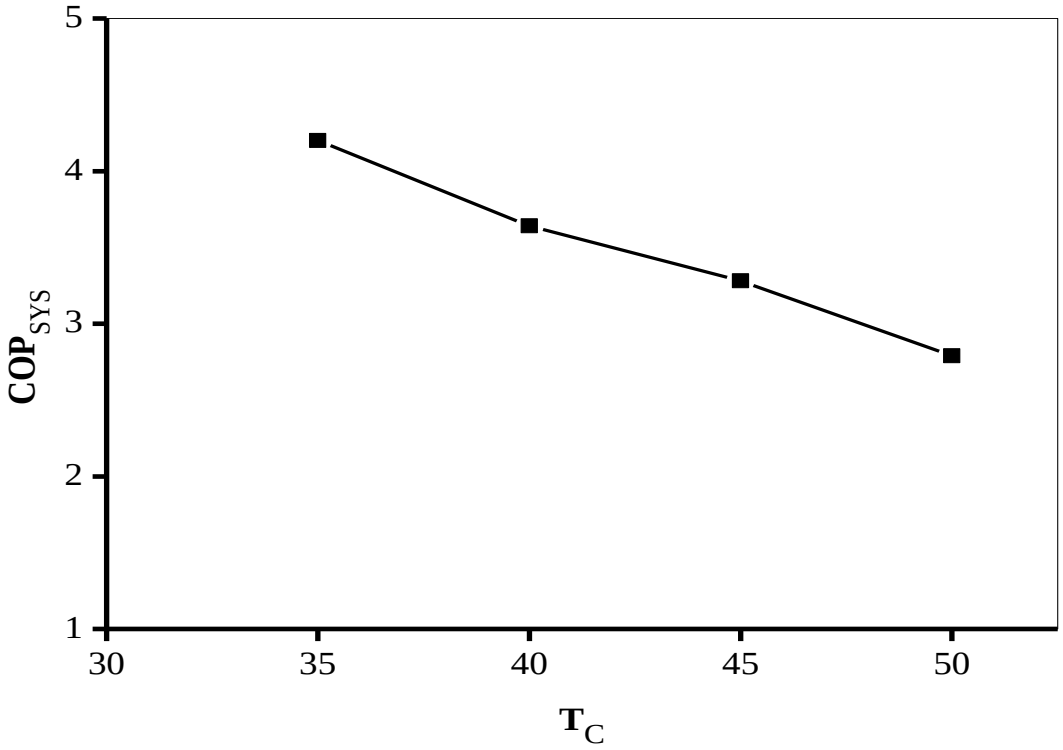

Fig. 4.17: The effect of condensing temperature T_C on COP_{SYS}.

The effect of condensing temperature on the COP of EEMECRS is examined. As indicated in Fig 4.17, the COP_{SYS} decreases with increasing condensing temperature, reason being that more work is required to be done in compressing the same amount of vapour to a higher pressure and thus COP decreases.

Chapter 5

Conclusion

- The performance of ejector is greatly influenced by geometric parameters. On increasing the ejector area Ø from 1.8 to 2.2, the COP of system decreases by 11.8%.
- Selection of appropriate refrigerant pair is found to greatly influence the COP of system as a whole. Refrigerants R142b and R1270 in lower and upper stage respectively gave best results and an overall COP of 3.28 is reached. While as the performance of system with refrigerants R134a and R116 was the least among 16 combinations with COP of 2.52.
- The introduction of ejectors into the system greatly reduces the work of compression and thereby increasing COP. For refrigerants R142b and R1270 in lower and upper stage respectively, the power input the system is reduced by 23% and COP is increased by 28% at Ø = 2. For Ø = 2.2 power input is reduced by 18% and COP is increased by 22%.
- The operating temperatures of four evaporators influence the ejector performance as well as system performance as a whole. For the evaporator 1 (EV_1), increasing temperature from -28^{o}C to -20^{o}C, the COP of system increases by 4.12%. For the evaporator 2 (EV_2), increasing temperature fro -45^{o}C to -35^{o}C, the COP of system increases by 4.83%. For the evaporator 3 (EV_3), increasing temperature from -55^{o}C to -48^{o}C, the COP of system increases by 6.02%. For the evaporator 4 (EV_4), increasing temperature from 8^{o}C to 15^{o}C, the COP of system increases by 11%.
- The intercooler temperature affects the COP of system and should be wisely chosen. On increasing the intercooler temperature the performance of lower stage deteriorates while as the performance of upper stage shows increase. The performance of system as a whole gives the best value at an optimized intercooler temperature. Any deviation from the optimized temperature leads to decreases in performance of system.

- Lowering of condensing temperature is always beneficial to system as a whole. On lowering condenser temperature from 50^{o}C to 35^{o}C, the COP of system is increased by 33%.

Future scope of research work

- The performance and working of EEMECRS needs to be investigated experimentally to verify the results of present work.
- Ejector model can be analysed using CFD, which will provide a better insight into the working of ejector over the present one-dimensional model.
- Exergetic analyses of EEMECRS can be performed to compute the irreversibilities.
- New configuration can be developed to cater the needs for any specific application.

REFERENCES

1. Aly ,N.H.,Karameldin,A., and Shamloul,A.A.,1999. Modelling and simulation of steam jet ejectors. *Desalination,*Vol 123,pp.1-8
2. Antonio Y. M., Périlhon C., Descombes G.,and Chacoux C., 2012. Thermodynamic modelling of an ejector with compressible flow by a one-dimensional approach. *Entropy*, Vol 14(4), pp. 599-613
3. Aphornratana S., and Eames I.W., 1997. A small capacity steam-ejector refrigerator: experimental investigation of a system using ejector with movable primary nozzle. *Int. J. Refrig.,*Vol 20(5), pp. 352-358
4. Arbel, A., and Sokolov, M., 2004. Revisiting solar-powered ejector air conditioner - the greener the better. *Solar Energ*, Vol 77(1), pp. 57-66.
5. Arora, C.P, 1996, *Refrigeration and Air Conditioning,* Tata McGraw-Hill, New Delhi, pp. 476.
6. Aye L., Charters W.W.S., and Rusly E., 2001. Combined solar and electric air conditioning system. *ISES Solar World Congress*, pp. 517-520.
7. Boumaraf L., and Lallemand A, 2009. Modeling of an ejector refrigerating system operating in dimensioning and off-dimensioning conditions with the working fluids R142b and R600a. *Applied Thermal Engineering*, Vol 29(2-3), pp. 265–274
8. Bruce Eng. ,Ejector Modeling in HYSYS,2009. Draft.
9. Chunnanond K., Aphornratana S. 2004. Ejectors: applications in refrigeration technology. *Renewable and Sustainable Energy Reviews*, Vol 8(2),pp. 129–155
10. Diaconu B.M., 2012. Energy analysis of a solar-assisted ejector cycle air conditioning system with low temperature thermal energy storage. *Renewable Energy*, Vol 37(1), pp. 266-276
11. Eames, I.W. , 2002.A new prescription for the design of supersonic jet-pumps: The constant rate momentum change method. *Appl. Therm. Eng.*, Vol 22(2), pp. 121–131.
12. Elbel S., and Hrnjak P., 2008. Ejector refrigeration: an overview of historical and present developments with an emphasis on air-conditioning applications, *International Refrigeration and Air Conditioning Conference.* Paper 884
13. El-Dessouky H., Ettouney H., Alatiqi I., and Al-Nuwaibit G., 2002. Evaluation of steam jet ejectors. *Chemical Engineering and Processing* ,Vol 41(6), pp. 551–561

14. Elakdhar, M., Nehdi, E., and Kairouani, L., 2007. Analysis of a compression/ejection cycle for domestic refrigeration. *Ind. Eng. Chem. Res.*, Vol 46(13), pp. 4639-4644.
15. Fabri J., and Paulon J., 1956. Theorie et experimentation des ejecteurs supersoniques air-air. *ONERA NT* ,Vol 36.
16. Fabri, J., and Siestrunck, R., 1958. Supersonic air ejectors. *Advances in applied mechanics*. Vol.5, pp.1-34.
17. Herna´ndez, J., Dorantes, R., Best, R., and Estrada, C., 2004. The behaviour of a hybrid compressor and ejector refrigeration system with refrigerants 134a and 142b. *Appl. Therm. Eng.* Vol 24(13).,pp.1765-1783
18. Huang,B.J.,Petrenko, V.A.,Chang, J.M., Lin,C.P.,and Hu,S.S, 2001. A combined cycle refrigeration system using ejector- cooling cycle as bottom cycle. *Int J. Refrigrat.* ,Vol 24(5),pp. 391-399
19. Keenan,H., Neumann E.P., and Lusterwerk F., 1950. An investigation of jet pump design by theory and experiment. *ASME J. Appl. Mech* ,Vol 17, pp. 299-309
20. Kairouani, L., Elakhdar, M., Nehdi, E., and Bouaziz,N.,2009. Use of ejectors in multi-evaporator refrigeration system for performance enhancement. *Int J. Refrigrat.* ,Vol 32(6),pp. 1173-1185s
21. Kornhauser, A.A, 1990 .The use of an ejector as a refrigerant expander. *Proceedings of USNC/IIR-Purdue refrigeration conference*, USA (1990)
22. Kshirsagar,D.S., and Deshmukh, M.M., 2013. Thermal design and performance of combined vapour compression-ejector refrigeration system using R600a. *Int. J. of Engineering Research and App.*,Vol 3 (2),pp. 1368-1380.
23. Le Grives, E.,and Fabri, J., 1969. Divers re´gimes de me´lange de deux flux d'enthalpie d'arreˆ t diffe´rentes. *Astronautica Acta* ,Vol 14,pp.203–213.
24. Liu F., and Groll E. A., 2008, Analysis of a two phase flow ejector for transcritical CO_2 cycle, *International Refrigeration and Air Conditioning Conference.* Paper 924.
25. Lu, L.T., 1986. Etudes the´orique et expe´rimentale de la production de froid par machine tritherme a e´jecteur de fluide frigorige`ne. *Ph.D. thesis, Laboratoire d'Energe´tique et d'Automatique, de l'INSA de Lyon, France*.
26. Ma X., Zhang W., Omer S.A., and Riffat S.B., 2010. Experimental investigation of a novel steam ejector refrigerator suitable for solar energy applications. *Appl. Therm. Eng.,* Vol 30(11-12), pp.1320-1325

27. Munday J., Bagster D., 1977. A new ejector theory applied to steam jet refrigeration. *Ind Eng Chem Process Des Dev.*, Vol 16(4), pp. 442-449
28. Nahdi, E., Champoussin, J.C., Hostache, G., Cheron, J., 1993. Optimal geometric parameters of a cooling ejector compressor. *Int. J. Refrigerat.*,Vol 16(1), pp. 67–72.
29. Ouzzane M., and Aidoun M., 2003. Model development and numerical procedure for detailed ejector analysis and design. *Appl. Therm. Eng.*, Vol 23(18), pp. 2337–2351
30. Paliwoda, P., 1968. A review paper on the experimental study on low-grade heat and solar energy operated halocarbon vapour jet refrigeration systems, Topical studies. *IIR Bulletin 1003*.
31. Petrenko, V.O., Huang, B.I., and Ierin, V.O., 2011. Design theoretical study of cascade CO2 sub-critical mechanical compression/butane ejector cooling cycle. *Int. J. Refrigerat.*, Vol 34(7), pp. 1649-1656.
32. Riffat S. B., Jiang L.,and Gan G., 2005. Recent development in ejector technology—a review. *International Journal of Ambient Energy*, Vol 26(1), pp.13-26
33. Sokolov, M., and Hershgal, D., 1989. Compression enhanced ejector refrigeration cycle for low grade heat utilization. *In: IEEE, Proceedings of the 24th Intersociety Energy Conversion Engineering Conference IECEC-89*, Vol 5, pp. 2543-2548.
34. Sokolov, M., and Hershgal, D., 1990. Enhanced ejector refrigeration cycles powered by low grade heat part1, 2 and3. *Int. J. Refrigerat.*, Vol 13(6), pp. 351-356.
35. Sun, D.W., Eames, W.I., and Aphornratana, S., 1996. Evaluation of a novel combined ejector absorption refrigeration cycle, I computer simulation. *Int J. Refrigarat.*, Vol. 19(3), pp. 172- 180.
36. Sun, D.W., 1997. Solar powered combined ejector-vapour compression cycle for air conditioning and refrigeration. *Energ. Convers. Manag.*, Vol 38(5), pp. 479-491.
37. Sun, D.W., 1998. Evaluation of a combined ejector-vapour-compression refrigeration system. *Int. J. Energy Res*. Vol 22(4), pp. 333-342.
38. Sriveerakul, T.,Aphornratana S, and Chunnanond K., 2007.Performance prediction of steam ejector using computational fluid dynamics: Part 1. Validation

of the CFD results. *International Journal of Thermal Sciences* , Vol 46(8), pp. 812–822

39. Sriveerakul, T.,Aphornratana S, and Chunnanond K., (2007).Performance prediction of steam ejector using computational fluid dynamics: Part 2. Flow structure of a steam ejector influenced by operating pressures and geometries. *International Journal of Thermal Sciences* , Vol 46(8) , pp. 823–833.
40. Ubelhack, H.T.,1972. One-dimensional inviscid analysis of supersonic ejectors, AGARDograph No 163,pp. 4-10
41. Valle J.G.D., Jabardo J.M.S., Ruiz F.C., and Alonso J.S.J., 2012.A one dimensional model for the determination of an ejector entrainment ratio. *Int. J. Refrig.*, Vol 35(4) , pp. 772-784
42. Vargaa S., Oliveiraa A.C., and Diaconua B., 2009. Numerical assessment of steam ejector efficiencies using CFD. *Int. J. Refrig.*,Vol 32(6) , pp. 1203-1211
43. Vidal,H., and Colle,S. ,2010. Simulation and economic optimization of a solar assisted combined ejector–vapour compression cycle for cooling applications .*Applied Thermal Engineering* .Vol 30(5) , pp. 478–486
44. Zhu Y, and Jiang P., 2012. Hybrid vapour compression refrigeration system with an integrated ejector cooling cycle. *Int. J. refrigerat.* ,Vol 35(1),pp. 68-78
45. Zhu ,L., Yu J., Zhou M., and Wang X.,2014. Performance analysis of a novel dual-nozzle ejector enhanced cycle for solar assisted air-source heat pump systems. *Renewable Energy*, Vol 63, pp. 735-740
46. Zhu, L., and Li ,Y., 2009.Novel ejector model for performance evaluation on both dry and wet vapors ejectors. *Int. J. Refrig.*, Vol 32(1), pp. 21-31

APPENDIX-A1

A1.1 MATLAB code for ejector modelling

```
function main
clc
clear all
warning('off','MATLAB:dispatcher:InexactMatch')
c=1;
m1=1;
k=input('enter the value of k:');
 disp('value of k:');
 k
 l=input('enter the value of length of ejector-L:');
 d1=input('enter the value of diameter of ejector-d1:');
t1=input('enter the value of primary fluid temperature i.e exit temp of ej1-t1:');
t=input('enter the value of secondary fluid temperature-t:');
o=t/t1;
o1=sqrt(o);
 disp('temp ratio of initial data: ');
 o
 disp('square root value of temp');
 o1
a3=input('enter the value of area a3;');
a5=input('enter the value of area a5;');
%a3=12;
%a5=6;
 q=input('enter the value of ejector area ratio:');
 disp('ejector area ratio(fie)-q:');
 q
 a3=input('enter the value for diffuser -a3:');
```

```
 ae3=input('enter the value for diffuser -ae3:');
%a3=12;
%ae3=4;
%z=4;
 disp('diffuser area ratio(fie)-:');
 z
tt1=t1-5;
tt=t-5;
p1=property('P','T',t1,'Q',1,'REFRIGERANT'); %% REFPROP SUBROUTINE
%p1=property('P','T',tt1,'Q',1,' REFRIGERANT ');
%p1=input('enter the value of pressure at exit of first ejector-pe4:');
%p=property('P','T',tt,'Q',1,' REFRIGERANT ');
%p=input('enter the value of pressure at exit of first ejector-pe4:')
p=property('P','T',t,'Q',1,' REFRIGERANT ');
a=p1/p;
 disp('expansion ratio with initial data:');
 a
 f=input('enter the friction factor value-f:');
%f=0.06
x=(k/(k+1))*(l/d1)*f;
 disp('constant used in momentum equation transformation:');
 x
 nd=input('enter the value of efficiency of diffuser-nd:');
nn=input('enter the value of efficiency of nozzle-nn:');
%nd=0.96;
%nn=0.9;
fn1=f1(m1);
disp('value of f(m1)is-f1:');
fn1
```

```
fn2=f2(k,m1)
disp('value of f(k,m1)is-a*/a-f2:');
fn2
m2=input('enter the value of mach no at section e2 for primary fluid-m1:');
%m2=0.1;
disp('values of function with dimensionless velocity at e2 for primary fluid -me2:');
fn3=f1(m2);
fn4=f2(k,m2);
fn5=f3(k,m2);
 disp('values of fn3:');
fn3
 disp('values of fn4:');
fn4
 disp('values of fn5:');
fn5
zm=k/(k-1);
b=((2/(k+1))^zm)*(1/fn5);
e=abs(b-a)
% abs=absolute
 disp('theortical value of expansion ratio-b:');
 b
disp('error value-e:');
 e
%j=0;
%j=j+e
 h=input('enter the value of change factor for value of m2:');
%check here0
%h=0.001;
mj=m2+h;
```

```
fn3=f1(mj);
fn4=f2(k,mj);
fn5=f3(k,mj)
b=((2/(k+1))^zm)*(1/fn5)
e=abs(b-a)
count_a=0;
count_b=0;
while(e>0.05)
      disp('RUNNING  LOOP');
      count_a=count_a+1
      h=input('enter the value of change factor for value of m2:');
     % h=.0001
      mj=mj+h;
      fn3=f1(mj);
      fn4=f2(k,mj);
      fn5=f3(k,mj);
      disp('new value of fn3:');
      fn3
      disp('new value of fn4:');
      fn4
      disp('new value of fn5:');
      fn5
      b=((2/(k+1))^zm)*(1/fn5)
      disp('new value of error-e:');
      e=abs(b-a)
end
disp('value of error-e:');
e
disp('value of m2final-m2:');
```

```
mj
f1f=f1(mj);
disp('value of m2final f1f=f1(mj):');
f1f
f2f=f2(k,mj);
disp('value of m2final f2f=f2(k,mj):');
f2f
f3f=f3(k,mj);
disp('value of m2final f3f=f3(mj):');
f3f
bf=((2/(k+1))^zm)*(1/f3f);
disp('value of b(final)or theortical final included error:');
bf
u=(1/a)*(q-(1/f2f))*(fn2);
disp('value of u(total factor with temprature ratio):');
u
uf=u/o1;
disp('value of u-final:');
uf
s=(f1f+(u*fn1))/(1+u);
disp('sample S is:');
s
a1=x+1;
d=((s*s)-(4*a1*1));
disp('value of d:');
d
if(d= =0)
   root1=(s)/(2*a1);
   root2=root1;
```

```
    disp('roots are real and equal');
elseif(d>0)
    root1=(s+sqrt(d))/(2*a1);
    root2=(s-sqrt(d))/(2*a1);
    disp('roots are real and distinct');
else
    root1=(s)/(2*a1);
    root2=sqrt(-d)/(2*a1);
    disp('roots are imaginary')
end
disp('root1 of m3:');
root1
disp('root2 of m3:');
root2
if(root1<1 & root2<1)
if(root1>root2)
    disp('root1 is used root');
    m3=root1;
elseif(root2>root1)
    disp('root2 is used root');
    m3=root2;
else
disp('undefined');
end
else
    if(root1<root2)
    disp('root1 is used root');
    m3=root1;
elseif(root2<root1)
```

```
    disp('root2 is used root');
    m3=root2;
    end
end

 disp('me3(dimensionless velocity at section e3):');
 m3
 fn6=f1(m3);
  disp('Fn6(f1(m3)):');
fn6
fn7=f2(k,m3);
disp('Fn7(f2(k,m3)):');
fn7
r=nd*z;
 disp('multiplication of diffuser efficiency and area ratio-r:');
r
ne=fn7/r;
 disp('the factor used to find m4-ne:');
ne
r1=m3/r;
 disp('value of r1:');
 r1
 r2=(r1)^(k-1);
 disp('value of r2:');
 r3=r2*(1-((k-1)/(k+1))*m3*m3);
 disp('value of r3:');
 r3
 r8=1/(k-1);
 r4=(r3)^r8;
```

```
disp('value of r4:');
r4
m4=r4;
fn8=f2(k,m4);
disp('value of f2(k,m4):');
fn8
fn9=f3(k,m4);
disp('frictional value of f3(k,m4)-fn9:');
fn9
w=(q*z*fn8)/((u+1)*fn9);
disp('value of driving pressure ratio(axii)is:');
w
rat=a/w;
disp('value of ratio(expansion ratio/axii)is:');
rat
pback=p1/w;
disp('value of back pressure for ejector:');
pback
uf
a
a1
t03=((1+uf*o)/(1+uf))*t1
end

function [xl]=f1(m)
xl=(m+(1/m));
%return x;
end
function  [ f,n ] = f2( k,m )
```

```
n=1/(k-1);
f=(((k+1)/2)^n)*m*((1-(((k-1)/(k+1))*m*m))^n);
end
function [g,s]= f3(k,m)
s= k/(k-1);
g=(1-(((k-1)/(k+1))*m*m))^s;
%return g;
end
```

A1.2. MATLAB code for lower stage of EEMECRS

```
function main
clc
clear all
warning('off','MATLAB:dispatcher:InexactMatch')
C=input('enter the value of cp:');
uej1=input('value of entrainment ration for ejector 1-uej1:');
uej2=input('value of entrainment ration for ejector 2-uej2:');
%uej1=m2/m1;
%uej2=m3/(m1+m2)
m1=1/((1+uej1)*(1+uej2))
m2=((uej1)/((1+uej1)*(1+uej2)))
m3=((uej2)/(1+uej2))
h6=property('H','T',tint,'Q',0,'REFRIGERANT');%318property('P','T',tt,'Q',1,REFRIG
ERANT')
p10=property('P','T',tev1,'Q',1,' REFRIGERANT');%te1
T10=input('Enter the value of temperature at 10 in K:');
[TS10 hs10 ss10 cs10]=property('THSC','P',p10,'Q',1,' REFRIGERANT');
h10=hs10+C*(T10-TS10)
s10=ss10+C*log(T10/TS10)
qev1=(h10-h6)/((1+uej1)*(1+uej2));
disp('heat absorbed in evaporator 1-qev1:');
```

```
qev1
p11=property('P','T',te2,'Q',1,' REFRIGERANT');%te2
T11=input('Enter the value of temperature at 11 in K:');
[TS11 hs11 ss11 cs11]=property('THSC','P',p11,'Q',1,' REFRIGERANT');
h11=hs11+C*(T11-TS11)
s11=ss11+C*log(T11/TS11)
qev2=(h11-h6)*((uej1)/((1+uej1)*(1+uej2)));
disp('heat absorbed in evaporator 2-qev2:');
qev2
p15=property('P','T',tev3,'Q',1,' REFRIGERANT');%te3
T15=input('Enter the value of temperature at 15 in K:');
[TS15 hs15 ss15 cs15]=property('THSC','P',p15,'Q',1,' REFRIGERANT');
h15=hs15+C*(T15-TS15)
s15=ss15+C*log(T15/TS15)
qev3=(h15-h6)*((uej2)/(1+uej2));
disp('heat absorbed in evaporator 3-qev3:');
qev3
p1=input('enter the value of pressure at exit of second ejector:');
T1=input('Enter the value of temperature at exit of second ejector:');
[TS1 hs1 ss1 cs1]=property('THSC','P',p1,'Q',1,' REFRIGERANT');
h1=hs1+C*(T1-TS1)
s1=ss1+C*log(T1/TS1)
[pc sc cc]=property('PSC','T',tint,'Q',1,' REFRIGERANT');
%it is t=318=45
t2=tint*exp((s1-sc)/C)
pc
h2=property('H','T',t2,'P',pc,' REFRIGERANT')
s2=property('S','T',t2,'P',pc,' REFRIGERANT');
a=h2-h1;
```

```
disp('the value of enthalpy drop-h2-h1:');
a
ncomp=(0.874-((0.0135)*((pc)/(p1))));
disp('value of compressor efficiency-ncomp:');
ncomp
c=a/ncomp;
w=c;
disp('value of work done in ejector refrigeration system-w:');
w
p=w/60;
disp('value of power required to drive compressor-p:');
p
re=qev1+qev2+qev3;
disp('value of refrigeration effect-re:');
re
cop=re/w;
disp('value of cop of ejector cycle-cop:');
cop
end
```

A1.3. MATLAB code for upper stage of EEMECRS

```
function main
clc
clear all
warning('off','MATLAB:dispatcher:InexactMatch')
C=input('enter the value of cp:');
uej=input('value of entrainment ration for ejector -uej:');
%uej1=m2/m1;
%uej2=m3/(m1+m2)
h6=property('H','T',tc'Q',0,'REFRIGERANT');%318property('P','T',tt,'Q',1,'REFRIGERANT')
```

```
p10=property('P','T',tev4,'Q',1,'REFRIGERANT');%qe1
T10=input('Enter the value of temperature at 10 in K:');
[TS10 hs10 ss10 cs10]=property('THSC','P',p10,'Q',1,"REFRIGERANT'');
h10=hs10+C*(T10-TS10)
s10=ss10+C*log(T10/TS10)
%qev1=(h10-h6)/(1+uej);
%qev1
p11=property('P','T',tint,'Q',1,'REFRIGERANT');
T11=input('Enter the value of temperature at 11 in K:');
[TS11 hs11 ss11 cs11]=property('THSC','P',p11,'Q',1, 'REFRIGERANT');
h11=hs11+C*(T11-TS11)
s11=ss11+C*log(T11/TS11)
t01=input('enter the value of temp at compressor exit:');
p01=input('enter the value of pressure at compressor exit:');
h01=property('H','T',t01,'P',p01, 'REFRIGERANT')%ref1
t2=input('enter the value of intercooler temprature:');
h02=property('H','T',t2,'Q',0, 'REFRIGERANT');ref1%
m2=(h01-h02)/(h11-h6)
m1=m2/uej
qev2=(h01-h02);
%qev2=(h11-h6)*m2;
qev1=(h10-h6)*m1
disp('heat absorbed in evaporator 2-qev2:');
qev2
p1=input('enter the value of pressure at exit of  ejector:');
T1=input('Enter the value of temperature at exit of  ejector:');
[TS1 hs1 ss1 cs1]=property('THSC','P',p1,'Q',1, 'REFRIGERANT');
h1=hs1+C*(T1-TS1)
s1=ss1+C*log(T1/TS1)
```

```
[pc sc cc]=property('PSC','T',tc'Q',1, 'REFRIGERANT');
%it is t=318=45
t2=323.15*exp((s1-sc)/C)
pc
h2=property('H','T',t2,'P',pc, 'REFRIGERANT')
s2=property('S','T',t2,'P',pc, 'REFRIGERANT');
a=(m1+m2)*(h2-h1);
disp('the value of enthalpy drop-h2-h1:');
a
ncomp=(0.874-((0.0135)*((pc)/(p1))));
disp('value of compressor efficiency-ncomp:');
ncomp
c=a/ncomp;
w=c;
disp('value of work done in ejector refrigeration system-w:');
w
p=w/60;
disp('value of power required to drive compressor-p:');
p
re=qev1+qev2;
disp('value of refrigeration effect-re:');
re
cop=re/w;
disp('value of cop of ejector cycle-cop:');
cop
end
```

A1.4. MATLAB code for lower stage of UMECRS

```
function main
C=input('enter the value of cp:');
qev1=input('enter the value of qev1:');
qev2=input('enter the value of qev2:');
qev3=input('enter the value of qev3:');
h6=property('H','T',tint,'Q',0,'REFRIGERANT')
%h9=property('H','P',pev1,'T',tev1, 'REFRIGERANT');
%h10=property('H','P',pev2,'T',tev2, 'REFRIGERANT');
%h13=property('H','P',pev3,'T',tev3, 'REFRIGERANT');
p9=property('P','T',tev1,'Q',1, 'REFRIGERANT')
T9=input('Enter the value of temperature at 9 in K:');
[TS9 hs9 ss9 cs9]=property('THSC','P',p9,'Q',1, 'REFRIGERANT');
h9=hs9+C*(T9-TS9)
%h9=input('enter the value of h9:');
p10=property('P','T',tev2,'Q',1, 'REFRIGERANT')
T10=input('Enter the value of temperature at 10 in K:');
[TS10 hs10 ss10 cs10]=property('THSC','P',p10,'Q',1, 'REFRIGERANT');
h10=hs10+C*(T10-TS10)
%h10=input('enter the value of h10:');
p13=property('P','T',tev1,'Q',1, 'REFRIGERANT')
T13=input('Enter the value of temperature at 13 in K:');
[TS13 hs13 ss13 cs13]=property('THSC','P',p13,'Q',1, 'REFRIGERANT');
h13=hs13+C*(T13-TS13)
%h13=input('enter the value of h13:');
m1=input('enter the value of m1:');
m2=input('enter the value of m2:');
m3=input('enter the value of m3:');
h1=(m1*h9+m2*h10+m3*h13)/(m1+m2+m3)
```

```
s1=input('enter the value of s1:');
s11=property('S','T',tint,'Q',1,"REFRIGERANT')
c11=property('C','T',tint,'Q',1, 'REFRIGERANT');
t2=tint*exp((s1-s11)/C)
pc=property('P','T',tint,'Q',1, 'REFRIGERANT');
%h2=h2s+c2s*(t2-T2s)
h2=property('H','T',t2,'P',pc, 'REFRIGERANT')
a=h2-h1;
disp('the value of enthalpy drop-h2-h1:');
a
ph=input('enter the value of pressure at compressor high pressure side-ph:');
pl=input('enter the value of pressure at compressor low pressure side-pl:');
ncomp=(0.874-((0.0135)*((ph)/(pl))));
disp('value of compressor efficiency-ncomp:');
ncomp
c=a/ncomp;
w=c;
disp('value of work done in ejector refrigeration system-w:');
w
p=w/60;
disp('value of power required to drive compressor-p:');
p
re=qev1+qev2+qev3;
disp('value of refrigeration effect-re:');
re
cop=re/w
```

A1.5. MATLAB code for upper stage of UMECRS

```
function main
m1=input('enter the value of m1:');
```

```
m2=input('enter the value of m2:');
C=input('enter the value of cp:');
qev1=input('enter the value of qev1:');
qev2=input('enter the value of qev2:');
h6=property('H','T',tc,'Q',0, 'REFRIGERANT')

p9=property('P','T',tev4,'Q',1, 'REFRIGERANT')
T9=input('Enter the value of temperature at 9 in K:');
[TS9 hs9 ss9 cs9]=property('THSC','P',p9,'Q',1, 'REFRIGERANT');
h9=hs9+C*(T9-TS9)
%h9=input('enter the value of h9:');
p10=property('P','T',tint,'Q',1, 'REFRIGERANT')
T10=input('Enter the value of temperature at 10 in K:');
[TS10 hs10 ss10 cs10]=property('THSC','P',p10,'Q',1, 'REFRIGERANT');
h10=hs10+C*(T10-TS10)
%m1=qev1/(h9-h6)
%m2=qev2/(h10-h6)
h1=(m1*h9+m2*h10)/(m1+m2)
s1=input('enter the value of s1:'); %1981.4 ; s11=property('S','T',318.15,'Q',1,'R142B')
c11=property('C','T',tc,'Q',1,'REFRIGERANT');
t2=tc*exp((s1-s11)/C)
pc=property('P','T',tc,'Q',1, 'REFRIGERANT');
%h2=h2s+c2s*(t2-T2s)
h2=property('H','T',t2,'P',pc, 'REFRIGERANT')
a=(m1+m2)*(h2-h1);
disp('the value of enthalpy drop-h2-h1:');
a
ncomp=(0.874-((0.0135)*((pc)/(p9))));
disp('value of compressor efficiency-ncomp:');
```

```
ncomp
c=a/ncomp;
w=c;
disp('value of work done in ejector refrigeration system-w:');
w
p=w/60;
disp('value of power required to drive compressor-p:');
p
re=qev1+qev2;
disp('value of refrigeration effect-re:');
re
cop=re/w
```

APPENDIX-A2

A 2.1 Transformation of momentum equation expression $mV + PA$

$$mV + PA = \rho AV^2 + PA = \left(\frac{P}{P_o}\right) \times P_o A \times \left(1 + \frac{\rho}{P} V^2\right) \qquad (A.1)$$

$$\frac{\rho}{P} = \rho AV^2 + PA = \frac{\rho_*}{P_*} \times \frac{\rho}{\rho_*} \times \frac{P_*}{P}$$

$$(1)\,\frac{P}{P_o}$$

$$\frac{T}{T_o} = \left(\frac{P_o}{P}\right)^{\frac{1-\gamma}{\gamma}} = \left(\frac{P}{P_o}\right)^{\frac{\gamma}{\gamma-1}}$$

$$C_P T_o = C_P T + \frac{V^2}{2}$$

Accounting for losses in nozzle,

$$\frac{V^2}{2} = \eta_n C_P T_o \left(1 - \frac{T}{T_o}\right) \qquad (A.2)$$

where , η_n is the nozzle isentropic efficiency.

$$V = \sqrt{2(C_P T_o - C_P T)}\eta_n$$

$$C_P = \frac{\gamma^r}{\gamma - 1}$$

where, r is given by r = R/M, M is the molecular weight of gas.

Therefore,

$$\frac{V^2}{2} = \frac{\gamma^r}{\gamma - 1} T_o \left(1 - \frac{T}{T_0}\right) \qquad (A.3)$$

$$V^2 = \frac{2kT_o}{k-1}\eta_n \left(1 - \left(\frac{P}{P_0}\right)^{\frac{k}{k-1}}\right)$$

$$a^2 = kRT = \frac{2kr}{k+1} T_o \qquad (A.4)$$

With equations *A.3* and *A.4* and by introducing dimensionless velocity M ($M=V/a_*$),we obtain

$$M^2 = \frac{V^2}{a^2} = \frac{k+1}{k-1}\eta_n \left(1 - \frac{T}{T_o}\right) \qquad (A.5)$$

$$M^2 = \frac{k+1}{k-1}\left(1 - \left(\frac{P}{P_0}\right)^{\frac{k}{k-1}}\right)$$

$$\frac{P}{P_o} = \left(1 - \frac{k-1}{k+1} \times \frac{M^2}{\eta_n}\right)^{\frac{k}{k-1}} \quad (A.6)$$

$$\frac{T}{T_o} = \left(1 - \frac{k-1}{k+1} \times \frac{M^2}{\eta_n}\right) \quad (A.7)$$

$$M^2 = \frac{k+1}{k-1}\left(1 - \left(\frac{P}{P_0}\right)^{\frac{k}{k-1}}\right)$$

(2) $\frac{\rho_*}{P_*}$

$$\frac{\rho_*}{P_*} = \frac{1}{RT_*} = \frac{k}{kRT_*} = \frac{k}{a^2} \quad (A.8)$$

(3) $\frac{\rho}{\rho_*}$

$$\frac{\rho}{\rho_*} = \frac{\rho}{\rho_0} \times \frac{\rho_0}{\rho_*}$$

$$\frac{\rho}{\rho_0} = \frac{P}{P_o} \times \frac{T_o}{T} = \left(1 - \frac{k-1}{k+1} \times \frac{M^2}{\eta_n}\right)^{\frac{1}{k-1}}$$

Therefore:

$$\frac{\rho}{\rho_*} = \left(\frac{k+1}{2}\right)^{\frac{1}{k+1}}\left(1 - \frac{k-1}{k+1} \times \frac{M^2}{\eta_n}\right)^{\frac{1}{k-1}} \quad (A.9)$$

(4) $\frac{P_*}{P}$

$$\frac{P_*}{P} = \left(\frac{k+1}{2} - \frac{k-1}{2} \times \frac{M^2}{\eta_n}\right)^{\frac{-k}{k-1}}$$

$$\frac{P_*}{P} = \left(\frac{k+1}{2} - \frac{k-1}{2}\frac{M^2}{\eta_n}\right)^{\frac{-k}{(k-1)}} = \left(\frac{k+1}{2}\right)^{\frac{-k}{(k-1)}}\left(1 - \frac{k-1}{k+1}\frac{M^2}{\eta_n}\right)^{\frac{-k}{(k-1)}} \quad (A.10)$$

By using equations *(A.6), (A.8), (A.9) and (A.10), (A.1)* can be rewritten as:

$$mV + PA = P_o A \times \left[\left(1 - \frac{k-1}{k+1} \times \frac{M^2}{\eta_n}\right)^{\frac{k}{k-1}} \times \frac{2 \times kM^2}{k+1}\left(1 - \frac{k-1}{k+1} \times \frac{M^2}{\eta_n}\right)^{\frac{1}{k-1}}\right]$$

$$mV + PA = P_o A \times \left[\left(1 - \frac{k-1}{k+1} \times \frac{M^2}{\eta_n} \right)^{\frac{1}{k-1}} \times (1 + M^2) \right]$$

$$mV + PA = P_o A \, f(k, M, \eta_n)$$

We have:

$m = m_*$

This gives:

$$\frac{A_*}{A} = \frac{\rho}{\rho_*} M$$

By using equation *(A.9)*

$$\frac{A_*}{A} = \left(\frac{k+1}{2} \right)^{\frac{1}{k-1}} M \left(1 - \frac{k-1}{k+1} \frac{M^2}{\eta_n} \right)^{\frac{1}{k-1}} = f_2(k, M, \eta_n) \qquad (A.11)$$

$$mV + PA = P_o A_* \frac{f(k, M, \eta_n)}{f_2(k, M, \eta_n)} = P_o A_* \frac{1 + M^2}{M \left(\frac{k+1}{2} \right)^{\frac{1}{k-1}}}$$

$$mV + PA = P_o A_* \left(\frac{2}{k+1} \right)^{\frac{1}{k-1}} \left(M + \frac{1}{M} \right)$$

We know:

$$f_1(M) = \left(M + \frac{1}{M} \right)$$

$$mV + PA = P_o A_* \left(\frac{2}{k+1} \right)^{\frac{1}{k-1}} f_1(M) \qquad (A.12)$$

And since V<< a_* → V/ a_*→0,

$$\frac{\rho_*}{\rho_0} = \left(1 - \frac{k-1}{k+1} \right)^{\frac{1}{k-1}} = \left(\frac{2}{k+1} \right)^{\frac{1}{k-1}}$$

Equation (*A.12)*, is then expressed as:

$$mV + PA = P_o \frac{\rho_*}{\rho_0} A_* f_2(M)$$

$$\frac{P_0}{\rho_0} = RT_0 = \frac{kRT_0}{k} = \frac{a_0^2}{k} = \frac{\frac{k+1}{2} a_*^2}{k} = \frac{k+1}{2k} a_*^2$$

$$mV + PA = \frac{k+1}{2k} a_*^2 \ \rho_* A_* f_3(M)$$

Finally we obtain:

$$mV + PA = \frac{k+1}{2k} a_*^2 \; mf_1(M) \qquad (A.13)$$

Calculation of stagnation pressure at section P_{0e3} in the section e3

The mass flow rate is given by:

$$m = A_* B_* \rho_* = A_* V_* \frac{P_*}{RT_*} = A_* \frac{a_*}{\sqrt{kRT_*}} \frac{\sqrt{k}}{\sqrt{RT_*}} \rho_*$$

$$\frac{a_*}{\sqrt{kRT_*}} = 1$$

$$m = A_* \rho_* \sqrt{\frac{k}{R}} \frac{1}{\sqrt{T_*}} \Rightarrow m = \frac{A_* \rho_*}{\sqrt{T_*}} \sqrt{\frac{k}{R}} \qquad (A.14)$$

By introducing (A_*/A) and (P_*/P_0) in the equation (*A.14*), we obtain:

$$m = A \frac{A_*}{A} P_0 \frac{P_*}{P_0} \frac{1}{\sqrt{T_0}} \frac{\sqrt{T_0}}{\sqrt{T_*}} \sqrt{\frac{k}{R}}$$

$$m = P_0 \frac{1}{\sqrt{T_0}} A \frac{A_*}{A} \frac{P_*}{P_0} \frac{\sqrt{T_0}}{\sqrt{T_*}} \sqrt{\frac{k}{R}} \qquad (A.15)$$

$$\frac{A_*}{A} = f_2(k, m)$$

And by knowing

$$\frac{P_*}{P_0} = \left(\frac{2}{k+1}\right)^{k/(k-1)}$$

and

$$\frac{\sqrt{T_0}}{\sqrt{T_*}} = \left(\frac{k+1}{2}\right)^{1/2}$$

Equation (*A.15*) becomes:

$$m = P_0 \frac{1}{\sqrt{T_0}} A f_2(k, m) \left(\frac{2}{k+1}\right)^{k/(k-1)} \left(\frac{k+1}{2}\right)^{1/2} \sqrt{\frac{k}{R}}$$

For the primary fluid, the flow rate expression is expressed as:

$$m' = P'_0 \frac{1}{\sqrt{T'_0}} A'_* \sqrt{\frac{k}{R}} \left(\frac{2}{k+1}\right)^{k/(k-1)} \left(\frac{k+1}{2}\right)^{1/2} \qquad (A.16)$$

And with an expression similar to (*A.16*), we can calculate the mass flow rate in section 3

$$m_{e3} = P_{0e3}\frac{1}{\sqrt{T_{0e3}}}A_{*e3}\sqrt{\frac{k}{R}}\left(\frac{2}{k+1}\right)^{k/(k-1)}\left(\frac{k+1}{2}\right)^{1/2} \quad (A.17)$$

The fictitious throat A_{*e3} can be expressed as:

$$\frac{A_{*e3}}{A_{e3}} = \left(\frac{k+1}{2}\right)^{1/(k-1)} M_{e3}\left(1-\frac{k-1}{k+1}M_{e3}^2\right)^{1/(k-1)}$$

$$f_2\,(k,m) = \frac{A_*}{A} = \left(\frac{k+1}{2}\right)^{1/(k-1)} M\left(1-\frac{k-1}{k+1}M^2\right)^{1/(k-1)}$$

then

$A_{*e3} = A_{e3}f_2\,(k, M_{e3})$

By combining the equation (*A.16*) attributed to the section (e2) and equation (*A.17*), we obtain:

$$\frac{m_{e3}}{m'_{e2}} = \frac{P_{0e3}}{P'_0}\sqrt{\frac{T'_0}{T_{0e3}}}\frac{A_{e3}}{A'_*}f_2\,(k, M_{e3}) \quad (A.18)$$

$$\frac{P_{0e3}}{P'_0} = \frac{m_{e3}}{m'_{e2}}\sqrt{\frac{T_{0e3}}{T'_0}}\frac{A'_*}{A_{e3}}\frac{1}{f_2\,(k, M_{e3})}$$

$$\frac{T_{0e3}}{T'_0} = \frac{1+U\theta}{1+U}$$

$$\frac{m_{e3}}{m'_{e2}} = 1+U$$

And by introducing the parameter $\emptyset = A_{e3}/A'_*$ we obtain:

$$\frac{P_{0e3}}{P'_0} = \frac{1 = U(\emptyset)^{1/2}}{\emptyset f_2\,(k, M_{e3})} \quad (A.19)$$